FINAL REPORT
FOR

INTAGLIATED PHOSPHOR SCREEN IMAGE TUBE PROJECT

Richard J. Hertel

ITT Aerospace/Optical Division
Fort Wayne, Indiana 46803

Contract NAS5-26417
15 May 1982

Prepared for

National Aeronautics and Space Administration
Goddard Space Flight Center
Greenbelt, Maryland 20771

A8127422

Table of Contents

List of Figures

List of Figures (continued)

List of Figures (continued)

List of Figures (continued)

List of Tables

REFERENCES

(1) "Resolution Model Study for Fiber Optic Window Interface at Intensified Film Cameras," Richard J. Hertel, NAS5-25452, 1 August 1980.

(2) Fiber Optics, Theory and Practice, Allen, W. B., Plenum Press, 1973, p. 161.

(3) Fiber Optics - Principles and Applications, N. S. Kapany, Academic Press, 1967, p. 212.

(4) High Performance Screens for Image Intensifiers, Piedmont, J. R., Finegold, R., EOSD Conference, Procedings, 1976, p. 615.

Section 1

INTRODUCTION

Photographic media are frequently used for detecting, recording, and archiving astronomy data. Even in this day of electronic astronomy, and with extensive knowledge of the idiosyncrasies of the photographic process, films and plates are still widely used. Combining electronic detection with film recording is particularly promising. The detection is by means of a high quantum efficiency, alkali metal photocathode in an image tube. If sufficient gain exists in the image tube, the film is selected for its recording and storage attributes and without consideration of its photon efficiency.

One means of assuring a high gain is to minimize the optical losses between the image tube and the film. Film in direct contact with an image tube phosphor screen has a very high coupling efficiency. Effective direct contact with the phosphor screen is achieved by using a fiber optic exit window on the image tube and placing the film in contact with that window.

A previous report, reference 1, examined the optical mechanisms of the image tube-film combination analytically and experimentally. That report showed the quantitative effects of finite phosphor screen and film thicknesses on the resolution of the image ultimately recorded in the film. The report concluded that a specially built image tube containing a phosphor screen prepared by the intagliation process would be useful.

The objectives of this study were to use current technology to produce a magnetic focus image tube that has an intagliated phosphor screen, to measure the modulation transfer function of such a tube by electronic means and by film tests, and to compare the results with tubes of more conventional construction. All of the objectives were accomplished.

Section 2 of this report describes the physical properties of the image tube and film combination. Section 2 also describes the analytical model of the optical interface and the salient features of the intagliated screen tube constructed especially for this study.

Section 3 describes the results of the electronic MTF tests of the intagliated image tube.

Section 4 covers the results of the densitometry of the tube and film test samples.

Section 5 contains the conclusions. Chief among the conclusions are that the intagliated screen is a help, but the thickness of the photographic film is also important.

Throughout this report, frequent reference is made to a previous study. Reference 1 is the final report for that study.

Section 2

PROPERTIES OF IMAGE TUBES, FILM, THEIR OPTICAL COUPLING, AND INTAGLIATED PHOSPHOR SCREENS

This section is a description of the important physical attributes of image tubes in general and intagliated phosphor screen models in particular. An excerpt from the previous study is used to describe the mathematical model of the tube and film coupling.

2.1 DESCRIPTIONS OF A STANDARD FIBER OPTIC IMAGE TUBE AND FILM COMBINATION (Reference 1)

A section view of the fiber optic faceplate and photographic film interface for a standard image tube is shown in Figure 2.1-1. The Y axis in the figure is parallel to the optical axis of the image tube. Photoelectrons, accelerated to 15 keV, travel in a helix which has an axis that is parallel to the Y axis. When the electrons reach the output end of the tube, they pass through a thin aluminum layer and then strike the phosphor screen. The substrate for the phosphor screen is the fiber optic window. The section view in Figure 2.1-1 shows three window fibers and part of a fourth. On the scale of the figure, most of the faceplate thickness is not shown, only the interfaces.

2.1.1 Aluminum Layer

As electrons reach the output phosphor screen, they first must penetrate a thin aluminum layer covering the screen. This aluminum layer serves two functions. It provides a ground plane for the phosphor screen and it reflects a fraction of the emitted light towards the exit windown.

The aluminum layer on the phosphor screen is the result of an evaporation and deposition process. A witness plate located nearby is used to control the process. Measurements of the resistance and optical transmission of the witness plate coating give an average aluminum thickness of 0.02 micrometers. Electrons of 15 keV energy lose about 100 eV when passing through this layer.

2.1.2 Phosphor Screen

The phosphor screen in a high resolution image tube is 6 to 8 micrometers thick and consists of a distribution of particle sizes from <0.3 micrometers to as large as 3 micrometers. Most are 1 to 2 micrometers in size. The screens are usually gravity or centrifuge settled and the particles are loosely packed. An average thickness of 6 to 8 micrometers is about as thin as possible for settled screens, while still achieving 100 percent area coverage and good absorption of 15 keV electrons.

Usual materials are P11, ZnS:Ag and P20, ZnCdS:Ag.

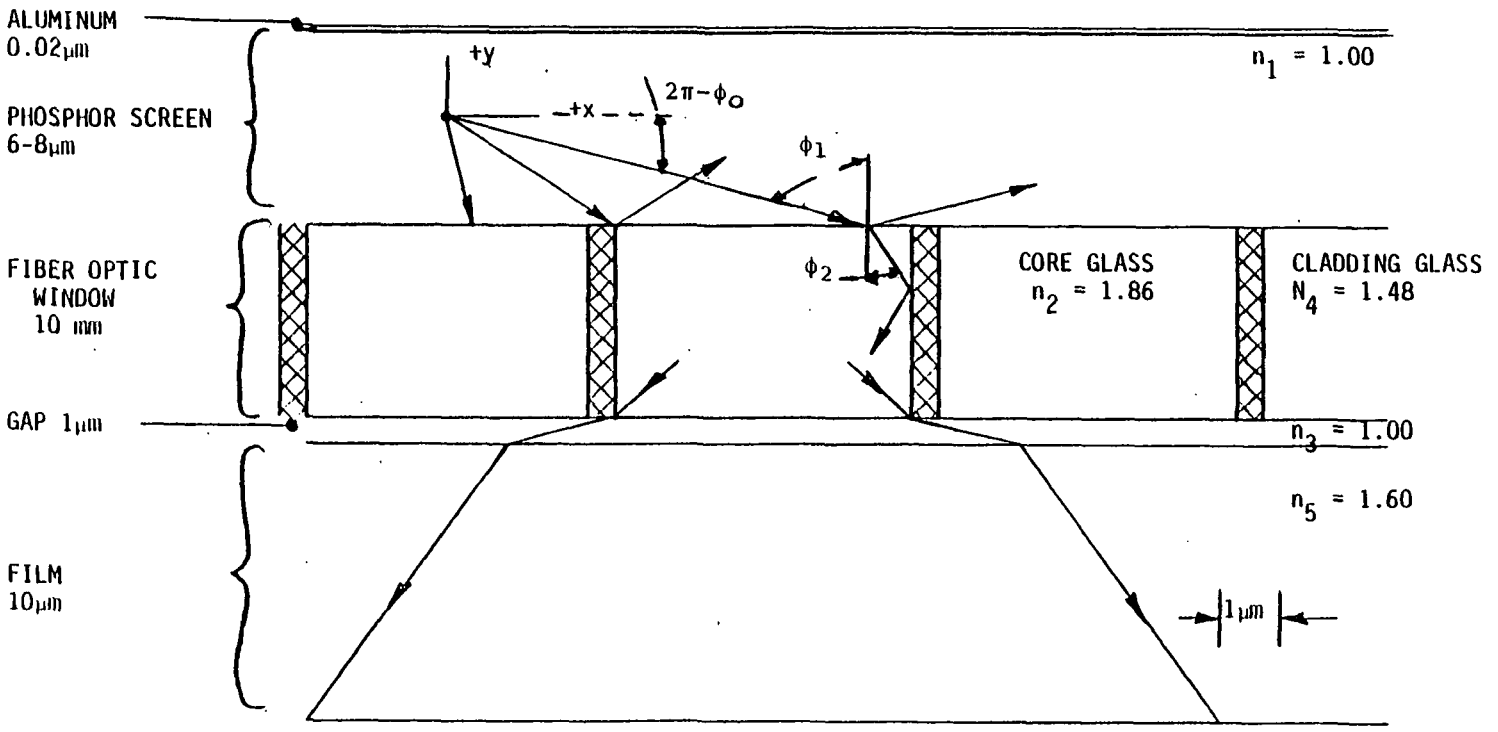

Figure 2.1-1. Section View of Fiber Optic - Film Interface. Fiber Optic Window Thickness is Not to Scale.

The following three figures, 2.1.2-1, 2.1.2-2, and 2.1.2-3, are scanning electron micrographs of a high resolution, P20 phosphor screen as used in a non-intagliated, magnetically focused, image tube. The views show aluminized and non-aluminized phosphor screen areas. The third figure, 2.1.2-3 is a stereophotograph. The visual impression, when viewed stereo-optically, is a layer at least 5 micrometers thick.

Settled phosphor grains on fiber optic windows emit light into 2 pi steradians in good approximation to a cosine distribution. Figure 2.1.2-4 shows an example of the measured angular light distribution for a settled phosphor screen. A second curve is for a theoretical phosphor material in complete optical contact; the resulting distribution is forward peaked. Because the measured results correspond to the no-optical contact case, the implication is that settled phosphor screens are not in optical contact with their windows; that light is incident onto the window from vacuum, not phosphor.

2.1.3 Fiber Optic Window

The substrate for the phosphor screen is the fiber optic window. This window is an array of glass fibers of high refractive index, each fiber clad with low refractive index glass. Groups of clad fibers are fused into a vacuum tight block. The block is cut perpendicular to the fibers to form a blank window. The blank window is ground and polished into its final shape. Windows used on image tubes usually have fibers in a 6 micrometer center-to-center hexagonal or square pack arrangement. Core glass index of refraction is typically 1.86, while the cladding glass is 1.48. These index values assure that virtually all light entering the end of a fiber will be totally reflected at the core-clad interface. The theoretical numerical aperature for meridonal rays, rays which intersect the fiber axis, is

$$NA = [\ n^2_{core} - n^2_{clad}\ ]^{0.5}$$

$$= (1.86^2 - 1.48^2)^{0.5}$$

$$= 1.13 > 1$$

It is highly desirable to use fiber plates that have unity or greater numerical apertures in high resolution image tubes. If the numerical aperture is less than unity, there exists a range of incident angles phi: $phi < phi_m <= pi/2$, $\sin(phi_m) = NA$, for which the rays propagate laterally in the fiber plate. These rays enter at too great an angle for total internal reflection at the core-cladding interface. They cross cladding layers and adjacent fibers eventually exiting many fibers distant from their entrance. Extra-mural absorption (EMA) material is included in the faceplate matrix to reduce the transmission of these rays. However, in 6 micrometer fiber plates, the amount of material that can be used is very limited.

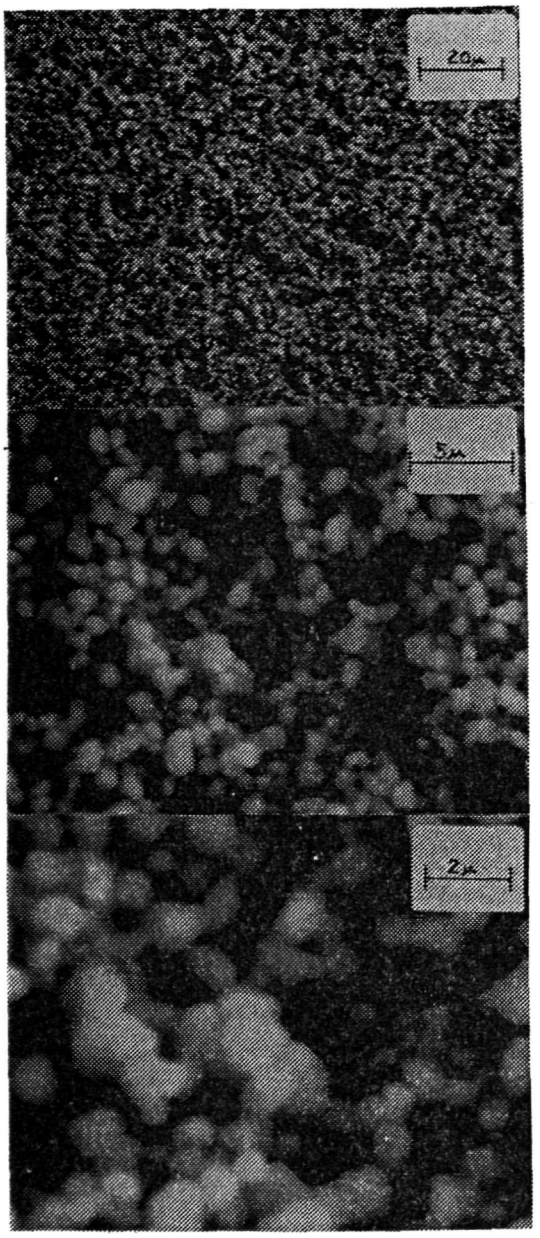

Figure 2.1.2-1. P20 Phosphor Screen of the Type Used in ITT Model F4089, 40 mm Magnetic Focus Image Tubes (Aluminized Side).

This is the view of the aluminized side of the screen. The incident energy was 20 keV onto the aluminum. The electrons passed through the aluminum and struck the phosphor grains. The image is the resulting pattern of secondary electrons collected in the scanning electron microscope detector. The thickness of the aluminum film is equivalent to 100 eV energy loss for 20 keV electrons.

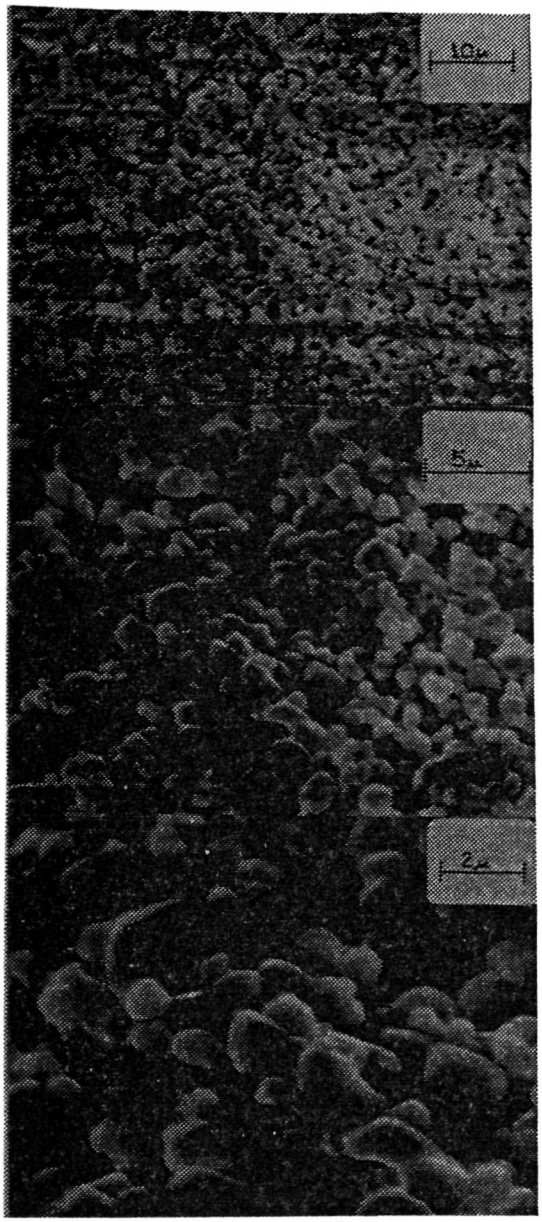

Figure 2.1.2-2. P20 Phosphor Screen of the Type Used in ITT Model F4089, 40 mm Magnetic Focus Image Tubes (Non-Aluminized Region).

This is the view of the phosphor screen in a region where it was not aluminized. The incident energy was 20 keV onto the phosphor. The image is the resulting pattern of secondary electrons collected in the scanning electron microscope detector. The streaks in the pictures are thought to be electrostatic charging of the phosphor grains. Normal SEM practice is to evaporate a thin film of gold onto the scanned object to minimize charging. No conductive coating was used here.

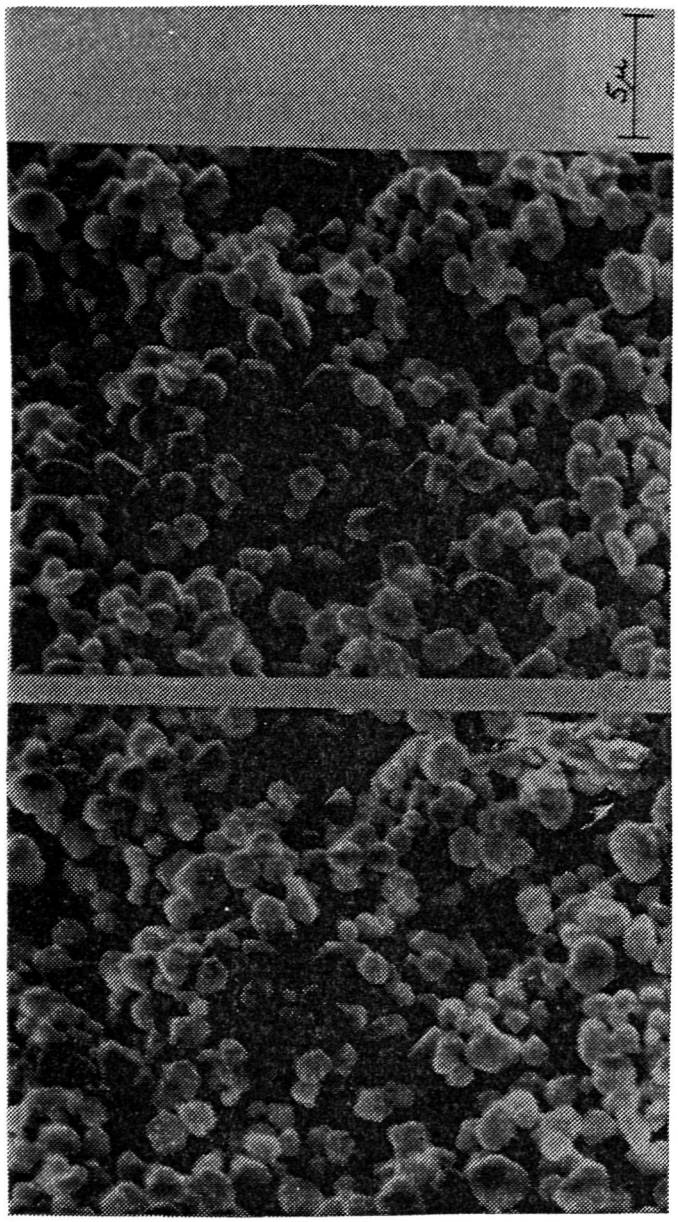

Figure 2.1.2-3. Stereographic View of P20 Phosphor Screen of the Type Used in ITT Model F4089, 40 mm Magnetic Focus Image Tubes (Non-Aluminized Region).

This is a stereographic view of the phosphor screen in a region where it was not aluminized. The sample was tilted 6 degrees between photographs. The incident energy was 20 keV onto the phosphor. The image is the resulting pattern of secondary electrons collected in the scanning electron microscope detector. The streaks in the pictures are thought to be electrostatic charging of the phosphor grains. Normal SEM practice is to evaporate a thin film of gold onto the scanned object to minimize charging. No conductive coating was used here.

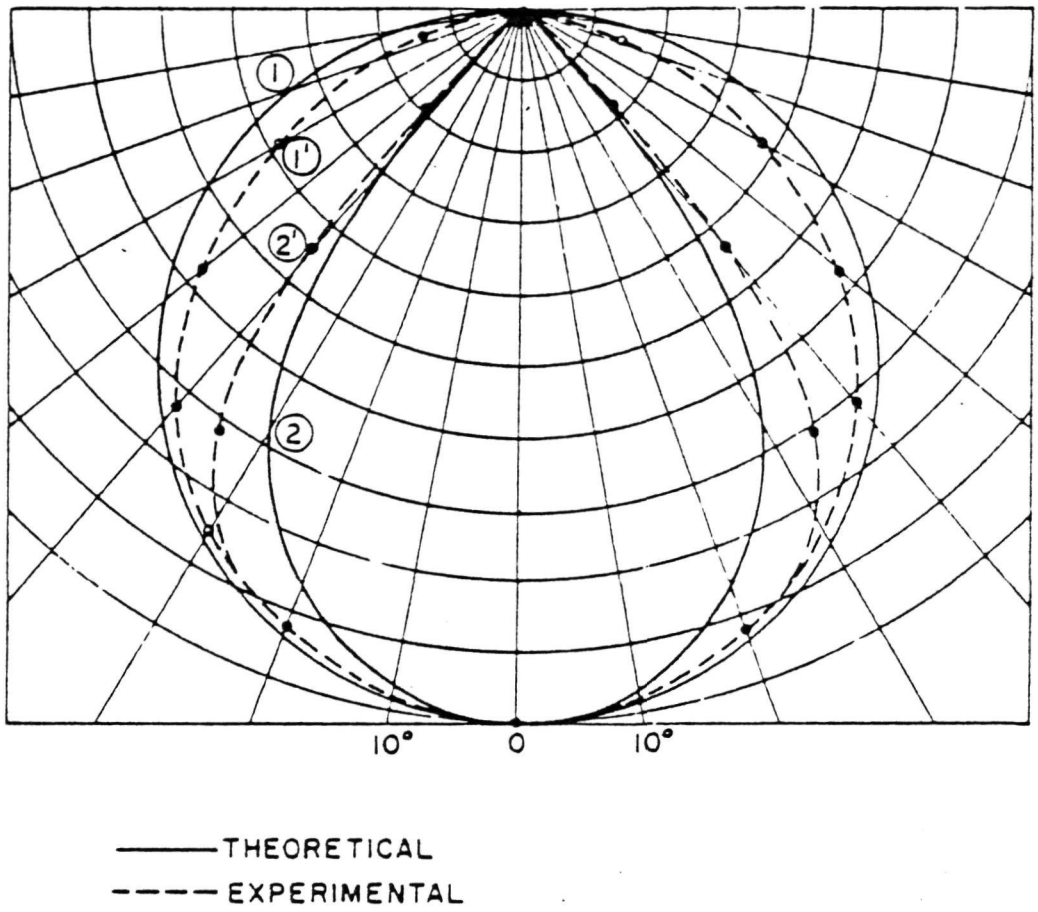

Figure 2.1.2-4. Angular Distribution of Energy Emitted by Phosphors: (1) Theoretical, No Optical Contact: (2) Theoretical, Complete Optical Contact: (1') Experimental, Settled Phosphor; and (2') Experimental, Transparent Phosphor.

A fiber collects and transmits light entering at $phi < phi_m$ in proportion to $(NA)^2$. Therefore, plates having fibers with NA = 0.93 and NA = 0.70 collect 86 and 49 percent of the amount of light collected by a NA = 1.0 plate. A NA = 1.0 plate collects all light in 2 pi steradians except for web and reflection losses.

The remaining portion of the light, 14 and 51 percent, represents rays outside the acceptance angle of the fibers. The result, for NA < 1 plates, is a cone of diffuse light in the plate whose most extreme rays are at a radius given by:

$$R = \frac{d_1 T}{d_2 \tan(pi/2 - phi_2) + d_3 \tan(phi_4)}$$

where T = 10 mm, thickness of the fiber plate.

$d_1 = d_2 + d_3$, 6 micrometers, the center-to-center spacing of the fiber

d_2 = 5.5 micrometers, diameter of the core glass

d_3 = 0.5 micrometers, thickness of the cladding glass

$n_1 \sin(phi_1) = n_2 \sin(phi_2)$

$n_2 \sin(pi/2 - phi_2) = n_4 \sin(phi_4)$

phi_1 = incident angle onto the faceplate

phi_2 = angle in core glass

phi_4 = angle in cladding glass

$n_1 = 1.0$

$n_2 = 1.75$ (NA = 0.93)

$= 1.64$ (NA = 0.70)

$n_4 = 1.48$

Figure 2.1.3-1 shows R versus phi_1 for several numerical aperture fiber plates. Note, the radius of the diffuse cone of light can be as large as several millimeters.

A more detailed argument would contain reflection and transmission effects on these lateral rays, plus an estimate of their distribution. More details do not change the conclusion: NA > = 1 fibers are highly desirable to control stray light.

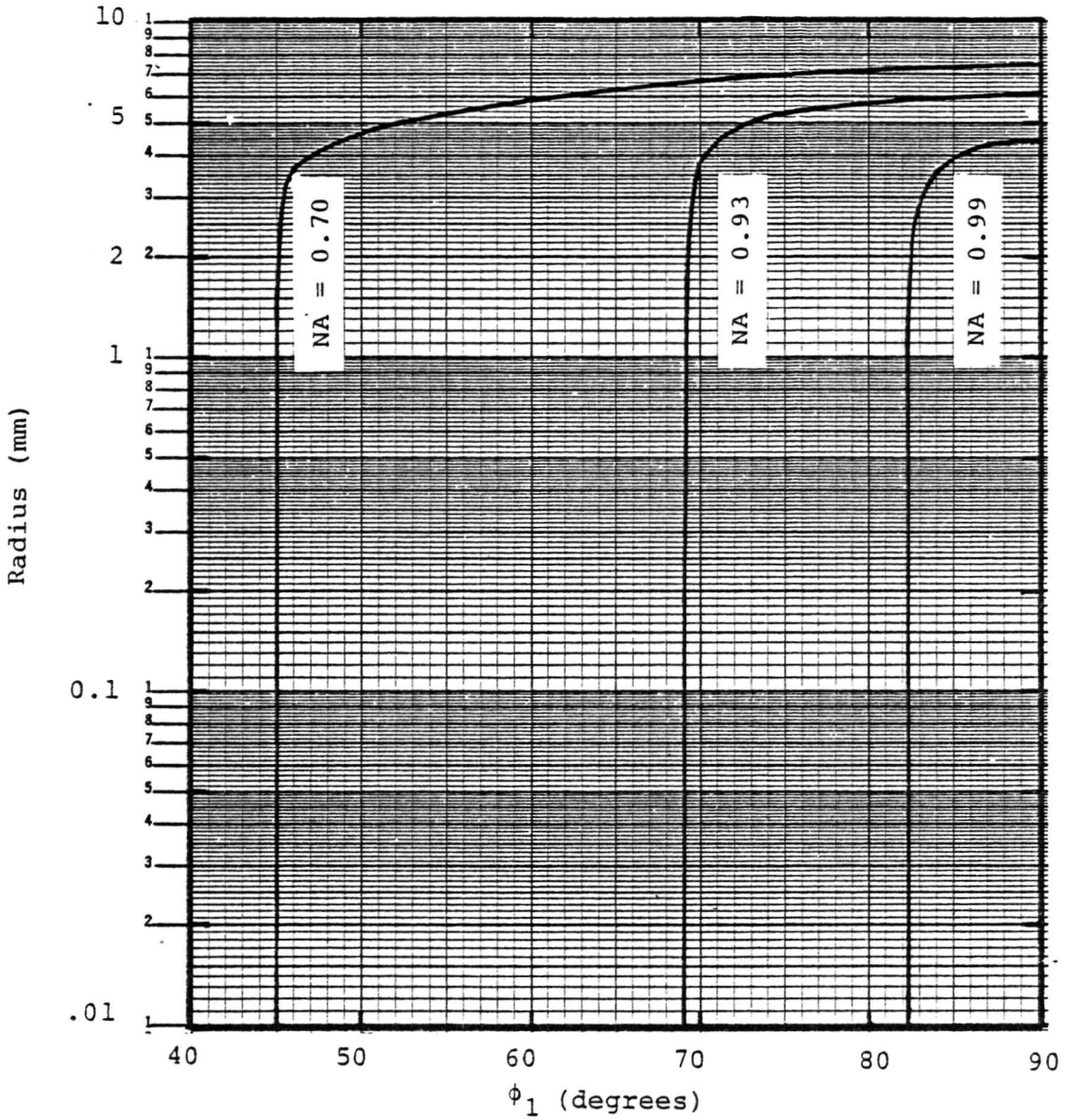

Figure 2.1.3-1. Diffuse Light Cone Radius Versus Incident Ray Angle for Several NA <1.

$T = 10mm$ $\quad d_3 = 0.5\mu m$

$d_1 = 6\mu m$ $\quad n_1 = 1.00$

$d_2 = 5.5\mu m$ $\quad n_2 = 1.781, 1.75, 1.64$

$n_4 = 1.48$

$$\phi_m \leq \phi_1 \leq 90$$

$$\sin\phi_m = NA = [n_2^2 - n_4^2]^{\frac{1}{2}}$$

2.1.4 Rays Exiting the Fiber Optic Faceplate

Ideally, a ray entering a fiber of a plane parallel plate at an angle phi will also leave the fiber at an angle phi. However, the azimuthal angle on leaving varies so rapidly with phi, plate thickness, fiber diameter, entrance position on the fiber, and so forth, that for all practical purposes the transmitted rays will spread to fill an annular cone of half angle phi. At some quite predictable distance (*) from the faceplate, the interior of this cone of rays becomes dark. The output of the fiber optic plate is the superposition of all light rays from all of the cones, for all angles phi, and for all fibers in the plate.

2.1.5 Photographic Film

The last element of the physical description of the image tube and film interface is the film. Photographic films have finite thickness. It is perhaps better to speak of the image being stored "in" not "on" the film. Scientific emulsions are 10 to 15 micrometers thick. High resolution aerial reconnaissance emulsions are 4 to 6 micrometers thick. Both film types usually have a 1 micrometer thick overcoat on the emulsion to protect it from damage such as scratches.

A film is sensitive to light over a full 2 pi steradian solid angle although the response may be modulated by cos (phi) for large incidence angles.

The index of refraction of the emulsion is 1.60, determined mainly by the gelatin and modified by the silver halide crystals.

2.2 RAY TRACE MODEL OF THE IMAGE TUBE - FILM INTERFACE (Reference 1)

The previous study created an analytical model of the image tube film interface based upon the preceding description of the physical hardware. The analytical model was used to estimate the line spread function and MTF of the image tube output when observed using low numerical aperture means such as a microscope objective lens and high numerical aperture means such as photographic film in contact with the fiber optic window. Figure 2.2-1 shows the geometrical arrangement used in the analytical model. The figure shows a fiber centered line of light incident onto the fibers in a fiber optic faceplate.

2.2.1 Ray Trace Model Results for the Microscopic Lens Case

Figure 2.2.1-1 shows a line spread function obtained when the model contains a microscope objective lens with numerical aperture 0.25. This line spread is the sum of two terms: the line spread at section AA and at section BB of Figure 2.2-1. The two separate line spread components are shown in Figure 2.2.1-2. The minor asymmetries are computer plotter limitations.

* The distance depends upon the diameter of the bundle rays and diameter of the fibers.

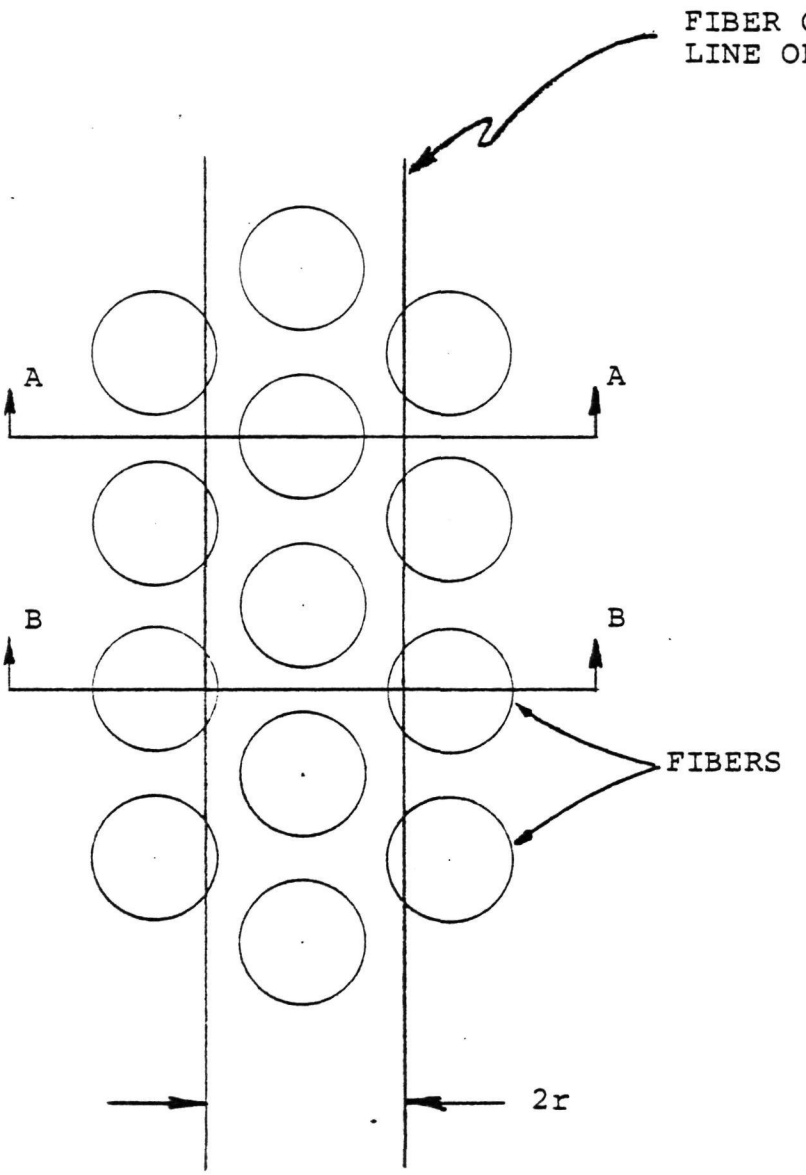

Figure 2.2-1. Geometrical Relationship Between Illumination and Fibers

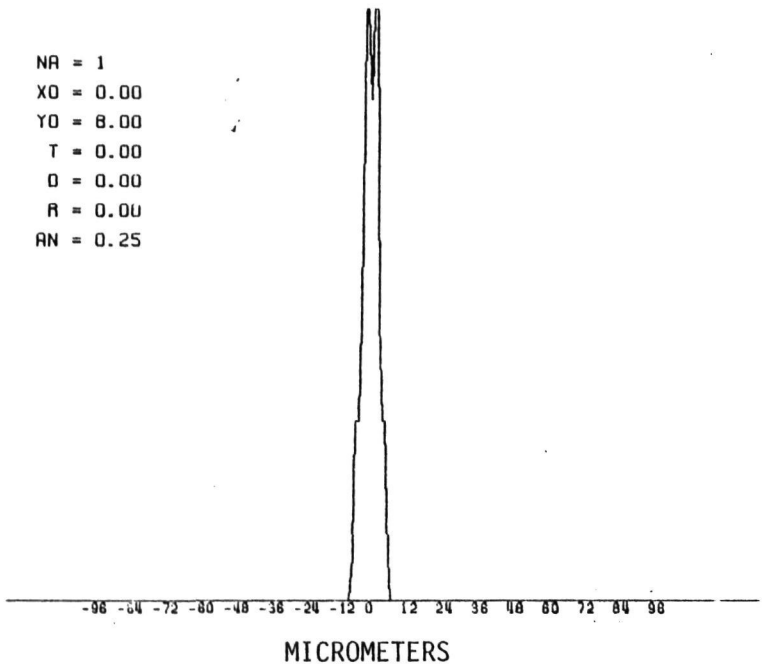

Figure 2.2.1-1. Line Spread Function Calculated for NA = 0.25 Microscope Objective Lens Case.

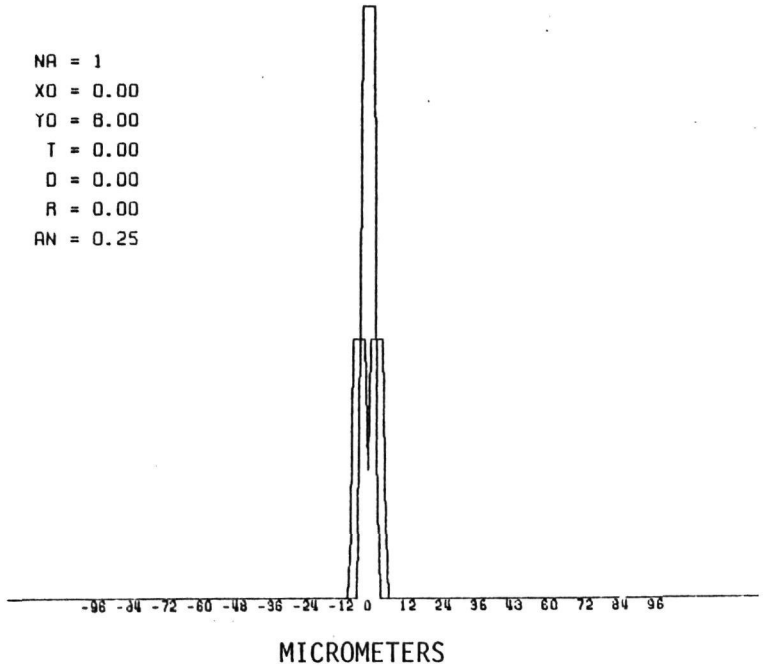

Figure 2.2.1-2. Line Spread Function Components Calculated for NA = 0.25 Microscope Objective Lens Case. Sections AA and BB of Figure 2.2-1.

Figures 2.2.1-3 and 2.2.1-4 show the corresponding MTF curves for the combined line spread and for the two separate components.

These calculated line spread functions are not as wide as usually observed in the microscope. Usually, several fibers are illuminated even for the narrowest of input lines. (*) This difference between model and hardware can be explained in part by the source size used in this calculation, i.e., a point source located 8 micrometers above the entrance of the faceplate. Figure 2.2.1-5 shows the results calculated for finite sized source, r = 2 micrometers. Careful examination shows an additional amount of energy at the base of the line spread.

Scattering and refraction of rays by the individual phosphor grains also broaden the line spread. These properties are not in the model.

Using microscopes and bar chart test patterns under tube test conditions, single stage magnetic focus image tubes exhibit 80 - 90 lp/mm, limiting spatial frequency, at a few percent modulation. This experimental data is plotted on Figures 2.2.1-3 and 2.2.1-4.

2.2.2 Calculated Film Results

Figure 2.2.2-1 represents the line spread and MTF at 5 micrometer depth in film. A small faceplate to film gap of 0.5 micrometer has been assumed. The source, at 8 micrometer and r = 2 micrometer size, is the same as used in one of the microscope lens cases. The fine structures on the line spread are the calculated contributions caused by the individual fibers. Film effectively has a very large numerical aperture, approximately 1.0. There are non-zero contributions to the line spread out to +/- 96 micrometers from the center of the line.

It is tempting to think much of the in film line spread width is because of the film thickness (5 micrometers) and the gap (0.5 micrometers). This is not so. Such small gaps and thicknesses have very little affect upon a line spread of the size shown here. Figure 2.2.2-2 is a case in which the film thickness and gap thickness are zero. There is very little change from Figure 2.2.2-1.

A more significant change in the line spread function can be obtained by modeling a thinner phosphor screen, assuming such a screen is physically realizable. Figure 2.2.2-3 is the line spread calculated for a source 4 micrometer above the fiber optic window. It is a narrower and, more importantly, there is much less energy at large distances from the center of the line.

* A most startling exception to this generally observed line shape occurred with the 10 micrometer intagliated plate in the specially built image tube. The individually illuminated fibers were clearly seen with remarkably dark neighboring fibers. See Sections 2.3.2, 3.1.1, and 3.2.2.

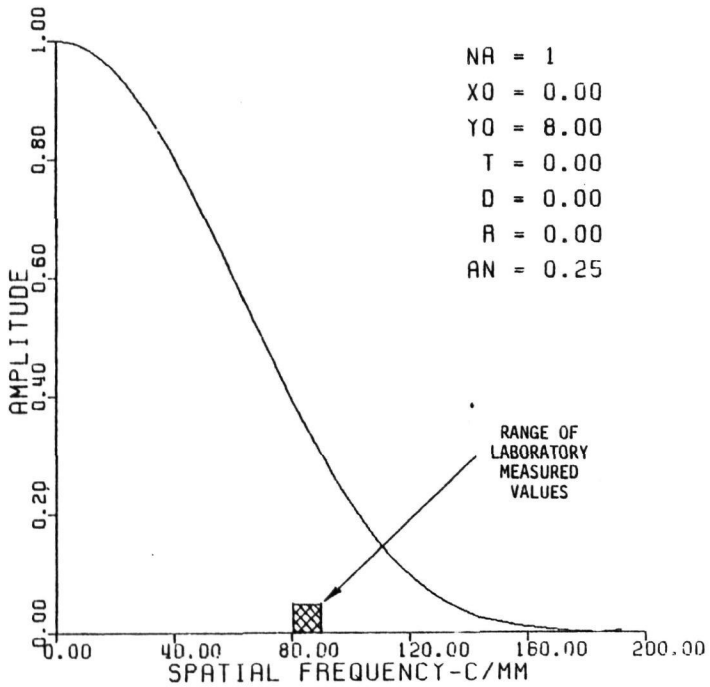

Figure 2.2.1-3. MTF Calculated for NA = 0.25 Microscope Objective Lens Case.

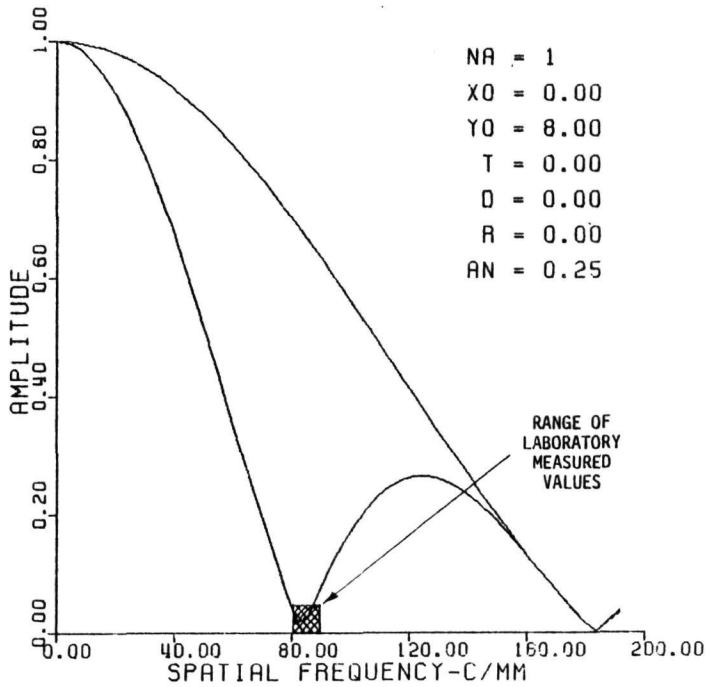

Figure 2.2.1-4. MTF Components Calculated for NA = 0.25 Microscope Objective Lens Case. Sections AA and BB of Figure 2.2-1.

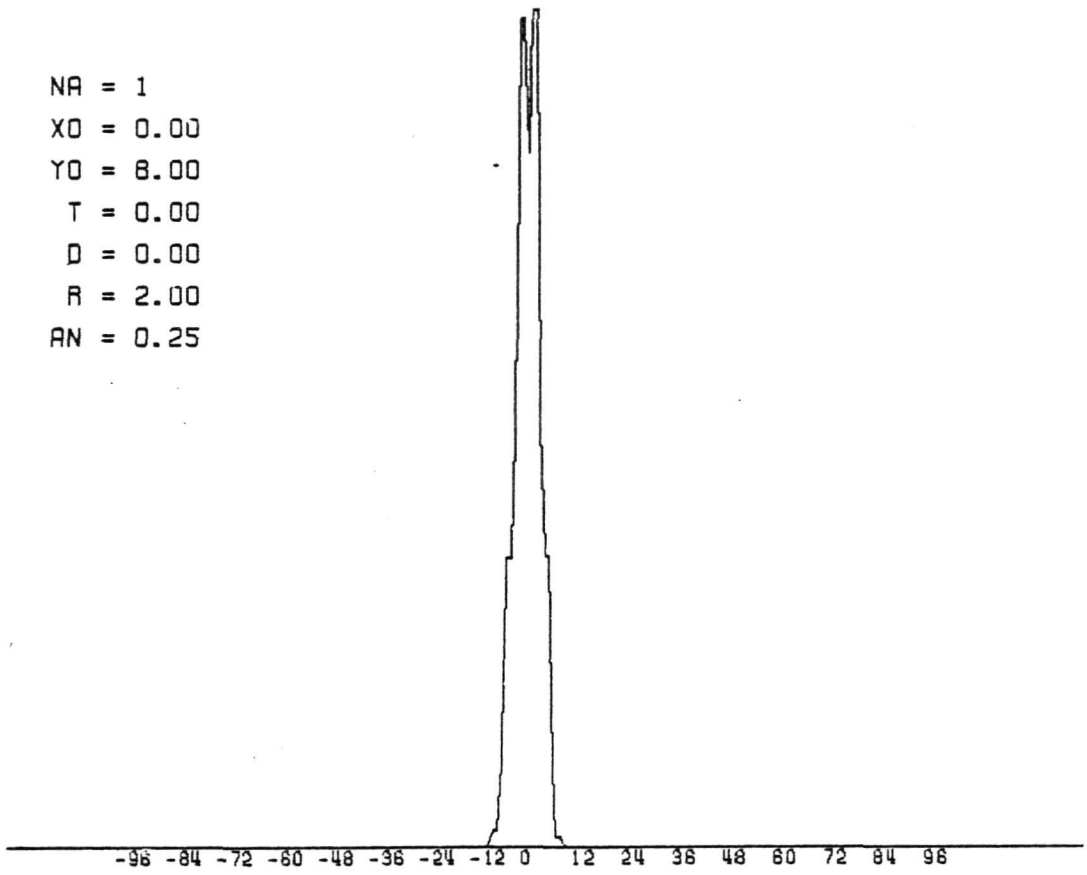

Figure 2.2.1-5. Line Spread Function Calculated for NA = 0.25 Microscope Objective Lens Case With Finite Source Size, r = 2 micrometers.

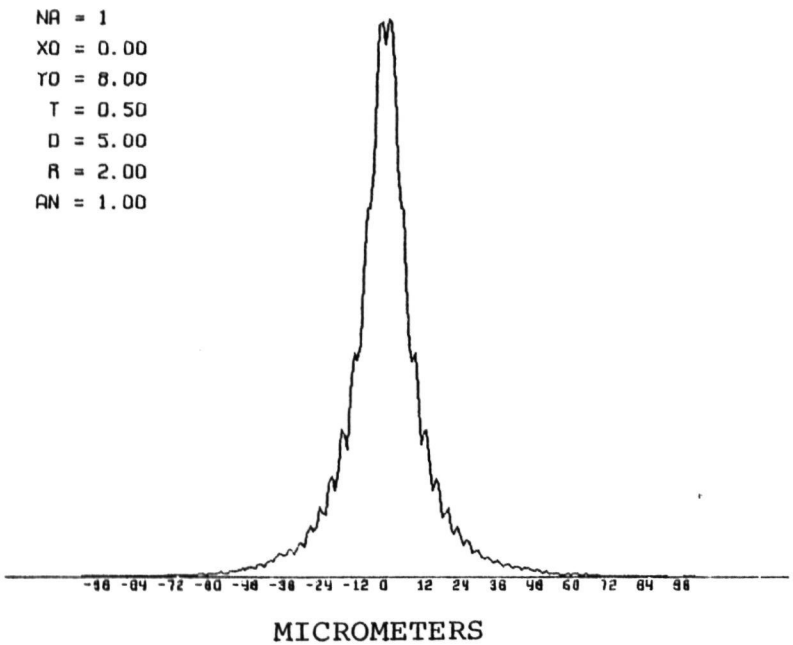

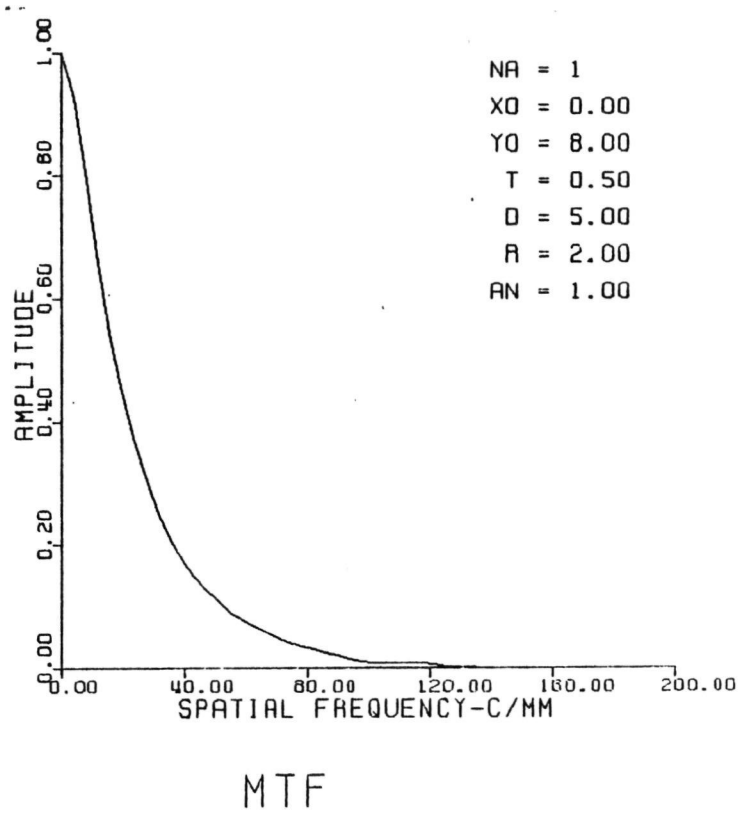

Figure 2.2.2-1. Line Spread Function and MTF Calculated for Image Tube and Film Combination Using r = 2 Micrometer Source and 5 Micrometer Depth in Film.

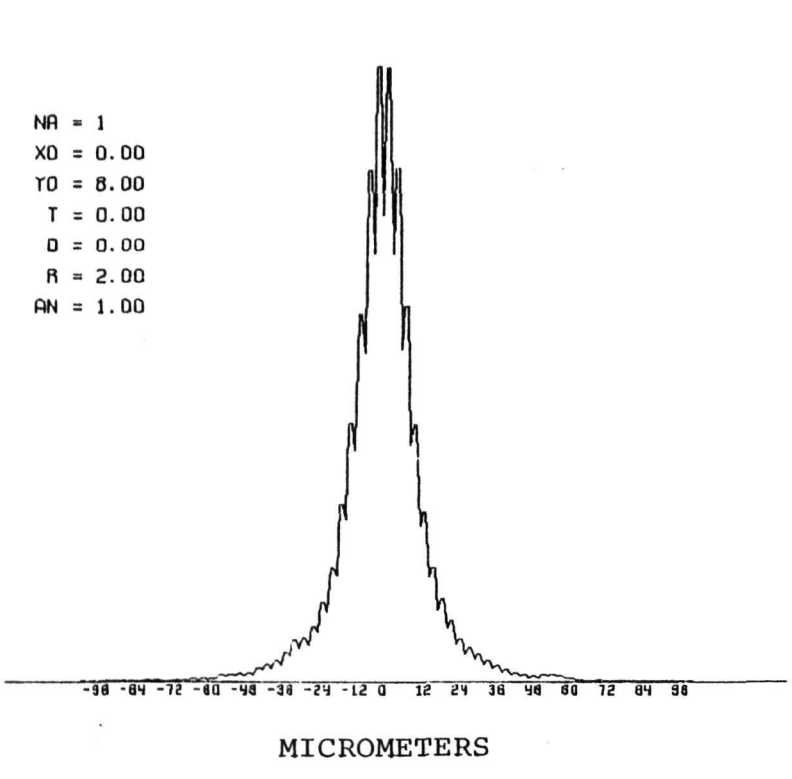

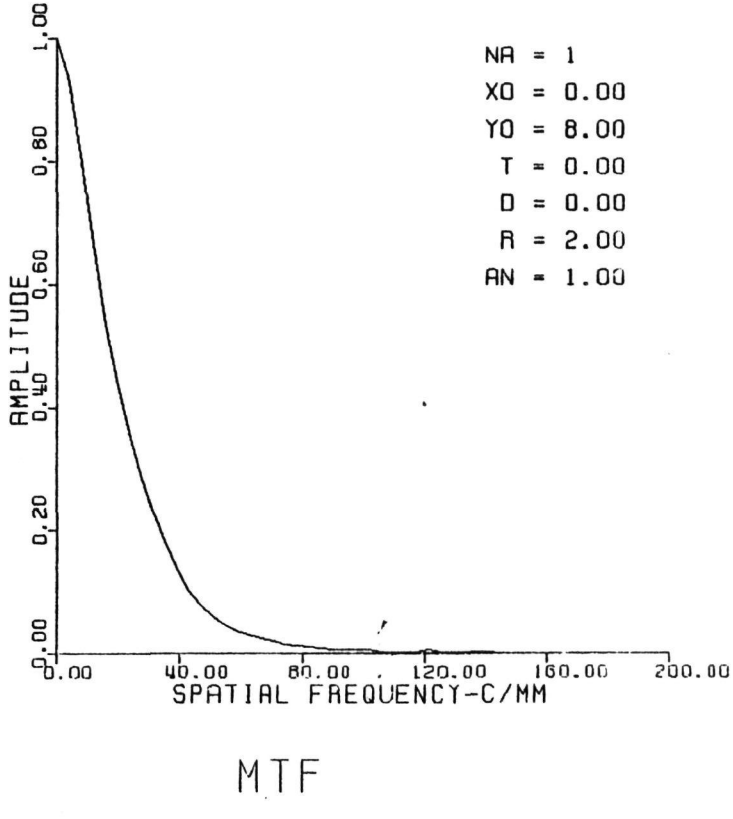

Figure 2.2.2-2. Line Spread Function and MTF Calculated for Image Tube and Film Combination Using r = 2 Micrometer Source and Zero Thickness Film and Gap.

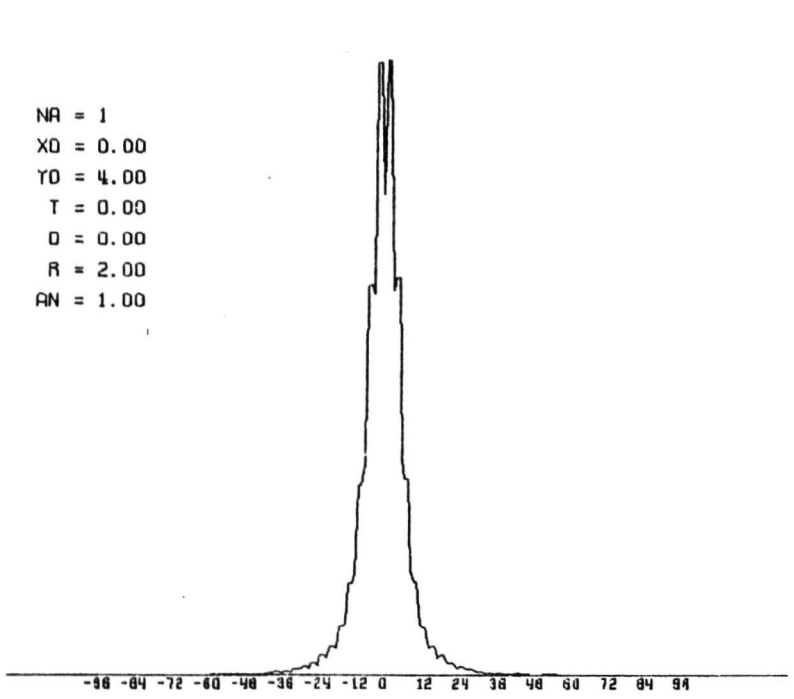

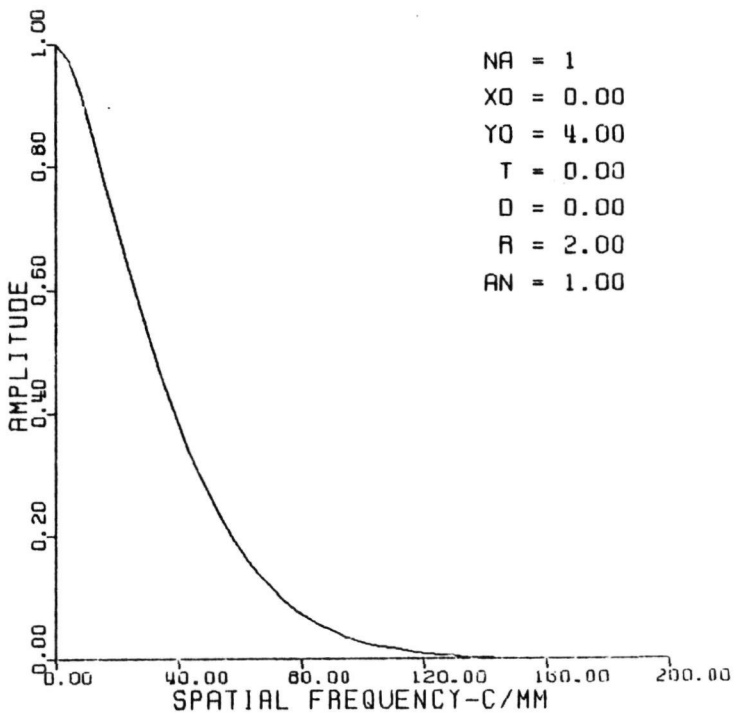

Figure 2.2.2-3. Line Spread Function and MTF Calculated for Image Tube and Film Combination Using r = 2 Micrometer Source, Zero Thickness Film and Gap and Thin Phosphor Screen.

2.2.3 Analytical Model Conclusions

Examination of the output of an image tube using a microscope will give narrower line spread images or better MTF response than the same tube used with film.

Film emulsion, overcoat thickness, and gap between the faceplate and film do not seem to be major contributors to the resolution loss.

The cause of the resolution loss seems to be a consequence of the large numerical aperture fiber optic faceplate, the sensitivity of film to light rays at large incidence angles, and the existence of large incidence angle rays in the phosphor screen. It is also likely that scattering in the screen plays a role.

Figure 2.2.3-1 shows a diagram of the process. In Figure 2.2.3-1A, the source is directly above and centered on a fiber, fiber 0. Rays that enter fiber 0 expose the film directly beneath fiber 0 and also, to a degree, the film under fiber 1 (and -1). Figure 2.2.3-1B shows what happens to rays from the source which strike fiber 1. These rays not only expose the film under fiber 1, but also the area under fibers 0 and 2. Figure 2.2.3-1C extends the discussion to rays entering fiber 2, 15 micrometers from the center of the source. These rays expose film under fibers 1 and 3 at a distance of more than 20 micrometers from the center of the source.

Rays making an angle greater than phi = arcsin (0.25) = 14 degrees do not pass the microscope lens.

Scattering in the phosphor layer results in an effectively larger source than the individual phosphor grains. Scattering also causes a range of incidence angles from 0 to pi/2 onto fibers adjacent to the central fiber.

Examination of Figures 2.1.2-1, 2.1.2-2, 2.1.2-3, the SEM photos of a phosphor screen, leaves little doubt that there is room for light to propagate laterally through the screen for several fiber diameters without being intercepted by a phosphor grain. Furthermore, phosphor grains are of necessity transparent to their own radiation. Therefore, even if a ray is intercepted, it will be refracted to a new direction, not greatly absorbed. The structure of the phosphor screen permits lateral light propagation.

On the basis of this model, it seems that control of the lateral rays in the phosphor layer is an important means to improve image tube film resolution. For this reason, an image tube with an intagliated phosphor screen (reference 4) and fiber optic window was proposed and this study program created.

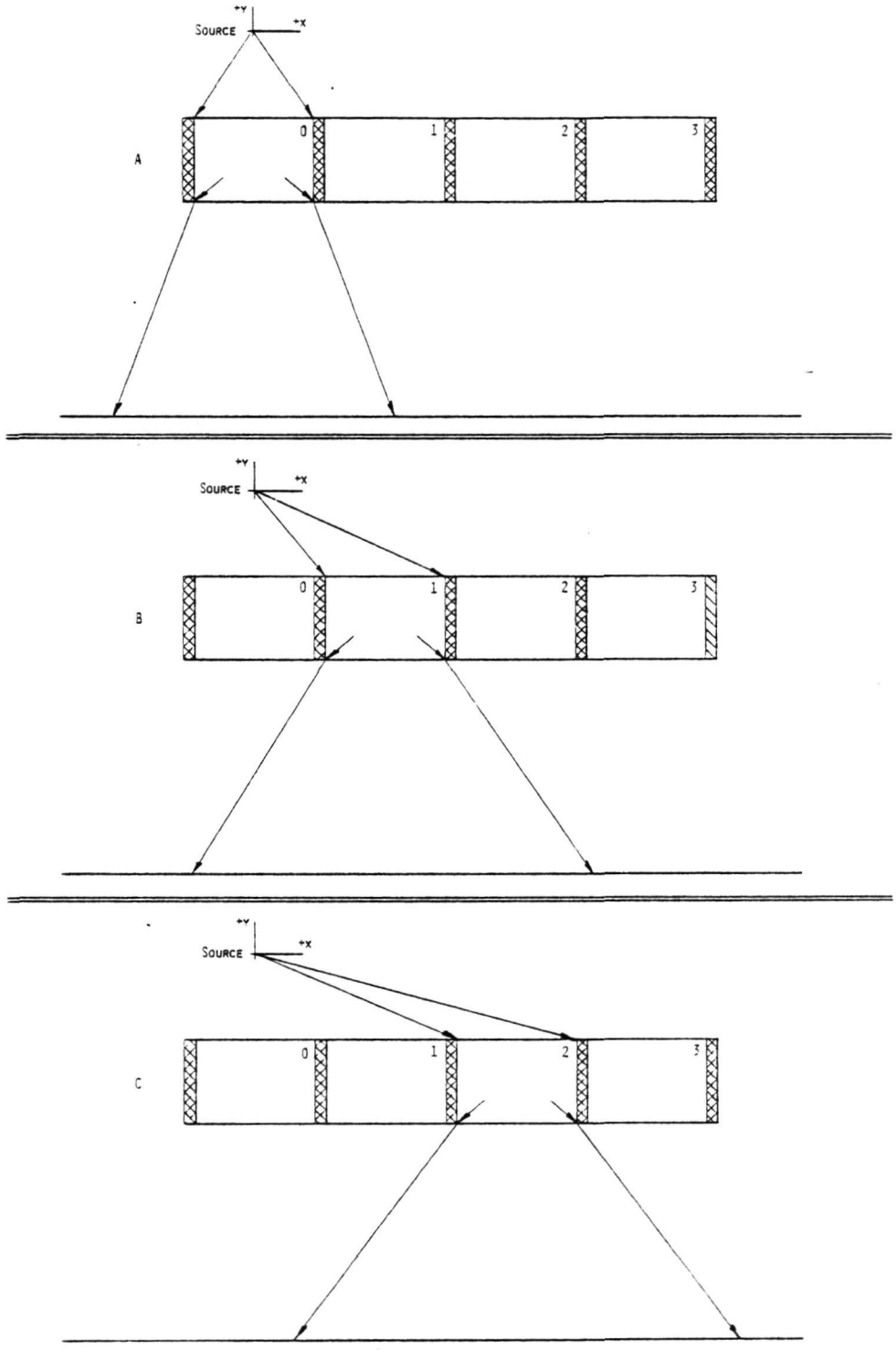

Figure 2.2.3-1. Cause of Resolution Loss in I^2 - Film Systems Using Large NA Fiber Optic Plates. Rays from the Source can Expose Portions of the Film at a Long Distance from the Source and from the Fiber Illuminated by a Ray from the Source.

2.3 INTAGLIATED FIBER OPTIC IMAGE TUBE

A major task on this contract was the construction of a magnetic focus image tube with an intagliated phosphor screen on a fiber optic window. Such a tube was constructed by ITT in their Electro-Optical Products Division (ITT-EOPD) at Fort Wayne, Indiana. ITT-EOPD used their F4089 40 mm image intensifier tube as the basic device. Two intagliated screens were incorporated in the one tube. The two screens were on plates having different fiber sizes; one was 6 micrometers and the other was 10 micrometers. The intagliation and deposition of the phosphor screens was done by ITT-EOPD in their Roanoke, Virginia facilities.

2.3.1 Phosphor Information

The fiber optic plates provided by ITT-EOPD Roanoke were for night vision goggles tubes. One of the plate's output surfaces had a sperical curvature to match to the optics for which the goggles tubes were designed. This curved surface was not acceptable for contact film work, so the plates were ground flat. As it happened, the grinding did not take place until after the intagliation had occurred. There is no reason to believe that the phosphor screens suffered from the extra handling.

Earlier intagliation efforts at Roanoke had produced P20 phosphor assemblies just meeting minimum screen efficiency requirements. There was concern whether or not the measured data was based on correctly calibrated standards, because intagliaged phosphors can have lower efficiency than conventional phosphors.

An exchange of image tubes between ITT-EOPD at Roanoke and Fort Wayne resulted in conflicting efficiency data. The problems associated with absolute efficiency measurement were never wholly resolved. However, all the phosphor data presented in this report were taken on the same setup and are consistent on a relative scale.

Six screen assemblies were made; four were deemed acceptable for efficiency and general appearance. There were two twister (*) plates (10 micrometer fiber spacing) and two straight plates (6 micrometer fiber spacing). In a demountable test at 6 kV, each pair of plates of the same fiber size had the same efficiency, but the twisters measured only half that of the straight plates. Strangely, this difference was not true in the completed tube. Based on visual inspection, assemblies No. 7 (straight) and No. 9 (twister) were selected for the image tube assembly.

The completed tube No. 068101A, with its two fiber optic output windows is shown in Figures 2.3.1-1 and 2.3.1-2. In Figure 2.3.1-1, it can be seen that the effective numerical aperture of the twisted (inverter) plate varies from the center (NA = 1.0) to the edge (NA nearly zero). This change is caused by the "waisting" of the outer

*Twister plates have the fiber bundle twisted 180 degrees from front to back to invert the image. See reference 2.

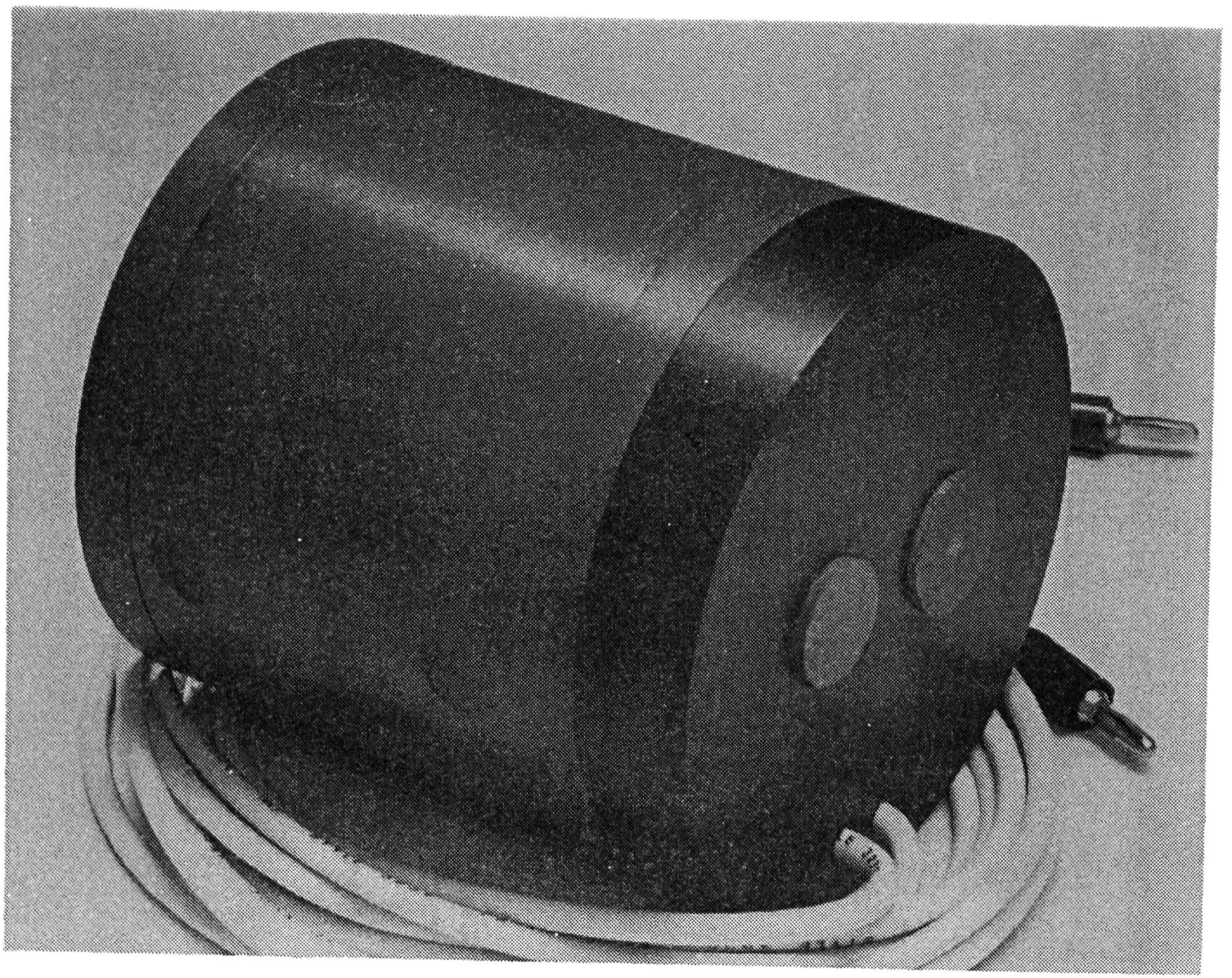

Figure 2.3.1-1. Potted Intagliated Phosphor Test Tube, F4089, No. 068101A.

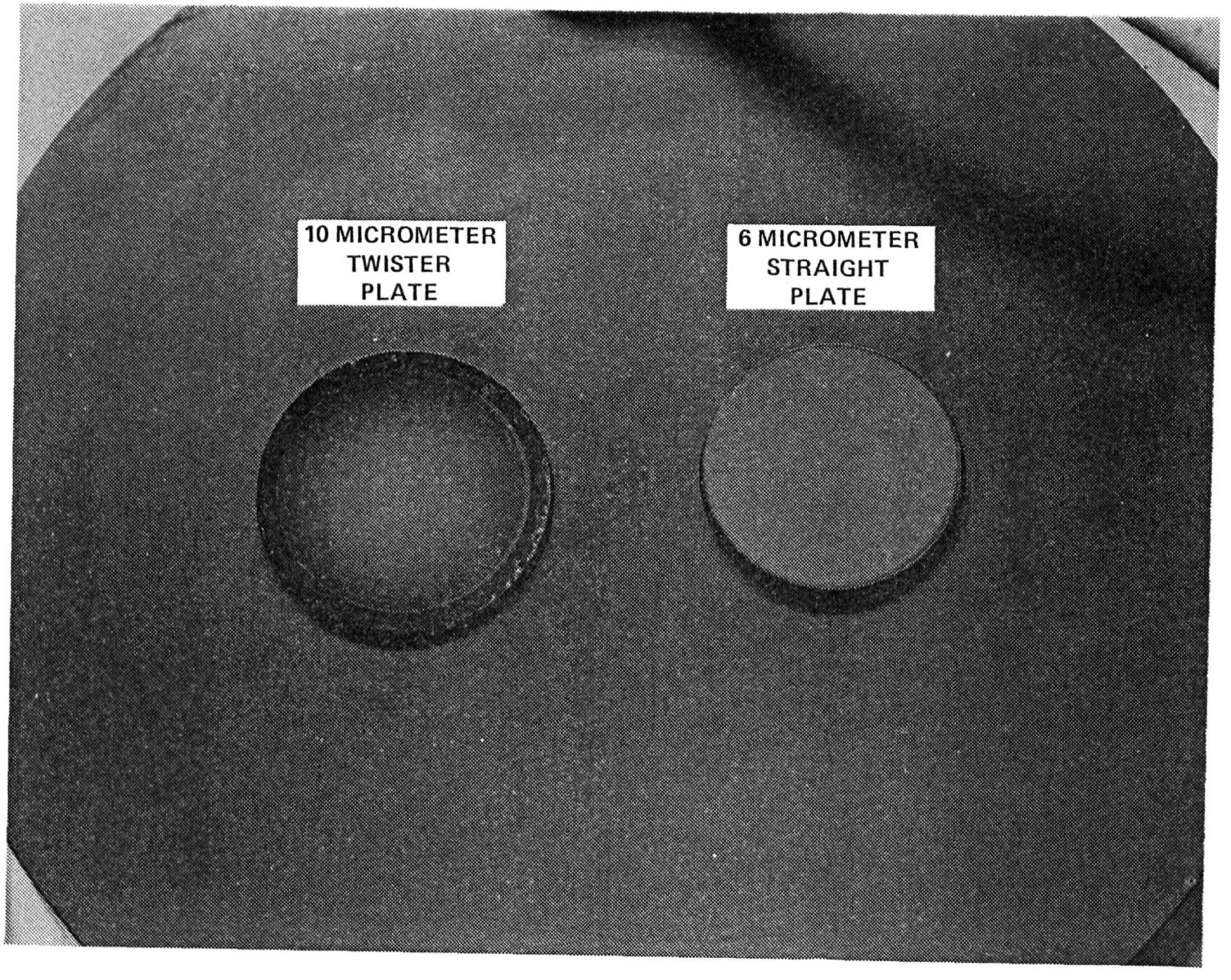

Figure 2.3.1-2. F4089 No. 068101A, Two 18 Micrometer Output Intagliated Phosphors

fibers when they are lengthened during the twisting process. It is necessary to pay attention to the physical location of the test image on the twister plate when making contact film measurements.

2.3.2 Tube Performance

The photocathode spectral response for the tube is shown in Figure 2.3.2-1. In Figure 2.3.2-2 shows the phosphor brightness measurements of the F4089's two intagliated fiber optic plates and a typical non-intagliated 6 micrometer F4089 phosphor assembly. The raw data and lumens per microampere values are shown in Table 2.3.2-1.

The variation in phosphor brightness across the 18 mircometer diameter of the plate with straight fibers was not clearly detectable in the test setup; this means it was less than 10 percent. Measurements of the twister plate were discontinued after reading Allan's comment (reference 2), because any measurement would seem to be highly dependent on the acceptance angle of the measuring system.

The visual limiting resolution of each of the two plates was nearly the same, and neither was the hoped for 80 - 90 lp/mm. The twister had 57 lp/mm and the straight plate 64 lp/mm. The twister produced an image of noticeably sharper contrast. This was also noted in subsequent MTF measurements; the dark areas appeared very dark.

At high magnification, what was certainly noticeable was the extra-mural absorption (EMA) rods of the fiber optic plate assembly. In coarse fiber optic plates, extra-mural absorption is accomplished by an extra sheath around the normally two part fiber. When the fiber-to-fiber spacing becomes 20 micrometers or less, as in the plates used in these experiments, the EMA sheath is replaced by absorbing rods among the fibers. These dark rods are easily seen in Figure 2.3.2-3, a photograph of the twister in F4089 No. 068101A. The illuminated circle of Figure 2.3.2-3 is 0.017 inch diameter. Shown in this figure, are some gray fibers, in which, presumably, there are fewer phosphor particles in the etched pits.

Figure 2.3.2-4 shows the phosphor output of the straight (6 micrometer spacing) fiber optic plate of F4089 No. 068101A. The arrangement of the EMA rods is the same as for the coarser plate, but it appears that the absorption is much less, at least the rods do not appear to be very black. What is disturbing is the multiplicity of blocked (black) fibers. The reason for these imperfections has not been determined but could be related to imperfections in the intagliation or deposition process. The scattered, but not really random arrangement, could also indicate a wrong piece of glass in one of the multi-bundles used to make the boule from which the plate was ultimately cut. As a result, core glass etchant did not work properly on this wrong piece of glass.

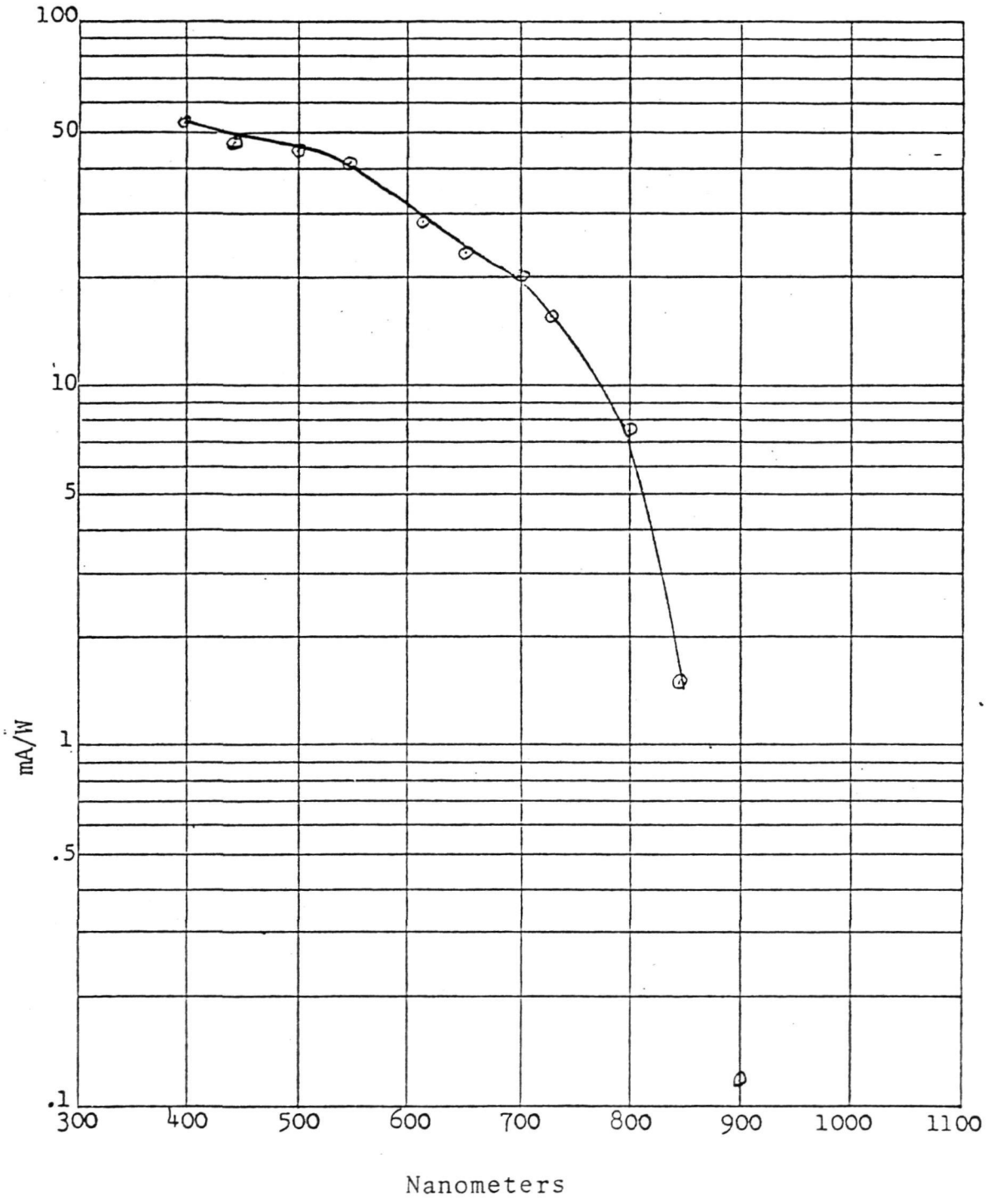

Figure 2.3.2-1. Photocathode Spectral Response F4089 No. 068101A.

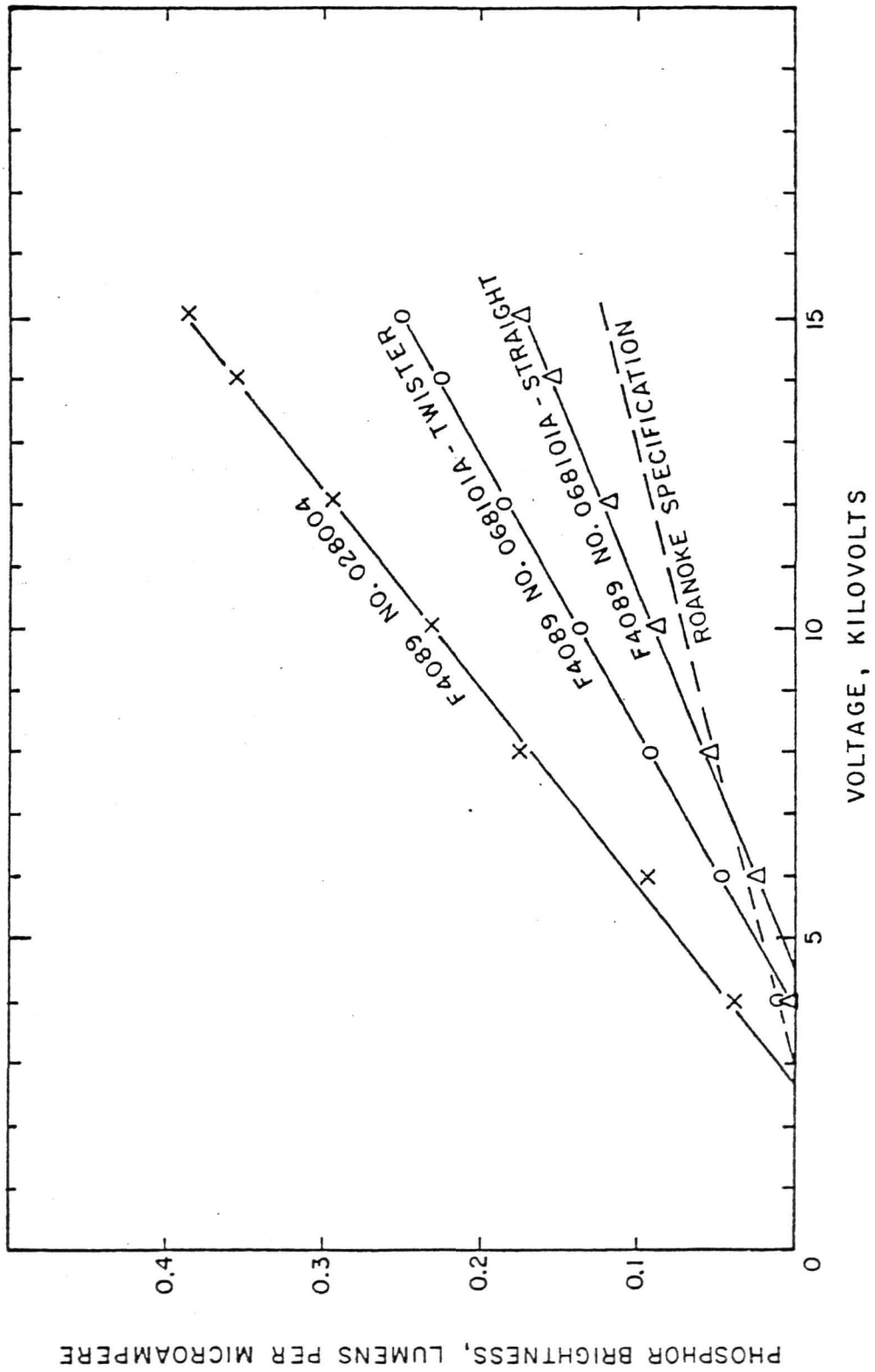

Figure 2.3.2-2. Phosphor Brightness Data

Table 2.3.2-1. Phosphor Brightness Data

PHOSPHOR VOLTAGE	F4089 NO. 068101A TWISTER		F4089 NO. 068101A STRAIGHT		F4089 NO. 28004	
	BRIGHTNESS[1]	BRIGHTNESS	BRIGHTNESS[1]	BRIGHTNESS	BRIGHTNESS[1]	BRIGHTNESS
KILOVOLTS	FOOT LAMBERTS	LUMEN/ μ A	FOOT LAMBERTS	LUMEN/μA	FOOT LAMBERTS	LUMEN/μA
15	0.0234	0.249	0.0162	0.172	0.71	0.387
14	0.0213	0.227	0.0144	0.153	0.65	0.354
12	0.0171	0.182	0.0111	0.118	0.54	0.294
10	0.0129	0.137	0.0080	0.085	0.42	0.229
8	0.0086	0.092	0.0050	0.053	0.32	0.174
6	0.0043	0.046	0.0023	0.024	0.17	0.093
4	0.0010	0.011	0.0005	0.005	0.07	0.038

[1] For 128 pA into a 0.5 inch diameter circle

[2] For 2.5 nA into a 0.5 inch diameter circle

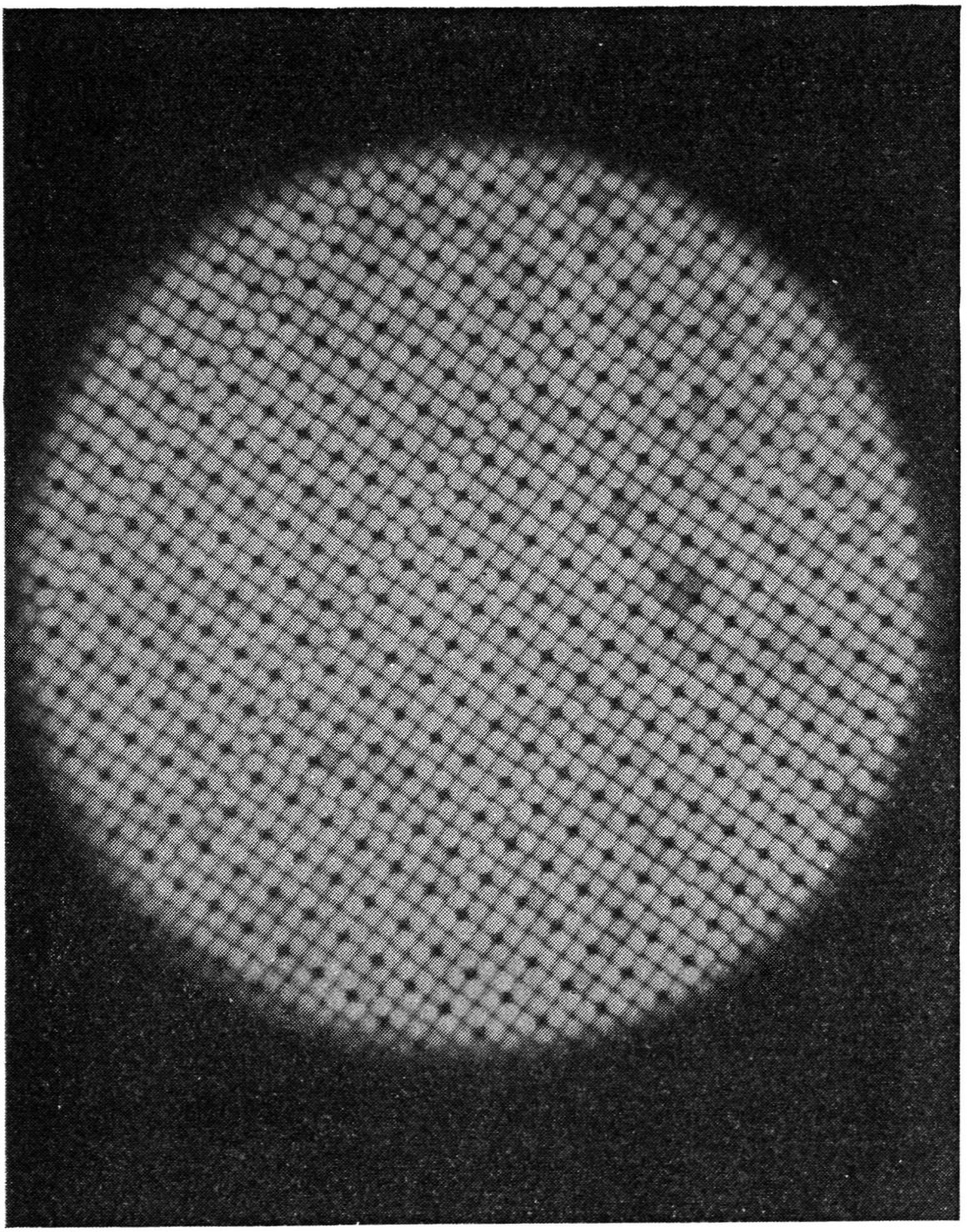

Figure 2.3.2-3. Illuminated 10 Micrometer Twister Fiber Plate, Intagliated

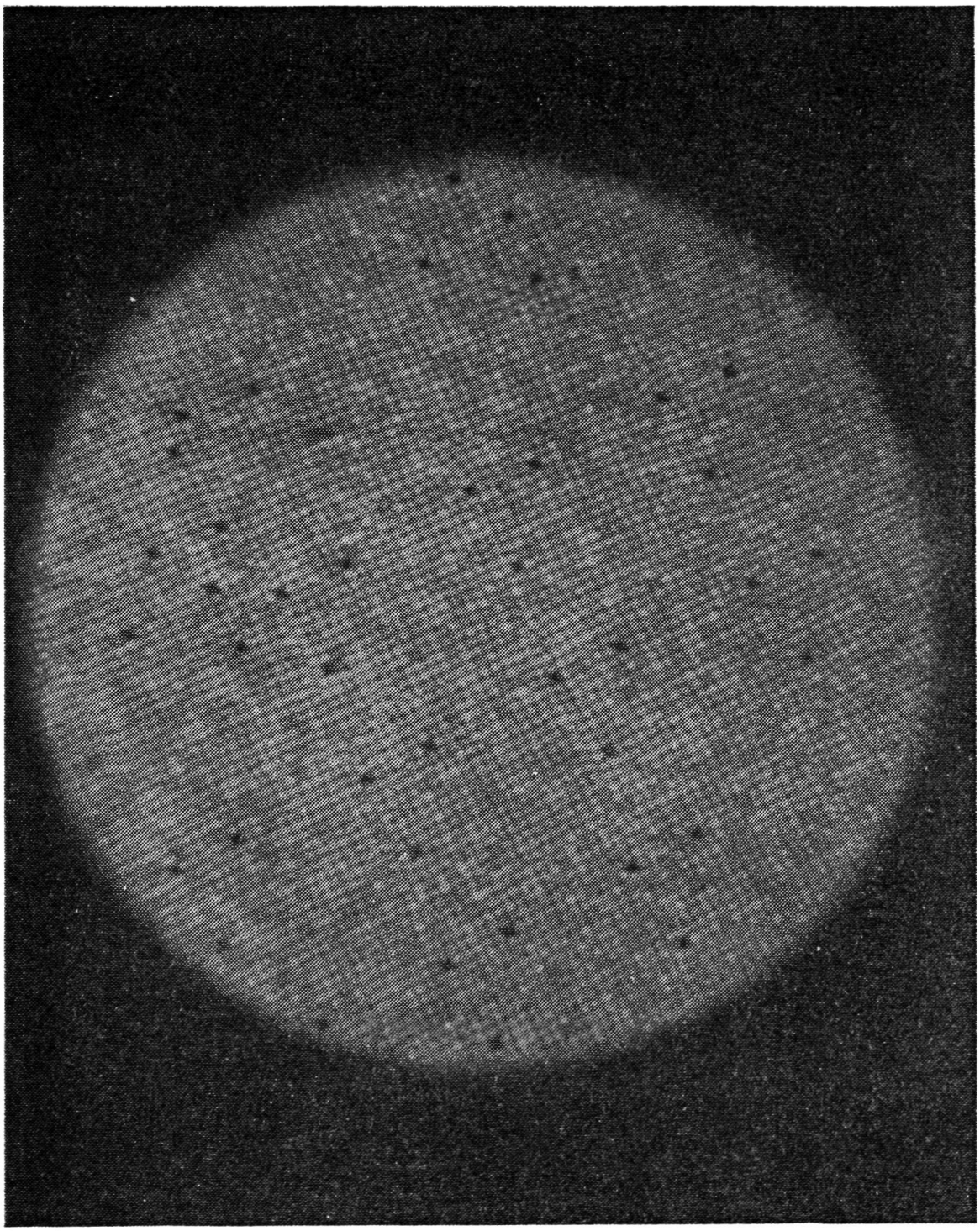

Figure 2.3.2-4. Illuminated 6 Micrometer Straight Fiber Plate, Intagliated

Figure 2.3.2-5 shows the phosphor on fiber optic of a standard F4089, No. 028004. The plate has 6 micrometer center-to-center fibers in a hexagonal pack. Here, as well as in Figures 2.3.2-3 and 2.3.2-4, the illuminated area is 0.017 inches in diameter. The black arc is an image used to establish focus.

After tube No. 068101A was built and examined, fiber optics similar to those used in No. 068101A, but not intagliated and not phosphored, were photographed through a microscope; see Figures 2.3.2-6, 2.3.2-7, and 2.3.2-8. Figure 2.3.2-6, a 10 micrometer twister, and Figure 2.3.2-7, a 6 micrometer straight plate, are at the same magnification. In Figure 2.3.2-8, the enlargement has been increased so that the spacing between EMA rods is nearly the same as that shown in Figures 2.3.2-6 and 2.3.2-8. It appears that there is relatively more rod area in the 10 micrometer spacing twister than in the 6 micrometer spacing straight plate. The "walls" of the 6 micrometer plate also seem relatively thinner, perhaps accounting for the higher phosphor efficiency of the straight plate. Caution, the twister's brightness is reduced at the edges by the longer path length.

2.3.3 Scanning Electron Microscope Photographs

Scanning electron microscope photographs of various intagliated and phosphored 10 micrometer fiber spacing assemblies are shown in Figures 2.3.3-1 through 2.3.3-6. These assemblies do not have the final aluminum layer over the surface of the fiber optic plate. To obtain the photographs, the plate had to be broken; some of the missing phosphor may have been lost during the breaking process.

One each of the unused 10 micrometer and 6 micrometer fiber spacing plates was broken and SEM photographs taken; see Figures 2.3.3-7 through 2.3.3-11. Of particular interest is Figure 2.3-11 (a 10 micrometer spacing plate), which shows the aluminum cover layer. Note the protrusion of some phosphor particles above the fiber optic surface, i.e., the channels are not uniformly filled.

In retrospect, it is disappointing that the etching is, it appears, only about 5 micrometers deep, rather than the 10 micrometers that was planned. The brightness measurements, Figure 2.3.2-2, of the phosphors show no serious saturation effects, so it would seem there was adequate thickness for the voltages used.

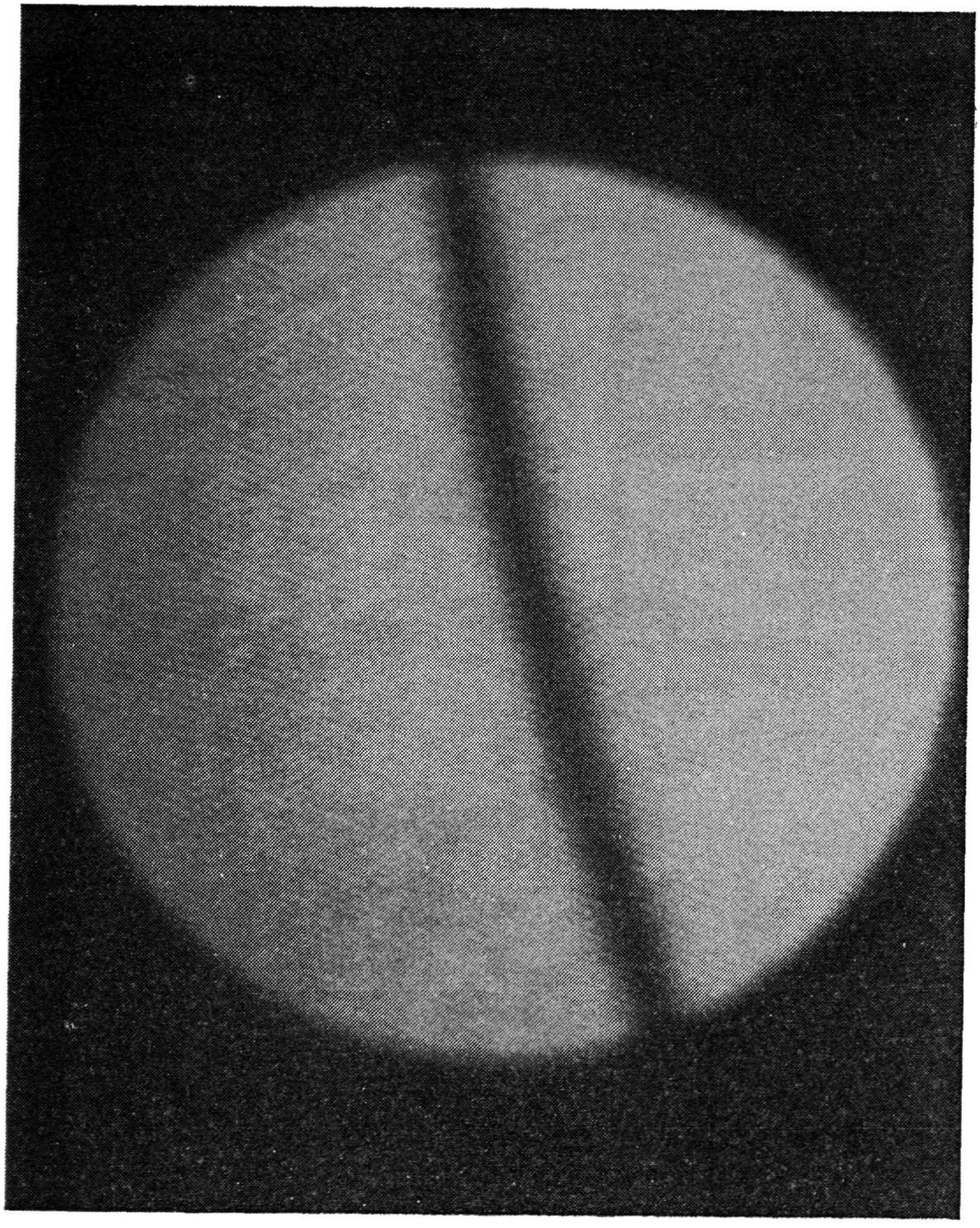

Figure 2.3.2-5. Standard 6 Micrometer F4089 Illuminated Phosphor Assembly

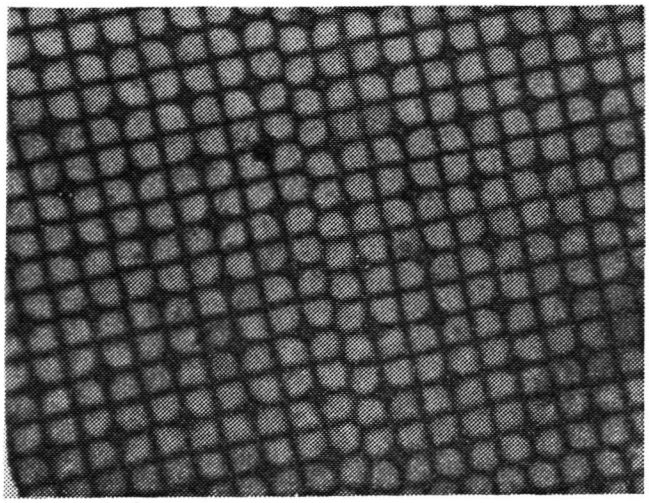

Figure 2.3.2-6. 10 Micrometer Twister Plate (not intagliated, not phosphored)

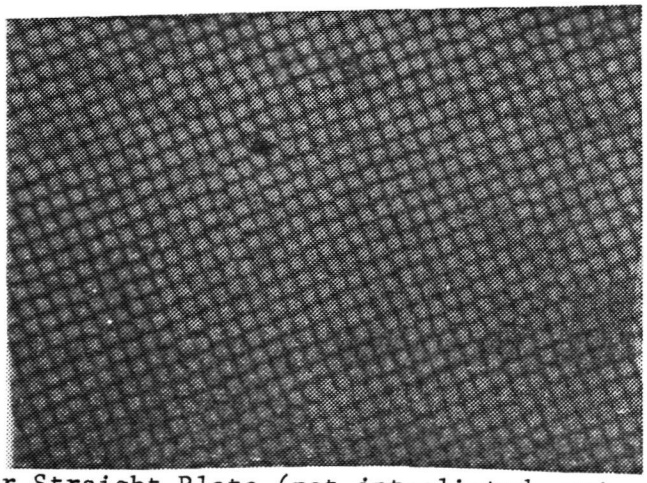

Figure 2.3.2-7. 6 Micrometer Straight Plate (not intagliated, not phosphored)

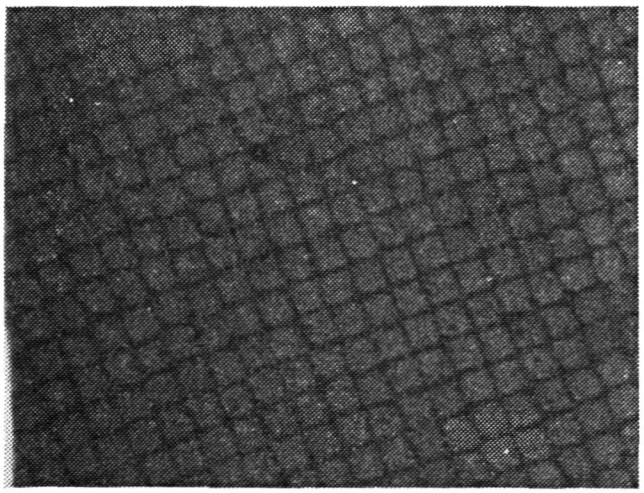

Figure 2.3.2-8. Same as Figure 2.3.2-7 Above, But at Higher Magnification

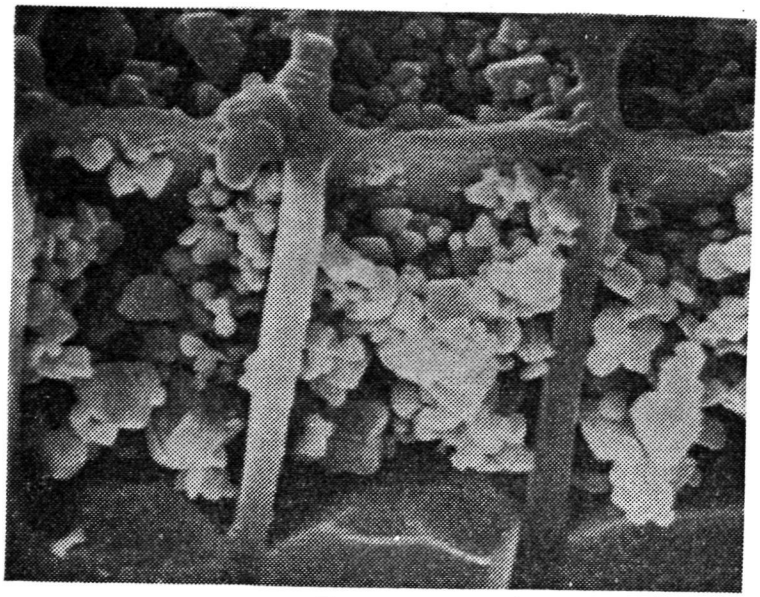

Figure 2.3.3-1. Intagliated Phosphor Before Lacquering - 5000X

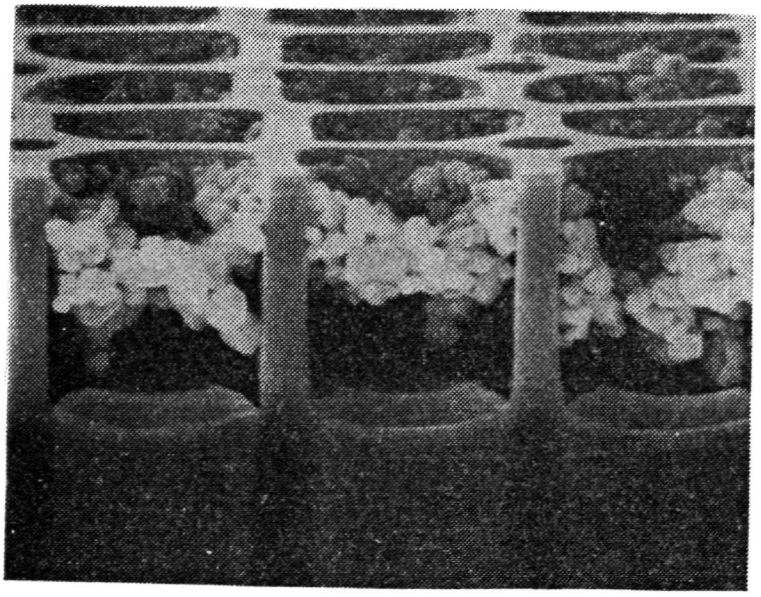

Figure 2.3.3-2. Same as Figure 2.3.3-1, Another Area - 4500X

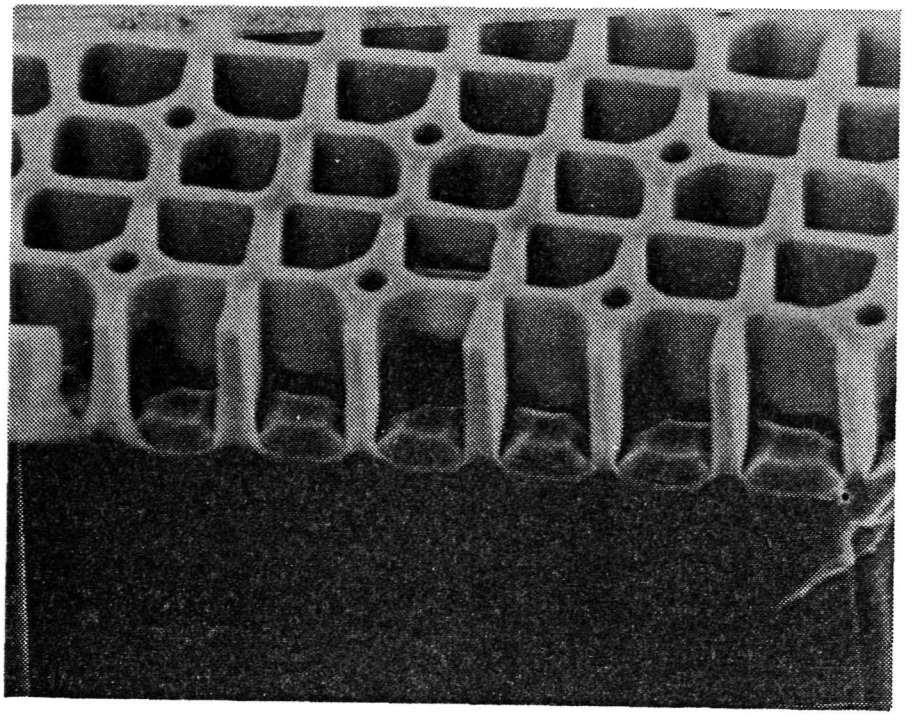

Figure 2.3.3-3. Etched Fiber Optics

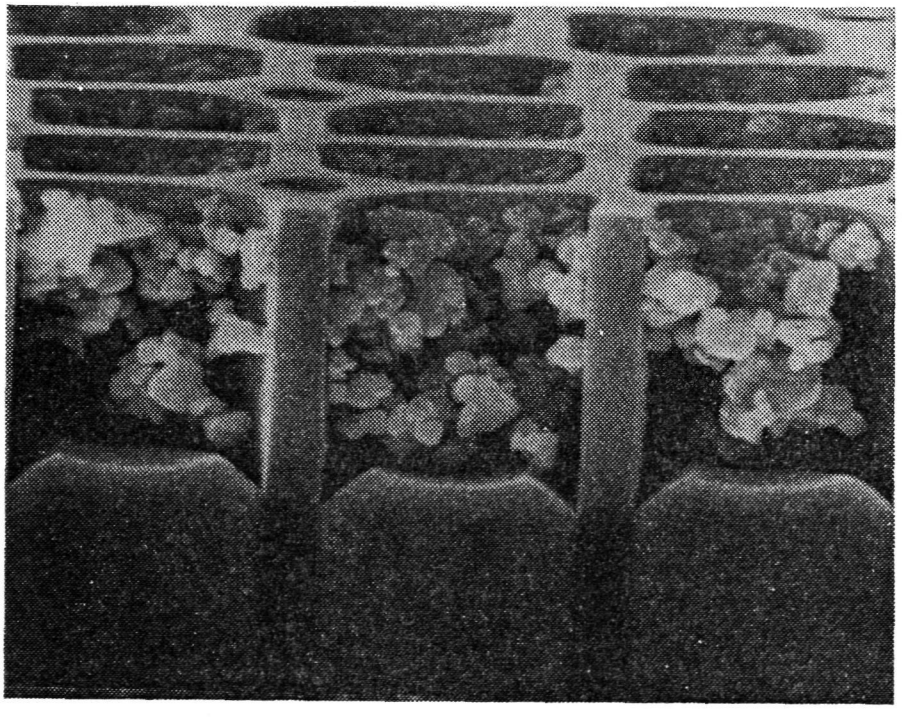

Figure 2.3.3-4. Etched and Phosphored Fiber Optic

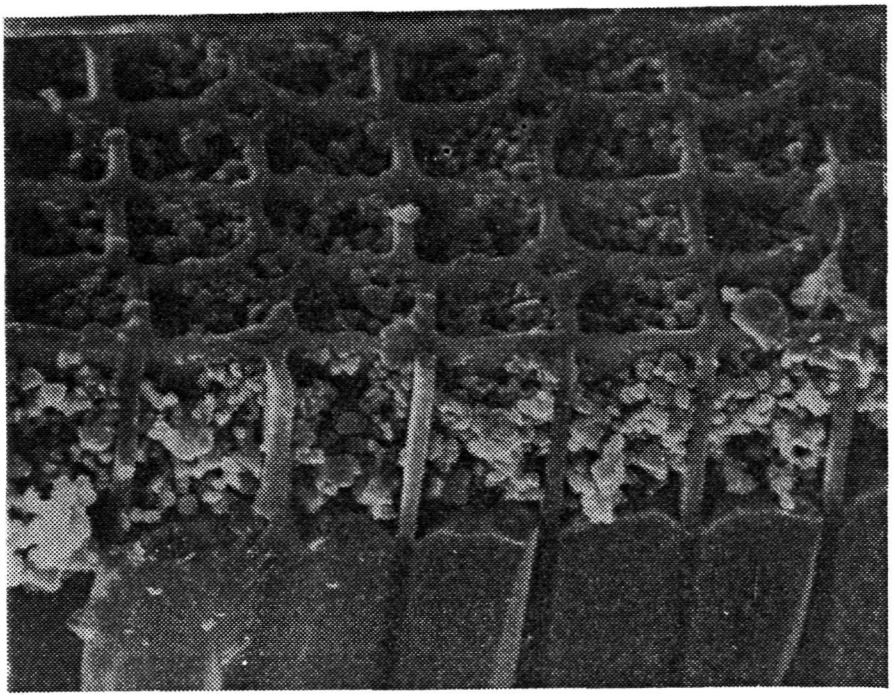

Figure 2.3.3-5. Phosphored Etched Plate (note filling)

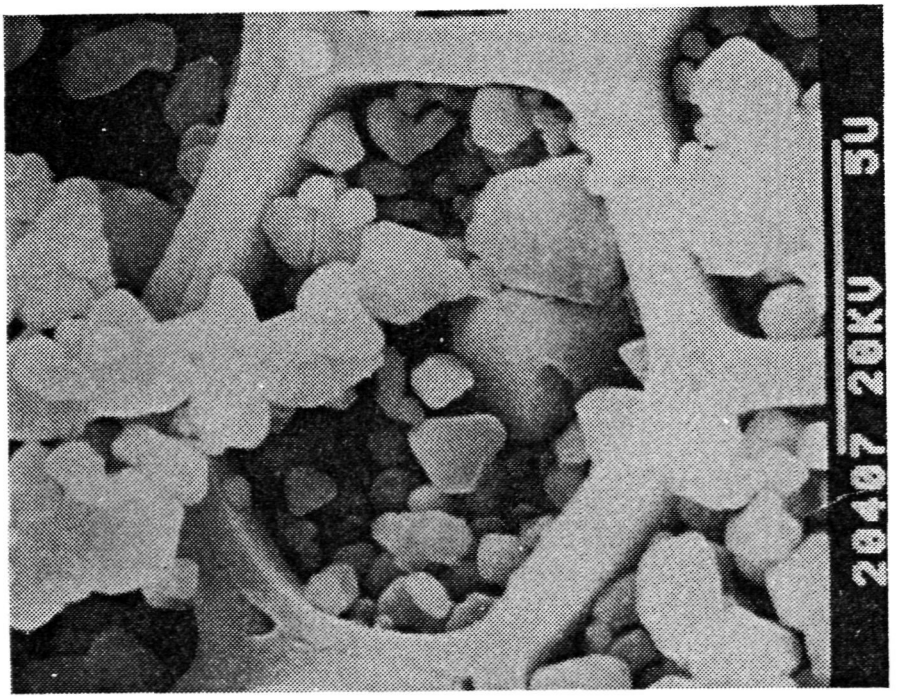

Figure 2.3.3-6. Phosphored Etched Plate, Top View

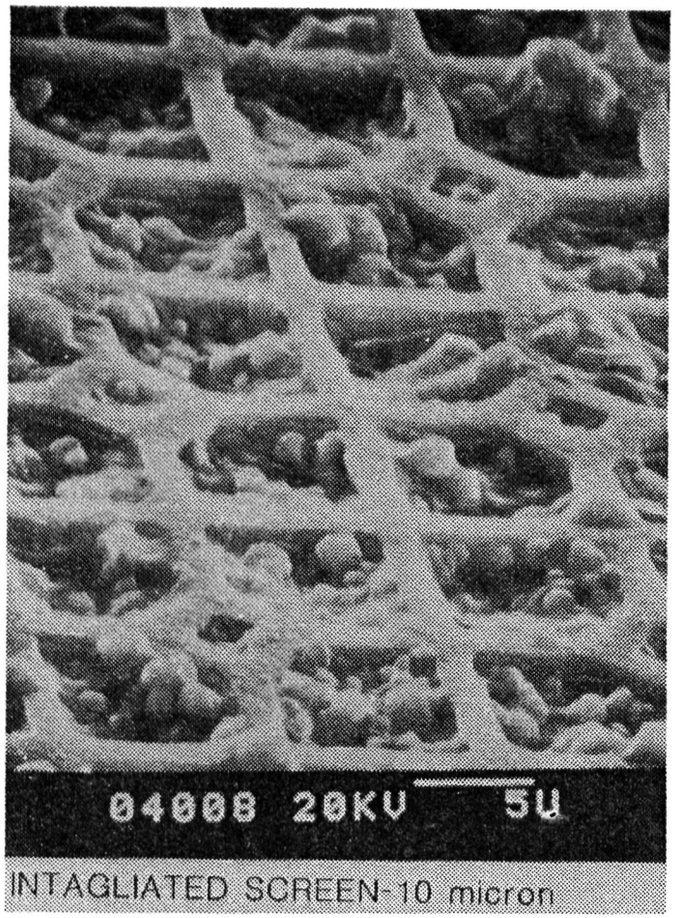

Figure 2.3.3-7. Aluminized Assembly

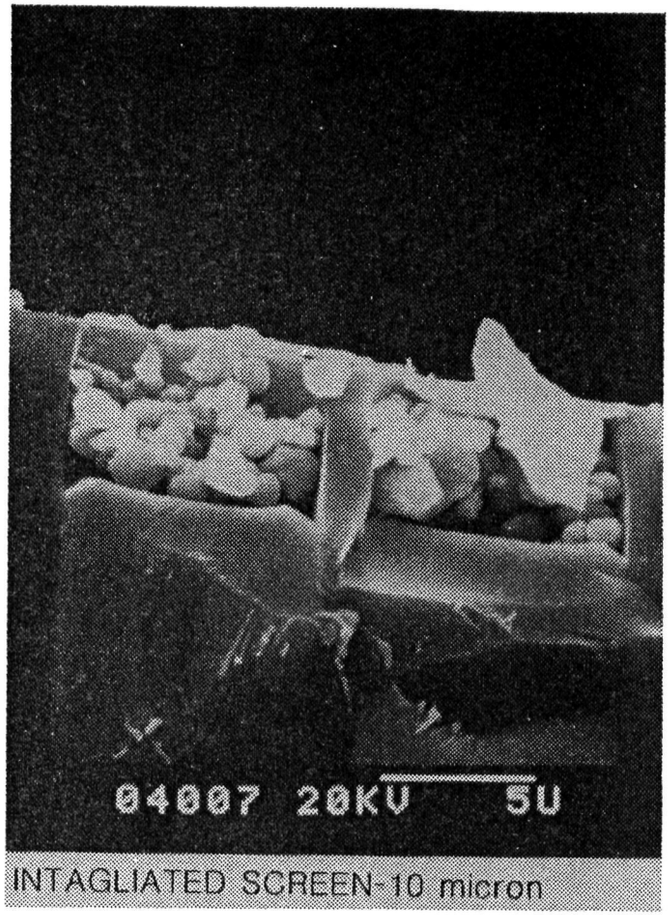

Figure 2.3.3-8. Same as Figure 2.3.3-9, But Side View

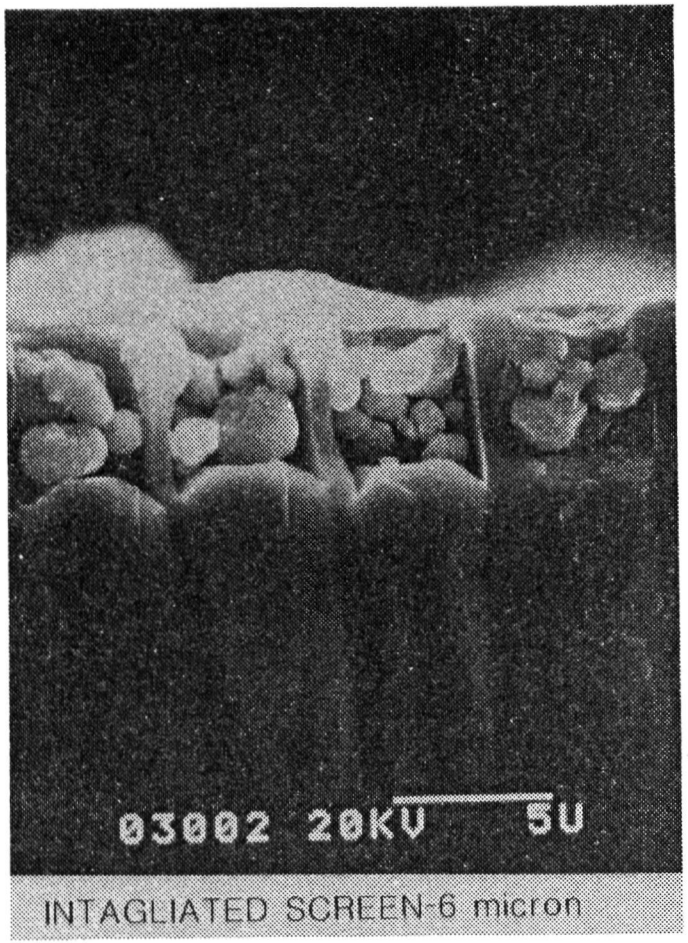

Figure 2.3.3-9. Side View of Aluminized Assembly

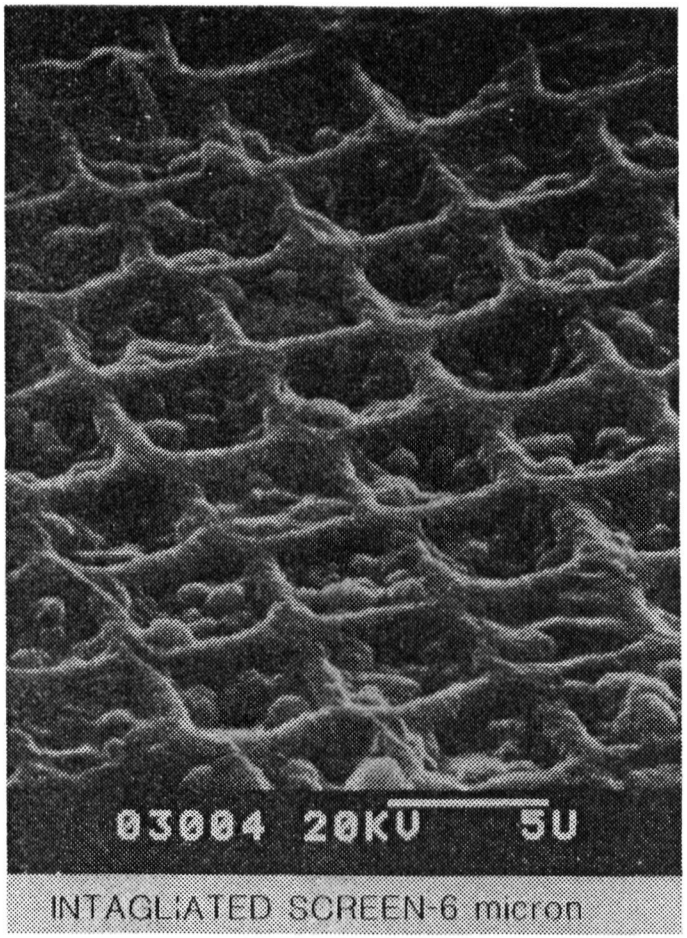

Figure 2.3.3-10. Top View of Aluminized Assembly

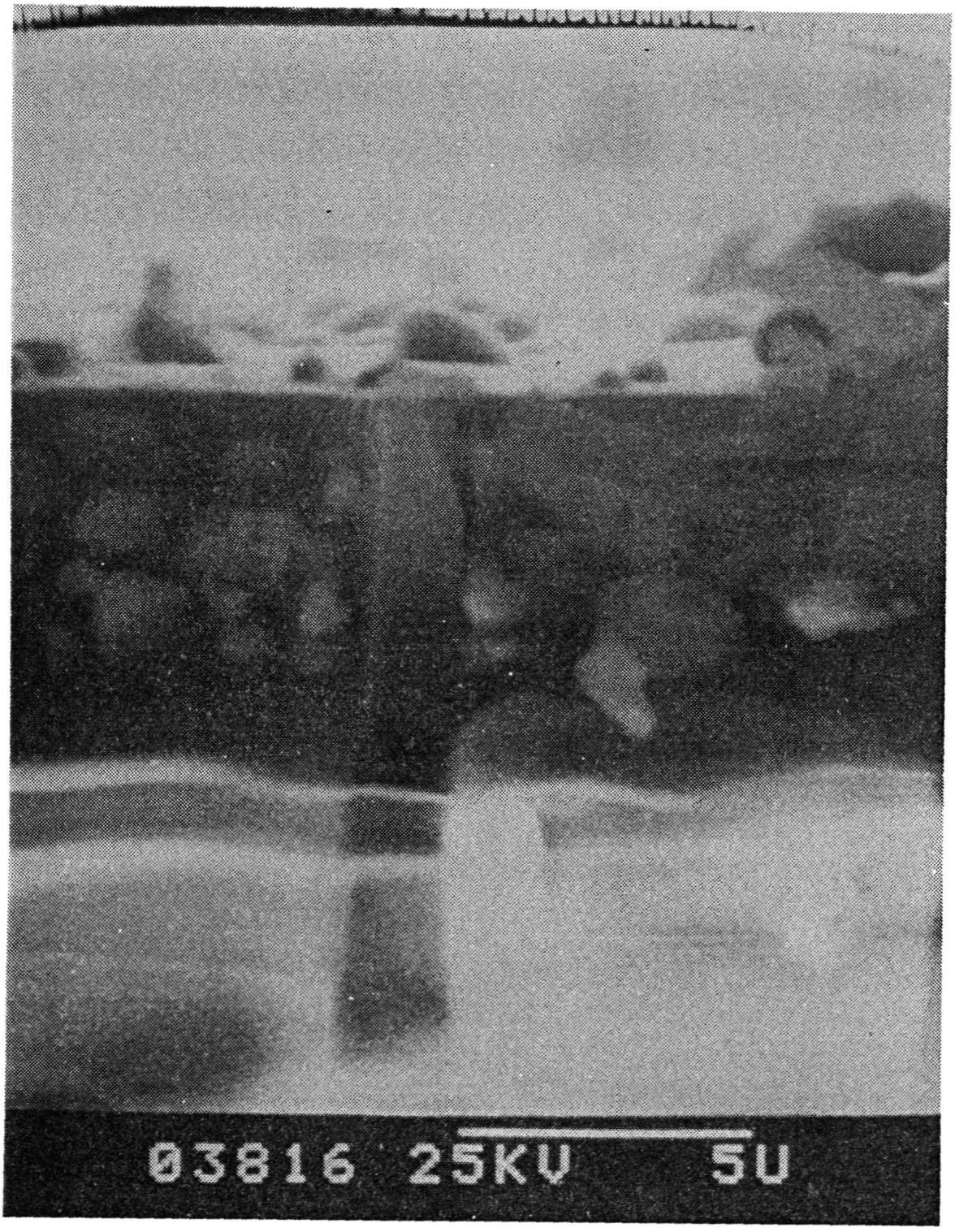

Figure 2.3.3-11. Aluminized Intagliated Phosphor (note "bumps")

Section 3

AN ELECTRONIC METHOD OF IMAGE TUBE SPATIAL FREQUENCY RESPONSE MEASUREMENT

The electronic process used here measures the spatial frequency response of an image tube. More specifically, it is the modulation transfer function that is calculated from measured line and point spread function data. This electronic process quantifies the image sampling properties of the image tube and is, in a sense, what an observer might see when viewing a spatial frequency test pattern at the phosphor screen of an image tube using a microscope. The difference between the electronically measured spatial frequency response and the spatial frequency responses derived from the analysis of direct contact film exposures is the subject of this study.

This section is the electronic case. The results of recent experimental work are presented and these results are compared with results from the previous study. Details of the measurement technique are described in the earlier study report. The specific arrangement of the MTF test equipment using two M = 10, NA = 0.25 lenses has a theoretical limit of MTF = 0.9 at 60 c/mm and MTF = 0.8 at 100 c/mm. The measured limits were MTF = 0.8 at 60 c/mm and MTF = 0.6 at 100 c/mm. These values are degraded slightly by the use of a M = 5, NA = 0.1 lens.

3.1 RESULTS OF ELECTRONIC MTF TESTS OF AN INTAGLIATED PHOSPHOR SCREEN IMAGE TUBE HAVING A 10 MICROMETER FIBER OPTIC PLATE

This series of tests was conducted under the following conditions:

Illumination Wavelength	- 600 +/- 10 nm (bandpass filter)
Image Tube Voltage	- 13.55 kV
Test Objects - Line Input	- 12.5 micrometer x 500 micrometers
- Point Input	- 25 micrometer diameter
Projection Lens	- M = 1/5, NA = 0.1
Analyzer Lens	- M = 10, NA = 0.25

3.1.1 Results of the Line Illumination Test

Figure 3.1.1-1 shows a printer plot of the intensity distribution at the image tube phosphor screen. The vertical scale is compressed approximately 2:1 when compared to the horizontal scale. This is due to the properties of the printer(1) and the particular scan pattern(2) chosen for the analyzer. The contour line enclosing

(1) 6 lines per inch vertically and 10 character per inch horizontally
(2) 1.40 micrometers per line vertically and 0.50 micrometer per character horizontally.

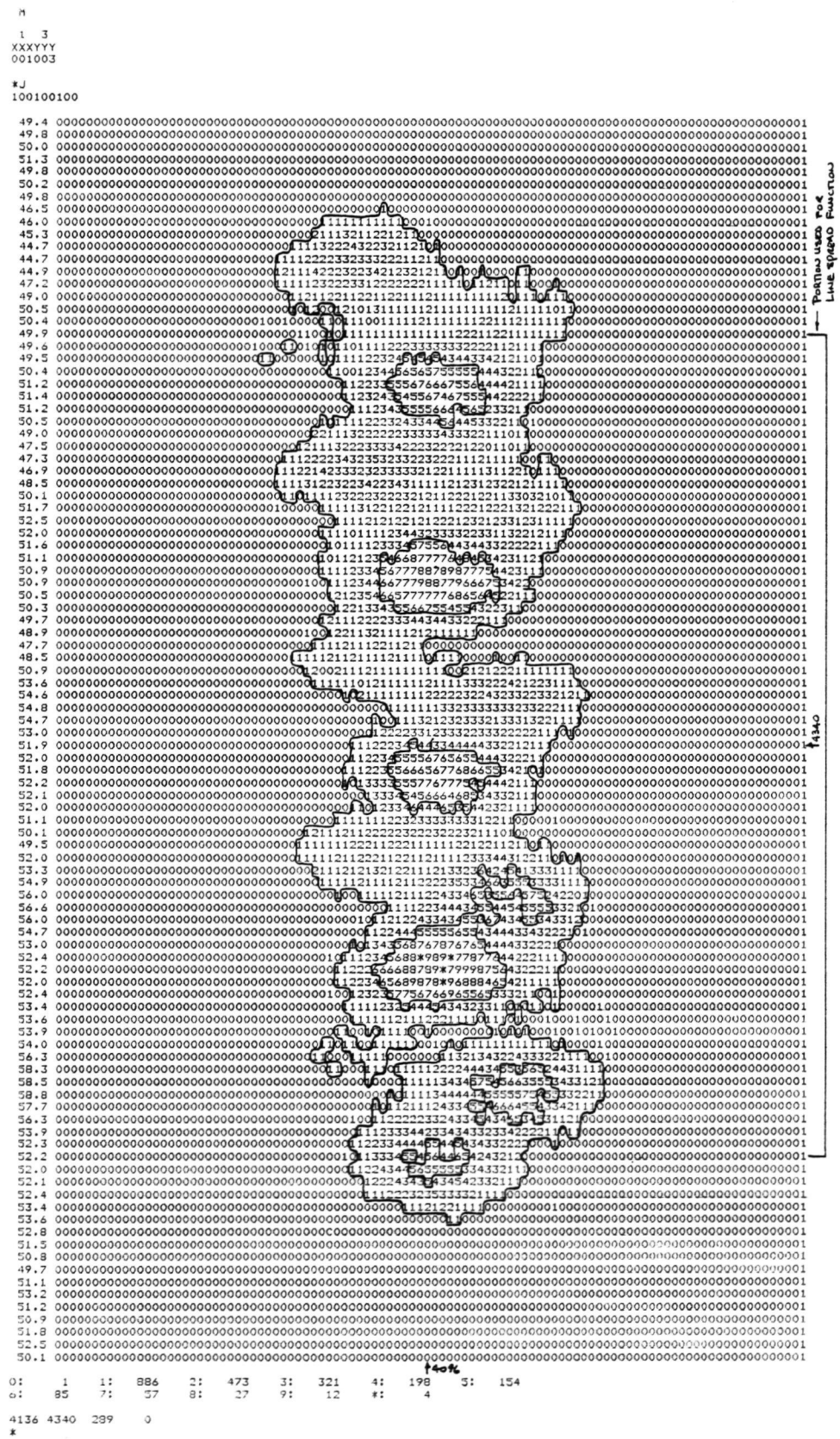

Figure 3.1.1-1. Raster Scan View of Image Tube Line Spread Function. Tube Has a 10 Micrometer, Intagliated, Fiber Optic Phosphor Screen. (600 nm)

the larger area contains all image samples having greater than 0.1 x of full scale intensity. The small area contour encloses all points greater than 0.5 x of full intensity.

Figure 3.1.1-2 is a photograph of the analyzer monitor. It is the view seen when looking through a microscope. The photographic view is slightly displaced from the contour view in Figure 3.1.1-1.

Both Figures 3.1.1-1 and 3.1.1-2 clearly show the individual fibers in the intagliated plate as well as the much darker webs among them. These figures can be compared with a similar figure from the earlier report, reproduced here as Figure 3.1.1-3. Figure 3.1.1-3 is of a 6 micrometer, non-intagliated fiber optic plate.

Figure 3.1.1-4 shows the line spread function and MTF of this 10 micrometer, intagliated plate tube. The line spread function was obtained by summing the intensity profiles of 41 line scans across the slit image. The purpose of the multiple scans was twofold. First, it averages the spatial noise of the fiber plate sampling of the slit image. Second, it averages the electrical noise of the lowlight level slit image. The spatial extent of the summation process is marked on Figure 3.1.1-1. The MTF table is a result of a Fourier Transform computation using the line spread function as the input data. The tabular part of Figure 3.1.1-4 shows the numerical data used to create the plots of the line spread function and the MTF results.

Figure 3.1.1-4 results can be compared to the earlier study. Figure 3.1.1-5 reproduces the corresponding results from the earlier work. Again, the earlier data is for a 6 micrometer, non-intagliated screen. At 50 c/mm, the present tube has an interpolated MTF = 0.30, while the previous tube exhibited an interpolated MTF = 0.13. The ratio of the two is 2.4:1. This is significant improvement, especially considering that the improved tube fiber optic plate has 10 micrometer fibers, not 6 micrometers.

3.1.2 Results of the Point Illumination Test

The stray light suppression properties of the 10 micrometer, intagliated phosphor screen were examined by projecting the image of a very small spot of light on to the photocathode. The spot size was 25 micrometer/5 = 5 micrometer diameter. Great care was taken to illuminate only a single fiber. This proved to be surprisingly easy to accomplish. Figure 3.1.2-1 shows the plotted and tabular results of the test. The zero of the MTF curve occurs at 108 c/mm, which implies about a 9 micrometer effective diameter of the illuminated core glass.

These plots are labeled as point spread data. The results are a measure of the image tube and fiber plate spatial sampling function. They are not a direct measure of the ability to detect and record spatial information from a scene. This is another way of saying that the Nyquist limit of a 10 micrometer plate corresponds to 20 micrometers or so spatial wavelengths. The two additional points on

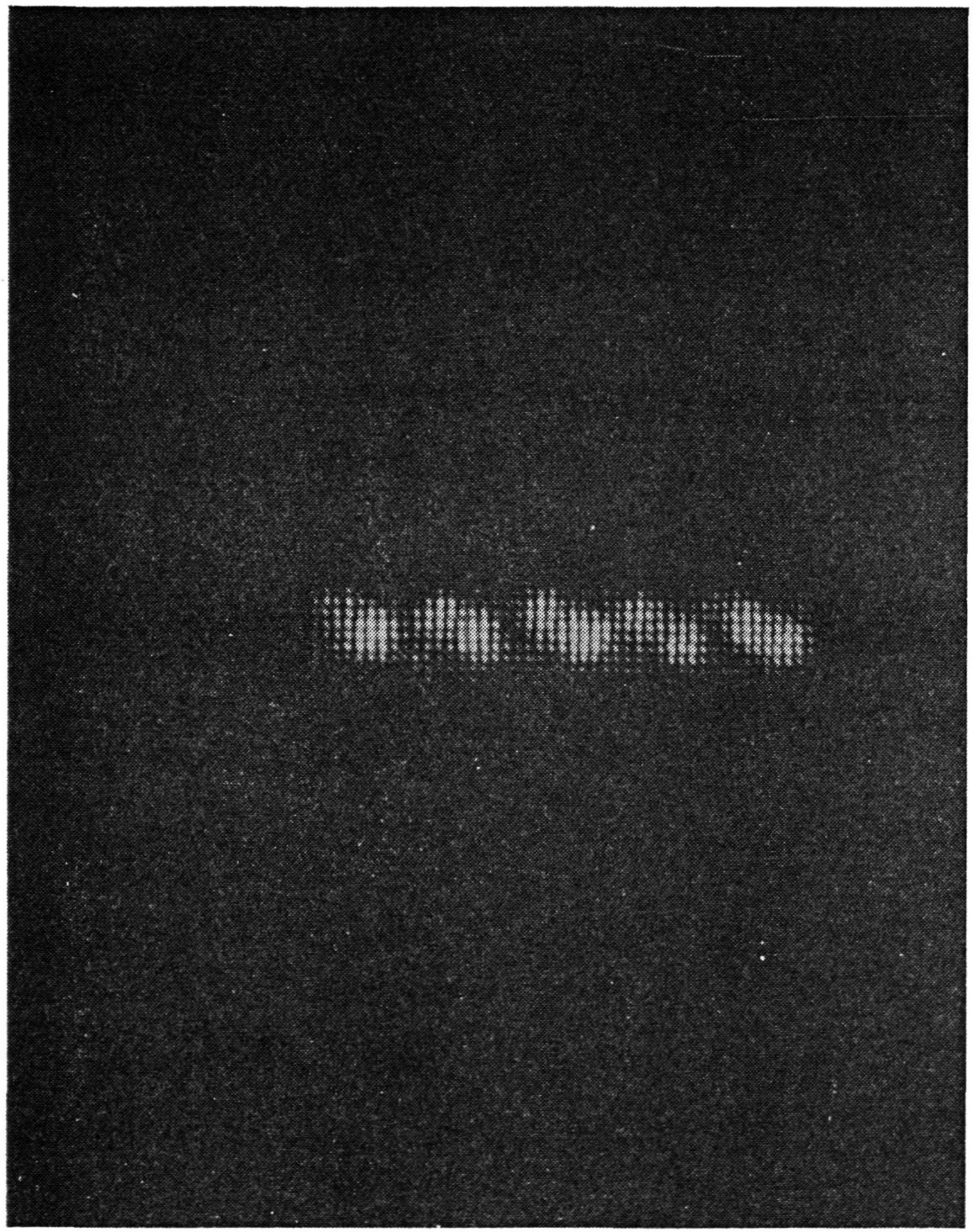

Figure 3.1.1-2. Monitor Photograph of Raster Scan View of Image Tube Line Spread Function. Tube Has a 10 Micrometer, Intagliated, Fiber Optic Phosphor Screen. (600 nm)

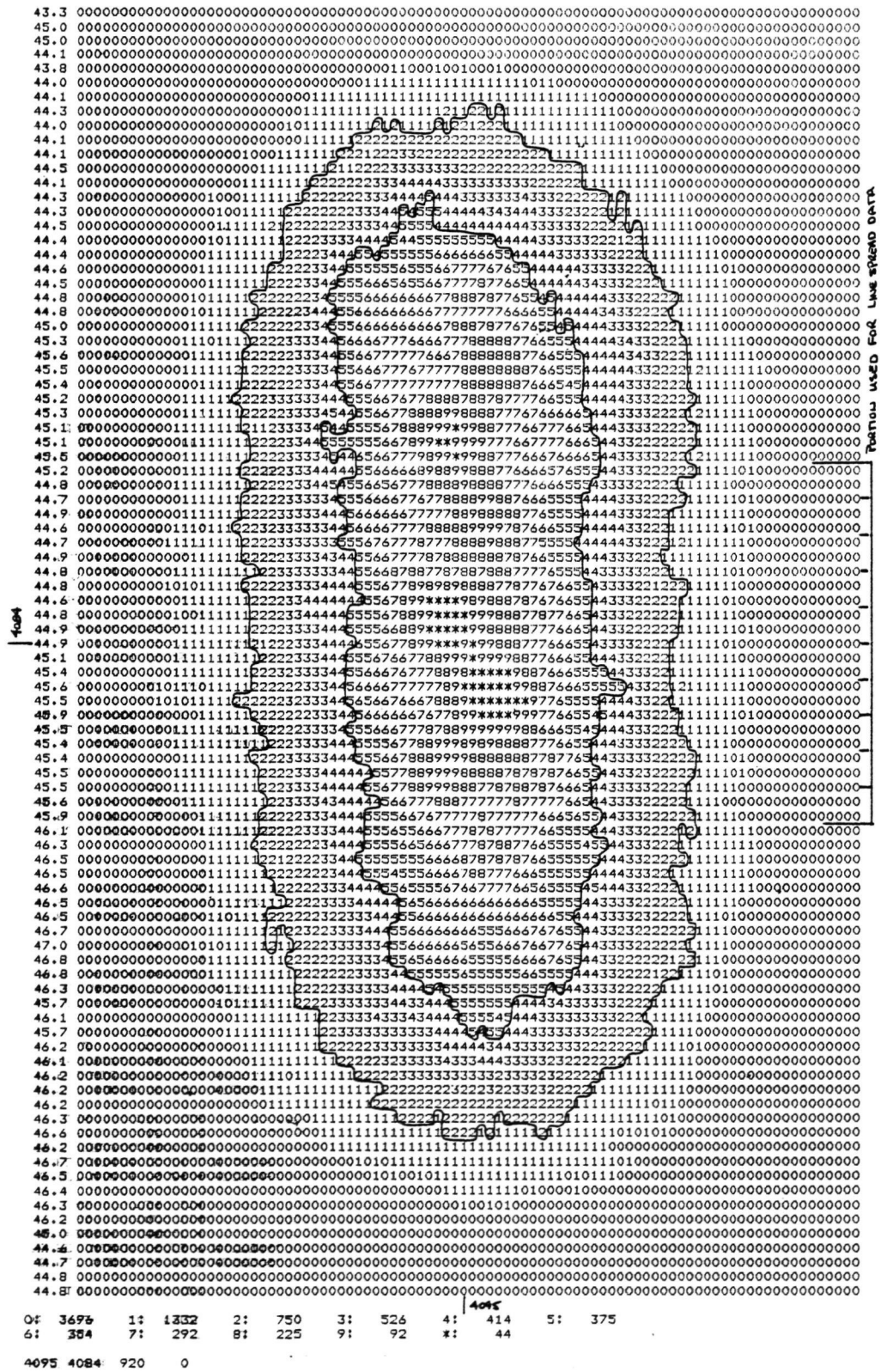

Figure 3.1.1-3. Raster Scan View of Image Tube Line Spread Function, Tube Has a 6 Micrometer, Non-Intagliated, Fiber Optic Phosphor Screen

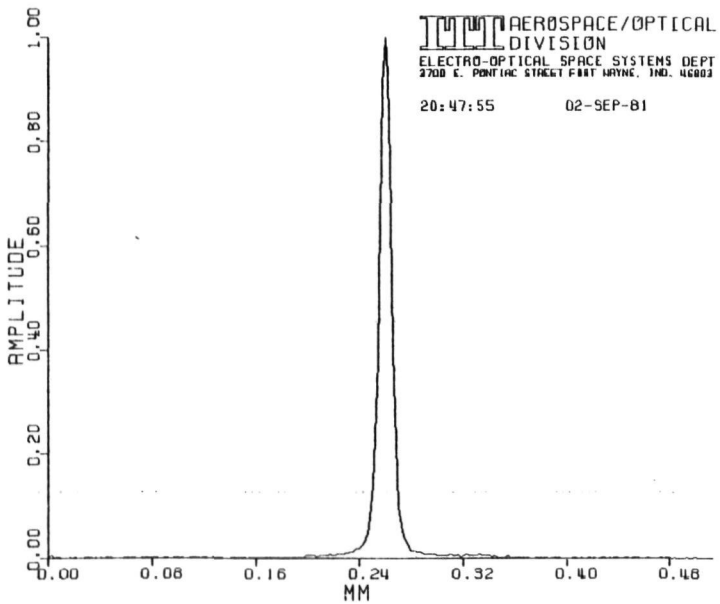

LINE SPREAD FUNCTION

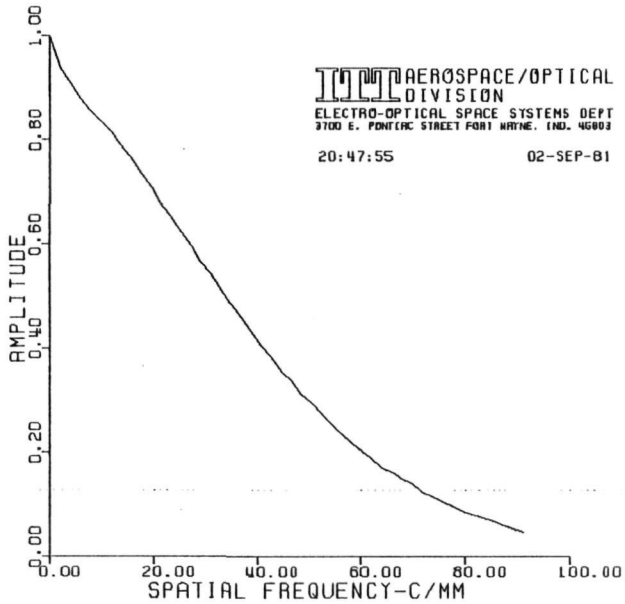

IMAGE TUBE MTF

Figure 3.1.1-4. Measured Line Spread Function and MTF of a Magnetic Focus Image Tube Having a 10 Micrometer, Intagliated, Fiber Optic Phosphor Screen (600 nm)

Sheet 1 of 2

LINE SPREAD DATA LISTING 20:47:55 02-SEP-81

213.	348.	265.	218.	120.	-13.	13.	52.	132.	92.	127.	80.	93.	65.	172.	248.
115.	32.	111.	59.	143.	88.	163.	184.	217.	92.	44.	32.	35.	104.	137.	181.
152.	108.	48.	100.	153.	140.	119.	129.	147.	110.	93.	42.	114.	124.	62.	94.
162.	154.	205.	138.	28.	53.	143.	116.	123.	195.	69.	180.	153.	100.	27.	199.
183.	188.	104.	78.	98.	65.	137.	208.	138.	132.	160.	170.	91.	266.	143.	191.
236.	168.	184.	157.	230.	213.	153.	155.	187.	195.	256.	188.	250.	286.	195.	196.
240.	231.	270.	369.	448.	324.	318.	272.	319.	397.	353.	475.	553.	504.	410.	580.
519.	681.	782.	919.	930.	984.	1439.	1426.	2051.	2388.	3899.	6434.	11553.	19147.	31490.	53938.
74952.	82458.	76487.	54572.	33023.	18246.	7989.	5221.	3429.	2577.	1770.	1305.	1226.	976.	962.	831.
710.	695.	592.	530.	569.	512.	410.	453.	404.	348.	535.	389.	389.	719.	281.	486.
539.	457.	358.	403.	515.	527.	398.	335.	459.	388.	265.	422.	272.	263.	220.	298.
349.	162.	130.	150.	128.	228.	123.	115.	179.	95.	98.	144.	206.	117.	164.	117.
96.	122.	129.	107.	127.	95.	94.	34.	56.	132.	121.	40.	179.	37.	67.	132.
62.	208.	13.	43.	273.	151.	62.	175.	14.	122.	112.	26.	-30.	145.	107.	64.
150.	112.	132.	77.	33.	26.	156.	11.	67.	74.	82.	116.	72.	142.	178.	-6.
143.	94.	47.	71.	62.	128.	80.	59.	126.	49.	78.	62.	18.	49.	26.	92.

X0=4096 Y0=4340 XSTEP= 4 YSTEP= 5

MTF AND PTF 20:47:55 02-SEP-81

SPATIAL FREQUENCY C/MM	MTF	PTF	SPATIAL FREQUENCY C/MM	MTF	PTF	SPATIAL FREQUENCY C/MM	MTF	PTF	SPATIAL FREQUENCY C/MM	MTF	PTF
0.0	1.000	0.0	1.9	0.938	-1.5	3.9	0.908	-3.1	5.8	0.878	-4.1
7.8	0.856	-5.2	9.7	0.835	-6.3	11.6	0.816	-7.7	13.6	0.791	-9.3
15.5	0.764	-10.8	17.5	0.735	-12.2	19.4	0.708	-13.6	21.3	0.678	-14.8
23.3	0.652	-16.1	25.2	0.622	-17.7	27.2	0.596	-19.2	29.1	0.565	-20.5
31.1	0.542	-22.0	33.0	0.510	-23.5	34.9	0.485	-25.1	36.9	0.458	-26.7
38.8	0.432	-28.1	40.8	0.405	-29.6	42.7	0.383	-31.5	44.6	0.354	-32.8
46.6	0.337	-34.6	48.5	0.311	-36.2	50.5	0.295	-37.8	52.4	0.272	-39.2
54.3	0.255	-41.5	56.3	0.235	-42.7	58.2	0.217	-45.0	60.2	0.201	-47.6
62.1	0.188	-48.5	64.0	0.171	-50.9	66.0	0.163	-52.6	67.9	0.148	-54.4
69.9	0.139	-56.0	71.8	0.122	-56.4	73.8	0.116	-60.3	75.7	0.105	-61.5
77.6	0.096	-64.1	79.6	0.086	-65.2	81.5	0.080	-66.7	83.5	0.073	-68.5
85.4	0.067	-71.7	87.3	0.060	-70.4	89.3	0.054	-73.6	91.2	0.048	-72.9

X0=4096 Y0=4340 XSTEP= 4 YSTEP= 5

Figure 3.1.1-4. Measured Line Spread Function and MTF of a Magnetic Focus Image Tube Having a 10 Micrometer, Intagliated, Fiber Optic Phosphor Screen (600 nm (continued)

Sheet 2 of 2

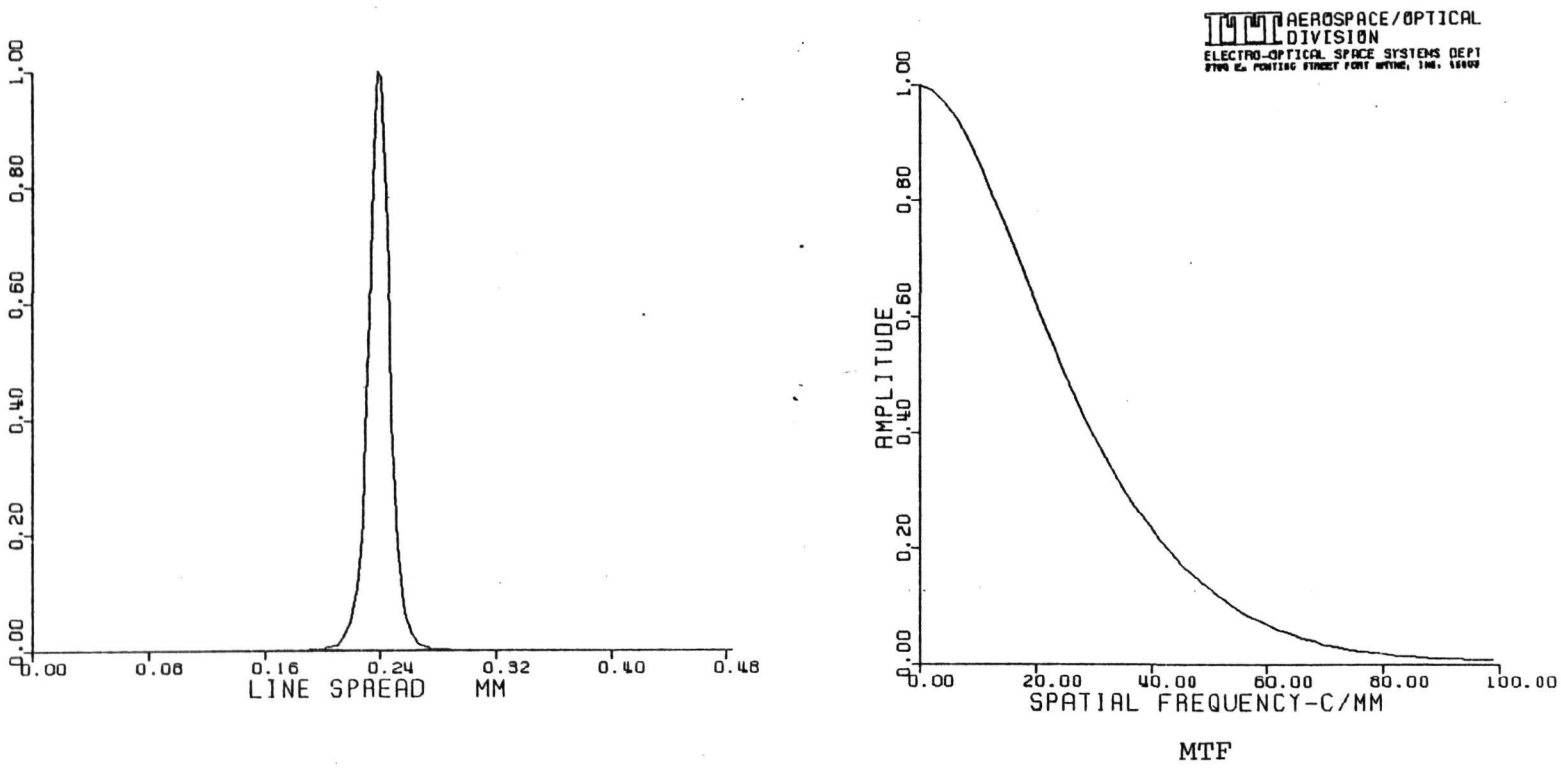

Figure 3.1.1-5. Measured Line Spread Function and MTF of a Magnetic Focus Image Tube Having a 6 Micrometer, Non-Intagliated, Fiber Optic Phosphor Screen (600 nm)

Sheet 1 of 2

LINE SPREAD DATA

52.	36.	37.												
47.	39.	50.	44.	39.	44.	59.	72.	70.	57.	71.	84.	71.	69.	68.	88.
92.	88.	84.	87.	79.	103.	82.	97.	94.	109.	111.	128.	108.	149.	200.	178.
240.	250.	283.	335.	312.	413.	478.	551.	667.	807.	1022.	1268.	1647.	2279.	2780.	3651.
5082.	7289.	10596.	14078.	18848.	25714.	35106.	48514.	71340.	101616.	141421.	188643.	244202.	296821.	326095.	322572.
288994.	238399.	183700.	129793.	88514.	60632.	39946.	26603.	18411.	12899.	8971.	6345.	4387.	3204.	2330.	1790.
1375.	1058.	972.	747.	656.	545.	484.	473.	359.	324.	303.	292.	268.	231.	215.	240.
218.	1[illegible]	151.	106.	162	116	151.	111.	115	103.	93.	93.	86.	103.	92.	87.
92.	86.	65.	47.	76.	46.	64.	61.	46.	48.	55.	55.	44.	39.	35.	54.
49.	29.	40.	36.	42.	34.	41.	43.	41.	40.	45.	39.	46.	33.	43.	27.
30.	37.	21.	27.	29.	25.	30.	29.	17.	21.	20.	32.	24.	30.	24.	16.
23.	20.	14.	30.	17.	24.	22.	14.	18.	22.	17.	22.	21.	22.	16.	24.
26.	17.	13.	19.	21.	26.	17.	15.	17.	18.	23.	11.	15.	11.	19.	14.

MTF AND PTF

SPATIAL FREQUENCY C/MM	MTF	PTF	SPATIAL FREQUENCY C/MM	MTF	PTF	SPATIAL FREQUENCY C/MM	MTF	PTF	SPATIAL FREQUENCY C/MM	MTF	PTF
0.0	1.000	0.0	2.1	0.991	2.5	4.1	0.971	4.9	6.2	0.942	7.4
8.2	0.904	9.8	10.3	0.861	12.1	12.4	0.813	14.5	14.4	0.762	16.7
16.5	0.709	18.9	18.5	0.656	21.0	20.6	0.604	23.1	22.7	0.553	25.2
24.7	0.505	27.2	26.8	0.459	29.2	28.8	0.416	31.1	30.9	0.376	33.1
33.0	0.339	35.0	35.0	0.304	37.0	37.1	0.273	38.9	39.1	0.244	40.9
41.2	0.218	42.9	43.3	0.194	44.9	45.3	0.172	46.9	47.4	0.152	48.9
49.4	0.135	51.0	51.5	0.118	53.0	53.5	0.104	55.0	55.6	0.091	57.1
57.7	0.079	59.1	59.7	0.069	61.1	61.8	0.060	63.1	63.8	0.052	65.0
65.9	0.045	66.8	68.0	0.039	68.6	70.0	0.034	70.4	72.1	0.029	72.3
74.1	0.025	74.1	76.2	0.022	76.2	78.3	0.020	78.4	80.3	0.017	81.0
82.4	0.015	83.9	84.4	0.014	87.2	86.5	0.012	-89.1	88.6	0.011	-84.7
90.6	0.010	-80.0	92.7	0.009	-74.4	94.7	0.008	-68.9	96.8	0.008	-62.9
98.9	0.007	-56.6									

Figure 3.1.1-5. Measured Line Spread Function and MTF of a Magnetic Focus Image Tube Having a 6 Micrometer, Non-Intagliated, Fiber Optic Phosphor Screen (600 nm) (continued)

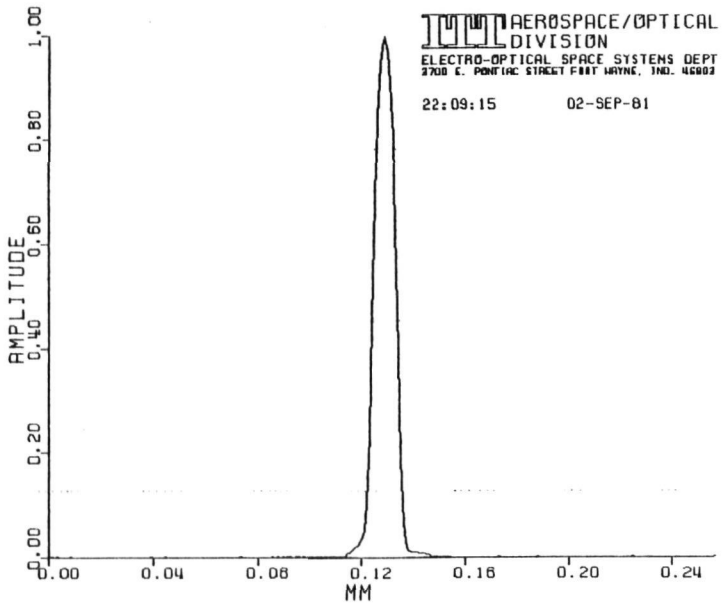

POINT SPREAD FUNCTION

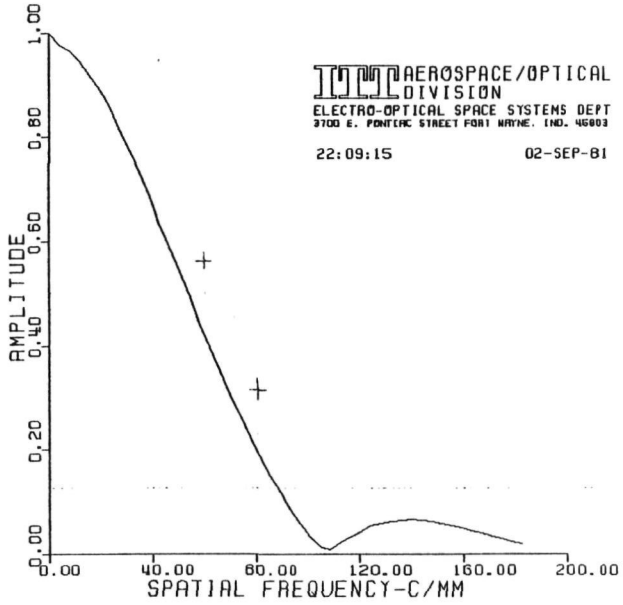

IMAGE TUBE MTF

Figure 3.1.2-1. Measured Point Spread Function and MTF of a Magnetic Focus Image Tube Having a 10 Micrometer, Intagliated, Fiber Optic Phosphor Screen

POINT SPREAD DATA LISTING 22:09:15 02-SEP-81

-78.	204.	-115.	214.	59.	112.	106.	-51.	196.	-10.	153.	16.	96.	132.	61.	182.
95.	163.	177.	65.	174.	58.	93.	35.	82.	129.	90.	112.	73.	99.	118.	124.
86.	145.	97.	137.	69.	180.	30.	199.	88.	17.	117.	57.	202.	59.	189.	40.
60.	139.	143.	82.	52.	140.	106.	155.	121.	40.	79.	159.	58.	109.	89.	132.
124.	134.	123.	154.	151.	103.	155.	150.	86.	200.	187.	162.	186.	129.	178.	79.
137.	97.	177.	105.	26.	236.	101.	222.	122.	195.	174.	231.	245.	128.	285.	232.
185.	213.	170.	192.	269.	253.	271.	307.	304.	226.	330.	389.	256.	218.	374.	340.
408.	544.	1115.	1320.	2100.	2619.	3392.	4767.	7546.	15854.	35122.	69203.	103881.	127954.	142930.	148251.
151390.	146720.	137824.	122384.	96120.	59979.	28243.	10185.	4441.	2232.	1666.	1336.	1434.	1172.	978.	1038.
785.	638.	542.	346.	423.	284.	266.	400.	279.	234.	178.	143.	94.	131.	124.	64.
180.	63.	155.	145.	118.	182.	141.	149.	104.	104.	140.	34.	199.	128.	46.	148.
119.	87.	89.	110.	104.	133.	89.	65.	147.	185.	111.	211.	62.	153.	63.	65.
47.	45.	156.	66.	132.	122.	64.	111.	23.	147.	80.	108.	98.	86.	72.	86.
94.	183.	123.	91.	80.	81.	104.	55.	99.	94.	25.	144.	55.	145.	35.	201.
73.	60.	62.	174.	122.	35.	66.	119.	62.	90.	32.	82.	84.	71.	76.	88.
78.	127.	28.	160.	74.	82.	29.	47.	171.	38.	142.	17.	164.	162.	56.	231.

X0=4142 Y0=4052 XSTEP= 2 YSTEP= 1

MTF AND PTF 22:09:15 02-SEP-81

SPATIAL FREQUENCY C/MM	MTF	PTF	SPATIAL FREQUENCY C/MM	MTF	PTF	SPATIAL FREQUENCY C/MM	MTF	PTF	SPATIAL FREQUENCY C/MM	MTF	PTF
0.0	1.000	0.0	3.9	0.978	0.3	7.8	0.964	0.5	11.6	0.944	0.8
15.5	0.919	1.0	19.4	0.889	1.2	23.3	0.855	1.5	27.2	0.816	1.7
31.1	0.775	2.0	34.9	0.732	2.2	38.8	0.685	2.5	42.7	0.638	2.6
46.6	0.590	2.7	50.5	0.542	2.7	54.3	0.493	2.8	58.2	0.444	2.8
62.1	0.398	2.8	66.0	0.351	2.7	69.9	0.307	2.7	73.8	0.265	2.6
77.6	0.224	2.6	81.5	0.186	2.7	85.4	0.150	2.7	89.3	0.117	2.4
93.2	0.086	2.8	97.0	0.059	3.3	100.9	0.034	4.7	104.8	0.012	5.2
108.7	0.006	-6.0	112.6	0.022	-0.1	116.4	0.035	0.9	120.3	0.046	1.8
124.2	0.054	2.3	128.1	0.060	2.5	132.0	0.063	2.8	135.9	0.065	3.3
139.7	0.066	3.5	143.6	0.065	3.5	147.5	0.063	3.0	151.4	0.059	3.5
155.3	0.056	2.6	159.1	0.051	3.2	163.0	0.046	3.4	166.9	0.040	3.0
170.8	0.035	2.5	174.7	0.029	3.9	178.6	0.024	1.9	182.4	0.019	3.1

X0=4142 Y0=4052 XSTEP= 2 YSTEP= 1

Figure 3.1.2-1. Measured Point Spread Function and MTF of a Magnetic Focus Image Tube Having a 10 Micrometer, Intagliated, Fiber Optic Phosphor Screen (continued)

Sheet 2 of 2

the MTF plot marked (+) are MTF = sin(x)/x for a 9 micrometer diameter fiber.

Figure 3.1.2-2 is a plot of the same point spread intensity data on a log intensity scale to accentuate the low level scattered light term. The second curve on the plot is the cumulative distribution function of the measured point spread data, I(x), across the diameter of the spot;

$$A(N) = \sum_{i=o}^{N} I(x_i).$$

About 95 percent of the total area under the point spread curve is contained within a 12.5 um (*) diameter about the center of the fiber.

3.2 RESULTS OF ELECTRONIC MTF TESTS OF AN INTAGLIATED PHOSPHOR SCREEN IMAGE TUBE HAVING A 6 MICROMETER FIBER OPTIC PLATE

This series of tests was conducted under the following conditions:

• Illumination Wavelength	600 +/- 10 nm (bandpass filter)
• Image Tube Voltage	13.80 kV
• Test Object - Line Input	12.5 micrometers x 500 micrometers
- Point Input	25 micrometer diameter
• Projection Lens	M = 1/5, NA = 0.1
• Analyzer Lens	M = 10, NA = 0.25

3.2.1 Results of the Line Illumination Test

Figure 3.2.1-1 shows a printer plot of the intensity distribution at the image tube phosphor screen. Again, the same scale compression exists as in the previous figures of this type. The contour lines are also similar, the larger enclosing all image points greater than 0.1 x of full scale and the smaller enclosing all points greater than 0.5 x of full scale. Note that full scale in this case is 8 and not the previous 9 to 10.

Figure 3.2.1-2 is a photograph of the analyzer monitor. While the individual fibers can be discerned, they are not as sharply defined as in the case of the 10 micrometer plate. The seemingly speckled nature of the image is a consequence of the very low photon rate in the image and the relatively high gain and short integration times used to create the display at the monitor.

Figure 3.2.1-3 shows the line spread function and the MTF of this 6 micrometer intagliated fiber optic plate. The interpolated MTF = 0.32 at 50 c/mm. This value should be compared with the MTF = 0.30 of the 10 micrometer intagliated plate and the MTF = 0.13 of the non-intagliated 6 micrometer plate of the previous study. Again, the improvement of the intagliated version of the image tube is significant.

* 10 micrometers for the fiber plus 2.5 micrometers for the analyzer.

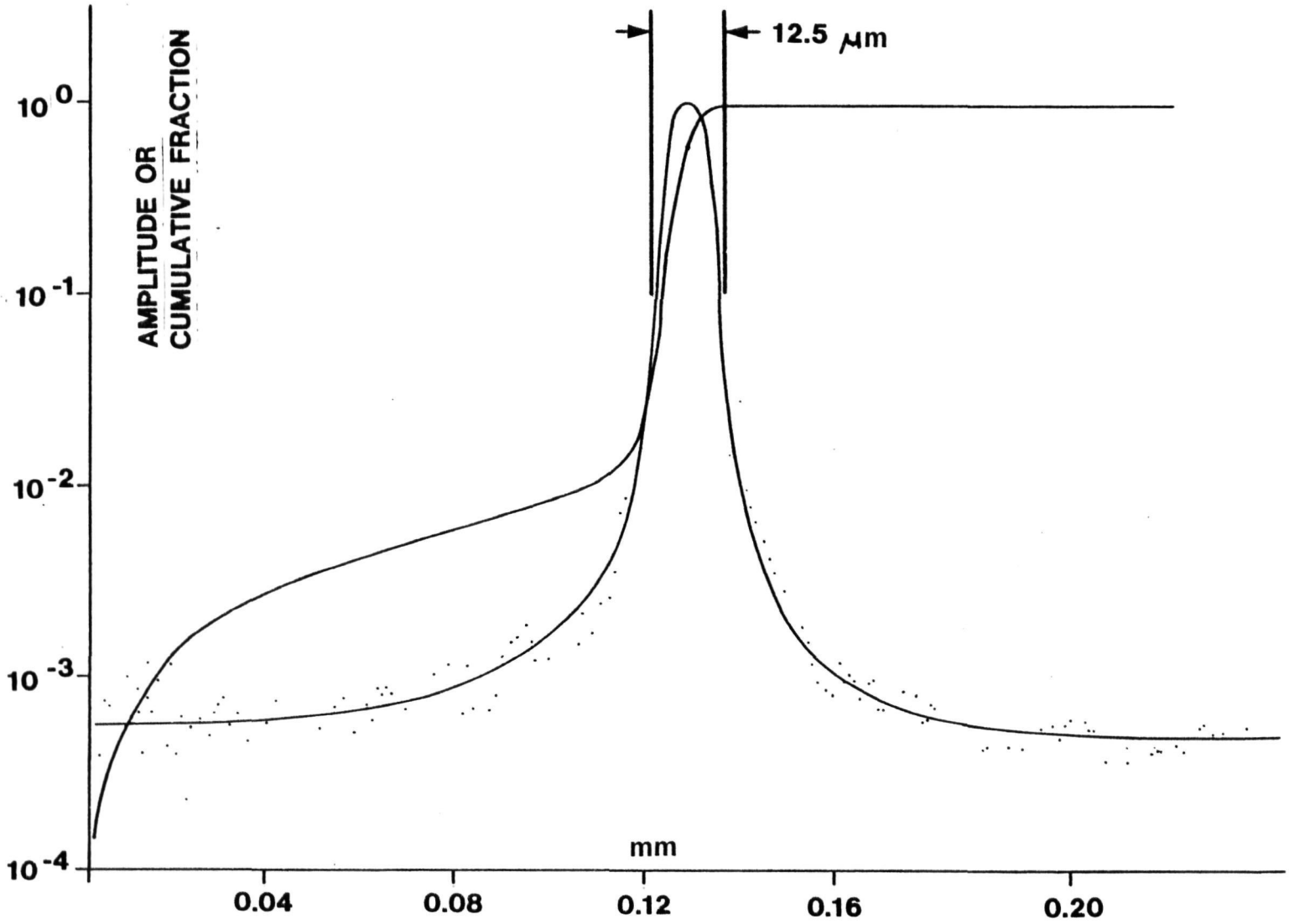

Figure 3.1.2-2. Measured Point Spread Function and Cumulative Distribution Function for a 10 Micrometer, Intagliated, Fiber Optic Plate. Same Data as Figure 3.1.2-1 Replotted on Log Scale.

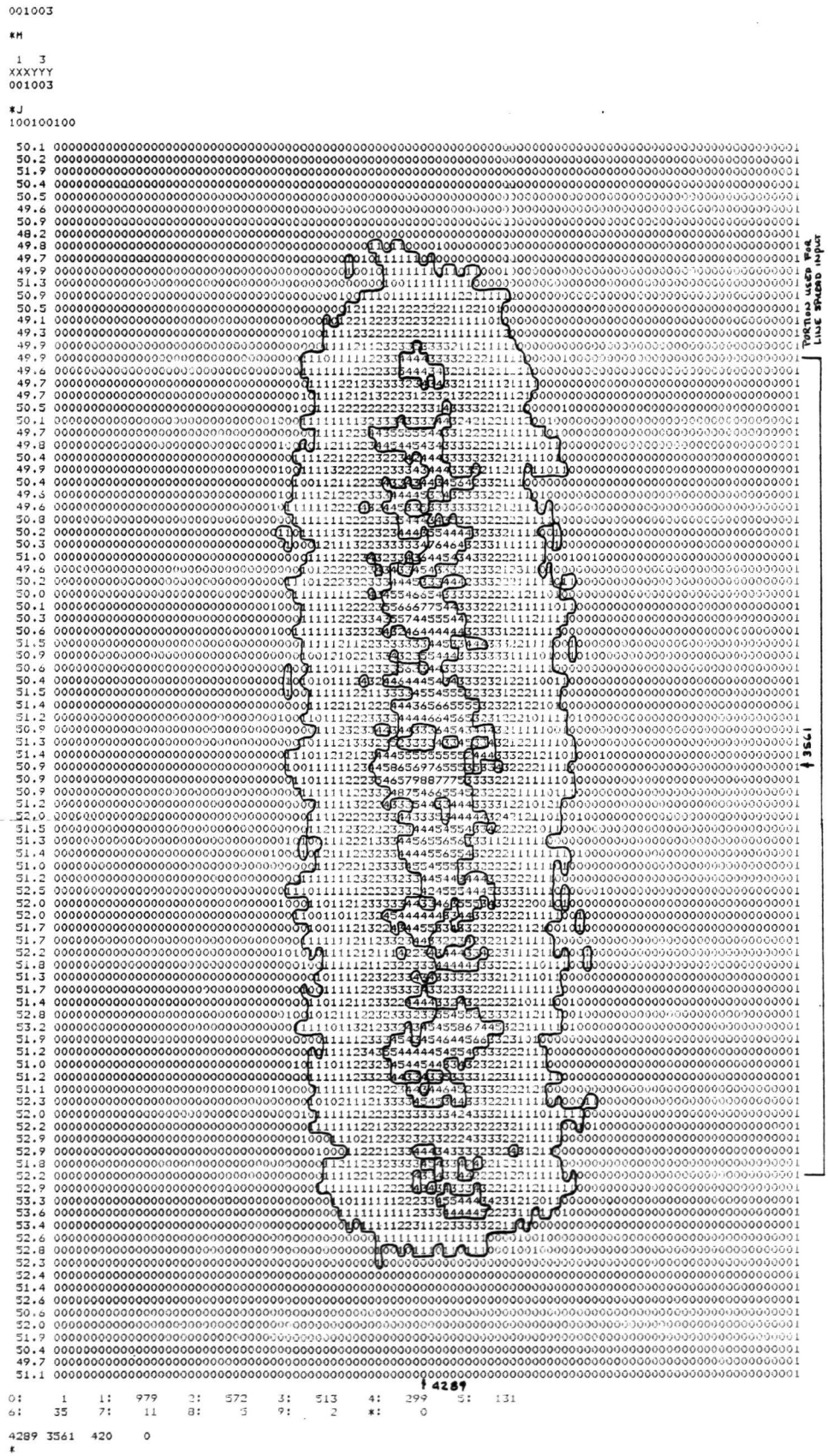

Figure 3.2.1-1. Raster Scan View of Image Tube Line Spread Function. Tube Has 6 Micrometer, Intagliated, Fiber Optic Phosphor Screen (600 nm).

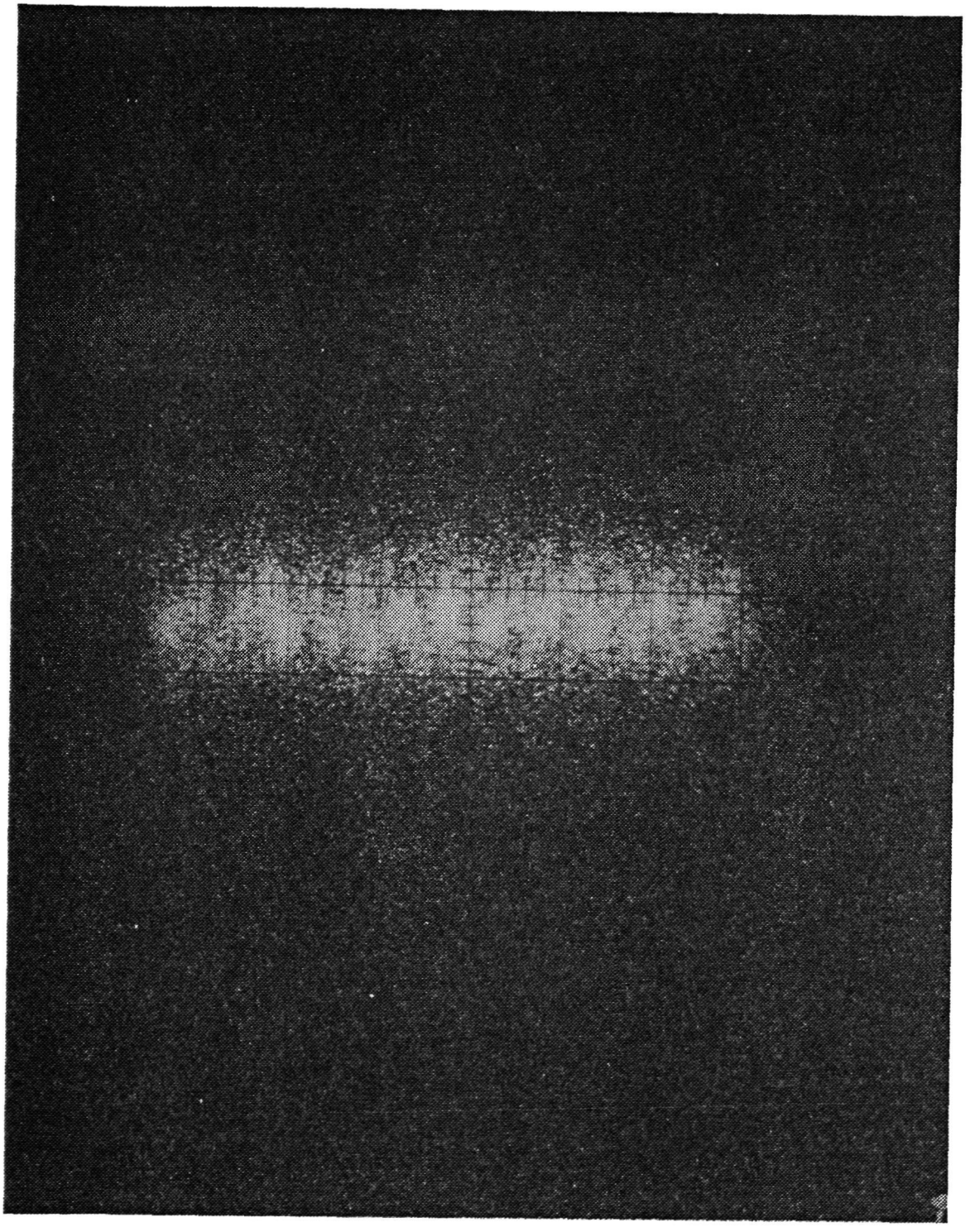

Figure 3.2.1-2. Monitor Photograph of Raster Scan View of Image Tube Line Spread Function. Tube Has 6 Micrometer, Intagliated, Fiber Optic Phosphor Screen (600 nm).

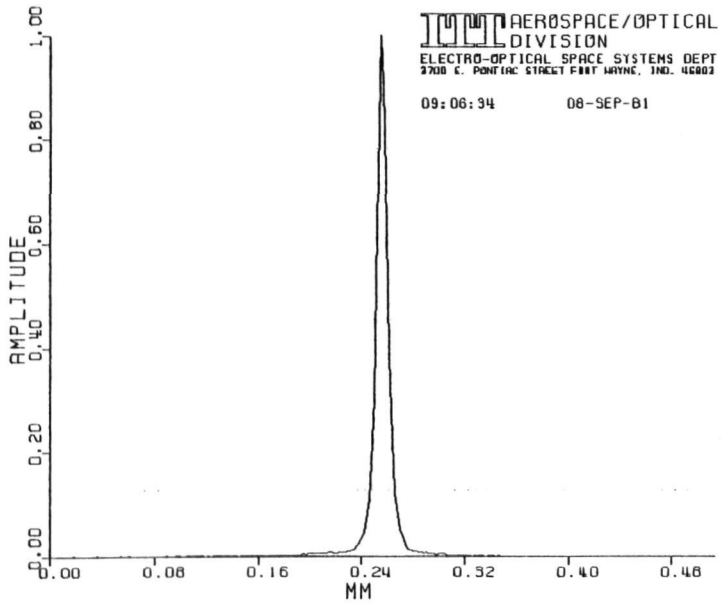

LINE SPREAD FUNCTION

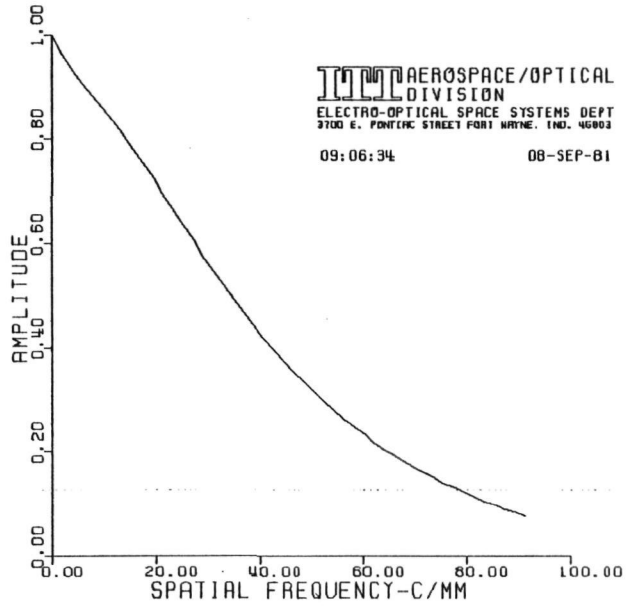

IMAGE TUBE MTF

Figure 3.2.1-3. Measured Line Spread Function and MTF of a Magnetic Focus Image Tube Having a 6 Micrometer, Intagliated, Fiber Optic Phosphor Screen (600 nm).

Sheet 1 of 2

LINE SPREAD DATA LISTING 09:06:34 08-SEP-81

66.	85.	0.	41.	78.	61.	80.	96.	81.	121.	70.	5.	63.	78.	94.	60.
67.	95.	118.	49.	72.	46.	104.	33.	69.	104.	74.	134.	46.	93.	137.	35.
100.	73.	71.	87.	82.	74.	81.	41.	105.	62.	35.	52.	118.	97.	80.	70.
118.	140.	98.	103.	134.	130.	129.	139.	117.	119.	159.	110.	144.	61.	135.	150.
183.	157.	189.	159.	183.	145.	118.	181.	84.	147.	129.	227.	186.	180.	205.	202.
180.	155.	203.	174.	251.	209.	242.	191.	316.	242.	300.	294.	271.	265.	279.	343.
251.	416.	274.	376.	411.	393.	424.	421.	387.	408.	460.	612.	611.	487.	576.	625.
642.	708.	838.	1021.	1184.	1398.	2059.	2981.	4132.	6600.	10271.	16672.	28292.	48960.	77121.	92833.
84530.	58591.	35926.	20830.	11471.	7332.	4592.	3443.	2312.	1394.	1237.	940.	888.	684.	633.	561.
612.	433.	485.	450.	324.	362.	388.	352.	229.	328.	303.	230.	256.	262.	164.	178.
233.	144.	109.	246.	179.	130.	121.	87.	182.	165.	146.	91.	129.	98.	99.	54.
90.	77.	107.	88.	73.	72.	48.	99.	37.	101.	61.	79.	79.	59.	93.	60.
12.	57.	44.	59.	103.	21.	36.	87.	50.	88.	62.	85.	25.	67.	75.	92.
53.	108.	64.	8.	47.	75.	6.	27.	16.	28.	56.	34.	33.	40.	67.	26.
36.	16.	48.	29.	10.	36.	70.	80.	74.	79.	40.	54.	32.	60.	48.	18.
72.	59.	73.	38.	-4.	55.	48.	10.	27.	59.	53.	40.	10.	41.	49.	64.

X0=4289 Y0=3561 XSTEP= 4 YSTEP= 5

MTF AND PTF 09:06:34 08-SEP-81

SPATIAL FREQUENCY C/MM	MTF	PTF	SPATIAL FREQUENCY C/MM	MTF	PTF	SPATIAL FREQUENCY C/MM	MTF	PTF	SPATIAL FREQUENCY C/MM	MTF	PTF
0.0	1.000	0.0	1.9	0.959	1.7	3.9	0.930	2.6	5.8	0.906	3.6
7.8	0.882	4.6	9.7	0.858	5.8	11.6	0.833	6.9	13.6	0.809	8.0
15.5	0.781	9.2	17.5	0.753	10.5	19.4	0.724	11.5	21.3	0.694	12.7
23.3	0.665	13.8	25.2	0.636	14.9	27.2	0.605	16.1	29.1	0.576	17.2
31.1	0.548	18.4	33.0	0.520	19.5	34.9	0.493	20.6	36.9	0.467	21.6
38.8	0.442	22.7	40.8	0.419	24.0	42.7	0.395	25.1	44.6	0.372	26.0
46.6	0.352	27.3	48.5	0.334	28.2	50.5	0.314	29.6	52.4	0.295	30.7
54.3	0.279	31.8	56.3	0.263	33.1	58.2	0.248	34.0	60.2	0.232	35.3
62.1	0.218	36.2	64.0	0.204	37.5	66.0	0.193	38.6	67.9	0.181	39.7
69.9	0.170	40.7	71.8	0.159	42.1	73.8	0.149	43.2	75.7	0.139	44.6
77.6	0.130	46.1	79.6	0.122	48.0	81.5	0.114	49.0	83.5	0.105	50.4
85.4	0.098	51.8	87.3	0.091	52.8	89.3	0.084	54.2	91.2	0.078	55.9

X0=4289 Y0=3561 XSTEP= 4 YSTEP= 5

Figure 3.2.1-3. Measured Line Spread Function and MTF of a Magnetic Focus Image Tube Having a 6 Micrometer, Intagliated, Fiber Optic Phosphor Screen (600 nm).

Sheet 2 of 2

3.2.2 Results of the Point Illumination Test

The stray light suppression properties of the 6 micrometer intagliated phosphor screen were examined by projecting the image of a very small spot of light on to the photocathode. The spot size was 25 micrometer/5 = 5 micrometer diameter. As before in the case of the 10 micrometer plate, great care was taken to align the light with a single fiber. This plate was more difficult to align than the 10 micrometer plate. Figure 3.2.2-1 shows the plotted and tabular results of the test. In this case, there is no pronounced zero in the MTF as was the case for the 10 micrometer plate. The missing zero implies the fiber plate sampling function is more triangular than rectangular. Once again, two additional points marked (+) have been added to the MTF plot. These correspond to the sin(x)/x response of a 6 micrometer sampling function. Correcting for the finite size of the input source and the limitations of the lenses would move the MTF curve closer to the sin(x)/x data points.

Figure 3.2.2-2 is a plot of the same point spread intensity data on a log intensity scale to accentuate the low level scattered light term. The second curve is the cumulative distribution function of the measured point spread data across the diameter of the spot. About 90 percent of the area under the point spread curve is contained within 12.5 micrometer diameter about the center of the fiber. This value should be compared with Figure 3.1.2-2 and its 95 percent value. The difference gives a quantitative footing to the better contrast of the 10 micrometer plate.

Figure 3.2.2-3 is perhaps the most exciting achievement of this study. The 5 micrometer spot of light was very carefully moved so that it centered on the web between the fibers. As can be seen, the bifurcated peak is quite visible. This figure should be compared with Figures 2.2.1-1 through 2.2.1-5 and 2.2.2-1 through 2.2.2-3 of the analytical model. The model predicted that such a feature could be seen if the stray light could be controlled.

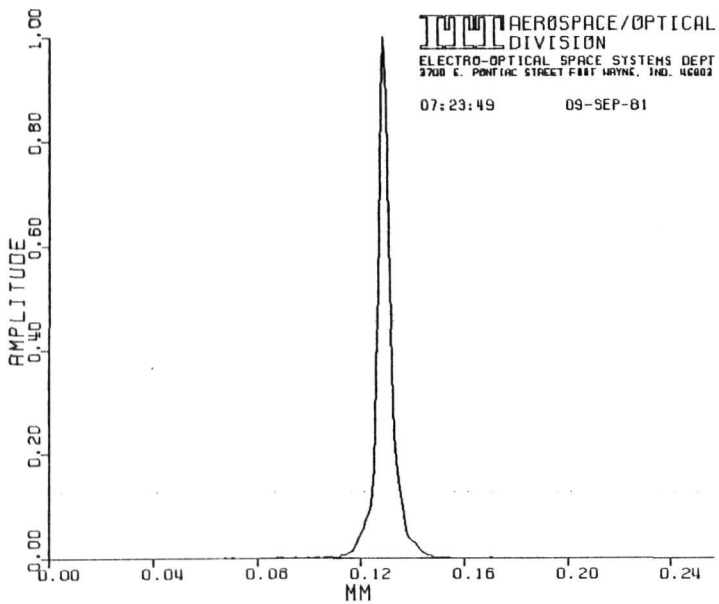

POINT SPREAD FUNCTION

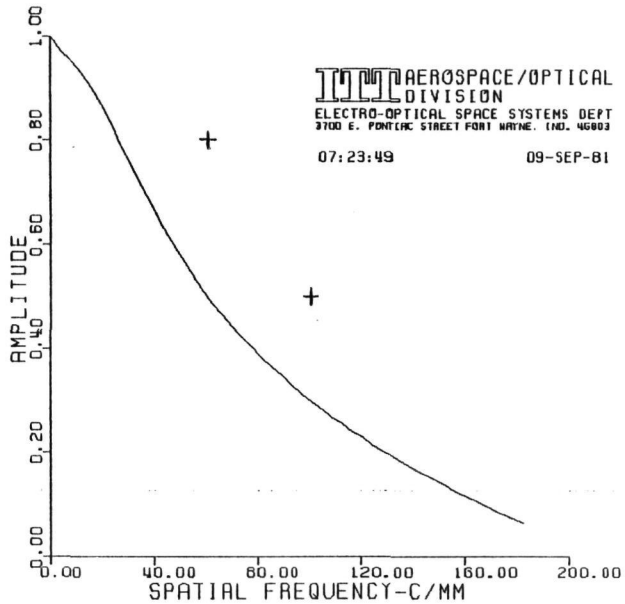

IMAGE TUBE MTF

Figure 3.2.2-1. Measured Point Spread Function and MTF of a Magnetic Focus Image Tube Having a 6 Micrometer, Intagliated, Fiber Optic Screen (600 nm). The 5 Micrometer Input Spot of Light Was Centered on a Single Fiber.

Sheet 1 of 2

POINT SPREAD DATA LISTING 07:23:49 09-SEP-81

43.	-24.	68.	70.	86.	81.	70.	122.	95.	108.	86.	50.	78.	47.	35.	45.
79.	75.	8.	76.	55.	76.	83.	76.	83.	69.	39.	61.	37.	131.	109.	49.
65.	29.	45.	40.	86.	61.	119.	84.	89.	65.	56.	64.	112.	109.	102.	103.
104.	113.	74.	46.	85.	99.	107.	116.	21.	51.	69.	51.	53.	109.	93.	67.
98.	63.	79.	138.	125.	107.	148.	73.	54.	85.	108.	58.	53.	81.	93.	93.
94.	62.	56.	87.	87.	96.	85.	158.	160.	144.	66.	92.	108.	121.	138.	107.
77.	93.	111.	138.	108.	133.	180.	170.	137.	219.	172.	216.	141.	262.	323.	407.
433.	663.	797.	1016.	1327.	1940.	3448.	5349.	6355.	8175.	9331.	11501.	18849.	38160.	68488.	96945.
109999.	97103.	68059.	40092.	25798.	18101.	14853.	10679.	7293.	4923.	4114.	3440.	3038.	2565.	1754.	1142.
791.	659.	574.	411.	328.	280.	256.	259.	179.	177.	121.	113.	75.	85.	118.	52.
56.	100.	122.	95.	68.	49.	96.	95.	98.	142.	101.	90.	60.	63.	100.	104.
45.	100.	105.	109.	79.	64.	78.	84.	81.	95.	110.	121.	53.	95.	48.	124.
79.	97.	93.	60.	88.	72.	87.	67.	77.	67.	78.	116.	44.	45.	51.	51.
16.	57.	6.	52.	62.	38.	29.	61.	63.	49.	94.	77.	66.	30.	39.	27.
42.	32.	68.	29.	38.	65.	62.	53.	51.	44.	26.	11.	66.	12.	9.	-7.
15.	82.	80.	105.	73.	63.	35.	57.	60.	77.	35.	39.	69.	16.	56.	59.

X0=4135 Y0=4095 XSTEP= 2 YSTEP= 1

MTF AND PTF 07:23:49 09-SEP-81

SPATIAL FREQUENCY C/MM	MTF	PTF	SPATIAL FREQUENCY C/MM	MTF	PTF	SPATIAL FREQUENCY C/MM	MTF	PTF	SPATIAL FREQUENCY C/MM	MTF	PTF
0.0	1.000	0.0	3.9	0.971	-0.4	7.8	0.952	-1.0	11.6	0.930	-1.3
15.5	0.902	-1.7	19.4	0.867	-2.0	23.3	0.830	-2.3	27.2	0.791	-2.4
31.1	0.752	-2.5	34.9	0.713	-2.5	38.8	0.675	-2.5	42.7	0.640	-2.5
46.6	0.606	-2.6	50.5	0.575	-2.4	54.3	0.543	-2.4	58.2	0.516	-2.4
62.1	0.489	-2.5	66.0	0.466	-2.3	69.9	0.443	-2.4	73.8	0.422	-2.3
77.6	0.402	-2.3	81.5	0.383	-2.3	85.4	0.364	-2.0	89.3	0.346	-1.9
93.2	0.329	-1.5	97.0	0.313	-1.3	100.9	0.297	-0.6	104.8	0.282	-0.0
108.7	0.267	0.7	112.6	0.254	1.6	116.4	0.241	2.4	120.3	0.230	3.3
124.2	0.216	4.4	128.1	0.203	5.2	132.0	0.193	5.9	135.9	0.181	7.0
139.7	0.170	7.3	143.6	0.160	7.8	147.5	0.149	8.1	151.4	0.139	8.4
155.3	0.128	8.4	159.1	0.118	7.5	163.0	0.109	7.8	166.9	0.100	6.8
170.8	0.091	6.6	174.7	0.083	5.1	178.6	0.074	4.6	182.4	0.066	4.0

X0=4135 Y0=4095 XSTEP= 2 YSTEP= 1

Figure 3.2.2-1. Measured Point Spread Function and MTF of a Magnetic Focus Image Tube Having a 6 Micrometer, Intagliated, Fiber Optic Screen (600 nm). The 5 Micrometer Input Spot of Light Was Centered on a Single Fiber. Sheet 2 of 2

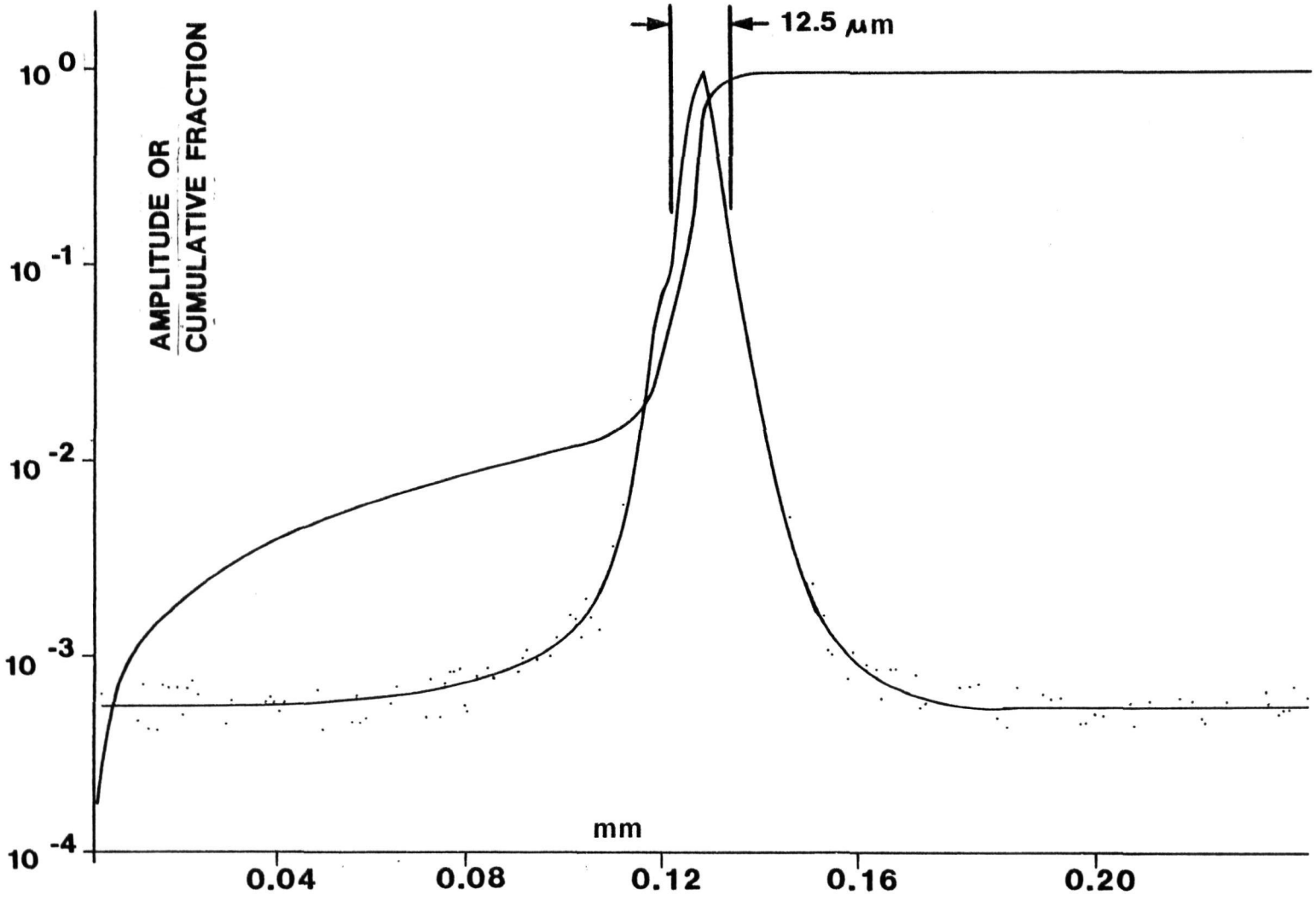

Figure 3.2.2-2. Measured Point Spread Function and Cumulative Distribution Function for a 6 Micrometer, Intagliated, Fiber Optic Plate. Same Data as Figure 3.2.2-1 But Replotted on Log Scale.

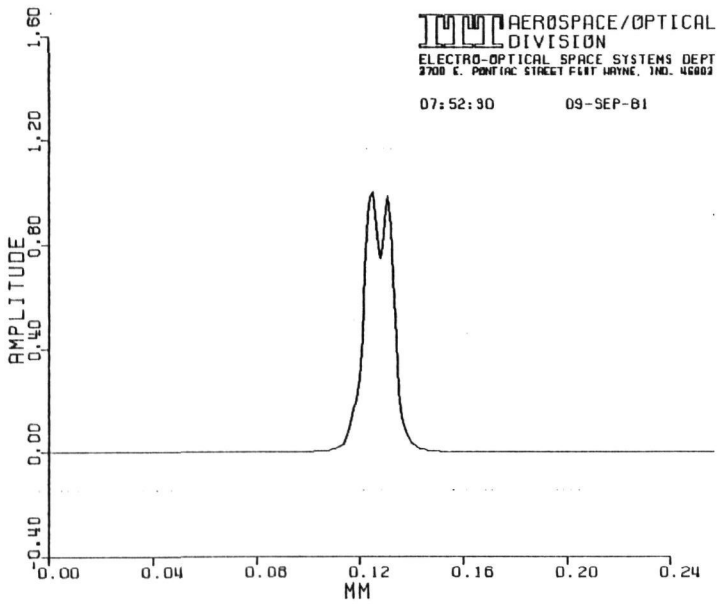

POINT SPREAD FUNCTION

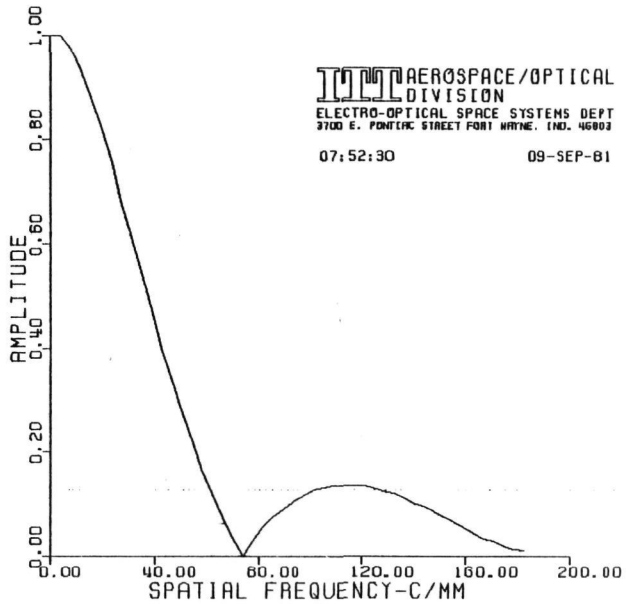

IMAGE TUBE MTF

Figure 3.2.2-3. Measured Point Spread Function and MTF of a Magnetic Focus Image Tube Having a 6 Micrometer, Intagliated, Fiber Optic Screen (600 nm). The 5 Micrometer Optical Input was Centered on the Interface Web Between Two Fibers.

CAMERA VIDEO OFFSET IS OUT OF RANGE. OFFSET IS 20

POINT SPREAD DATA LISTING 07:52:30 09-SEP-81

-27.	-120.	34.	-44.	-109.	-9.	-114.	-69.	4.	14.	-122.	21.	-9.	-1.	37.	-110.
-100.	-63.	-60.	19.	-127.	-122.	-135.	-80.	-26.	44.	-44.	-40.	-168.	-9.	-38.	-19.
-83.	-20.	72.	47.	2.	-43.	-20.	-71.	-3.	-25.	-69.	-3.	-58.	-35.	-98.	-71.
24.	-52.	-54.	23.	27.	-64.	-77.	-25.	-15.	-58.	-108.	20.	-81.	94.	-7.	-45.
-47.	-84.	43.	-16.	14.	-19.	-124.	35.	13.	-31.	23.	26.	-63.	-134.	-53.	-15.
-3.	-1.	177.	112.	76.	55.	60.	-25.	19.	-25.	163.	29.	89.	69.	125.	-14.
166.	154.	44.	204.	165.	235.	363.	285.	470.	416.	582.	441.	995.	1302.	1527.	1706.
2186.	2882.	5056.	7503.	11891.	15867.	18935.	27218.	42308.	66555.	86660.	93412.	95182.	86851.	75695.	70853.
75148.	88956.	93786.	82705.	63829.	41250.	22481.	12643.	10189.	7421.	5056.	3524.	2957.	1917.	1396.	1450.
1363.	681.	558.	418.	424.	286.	235.	58.	-39.	-13.	-57.	15.	46.	-40.	-70.	-50.
-41.	-105.	-10.	29.	-19.	24.	-4.	105.	36.	-94.	-127.	6.	-123.	-113.	-58.	-7.
-92.	-63.	75.	4.	-15.	-66.	35.	-4.	7.	-13.	-24.	-44.	-53.	-42.	87.	79.
99.	-58.	-115.	-48.	-28.	-97.	-78.	23.	28.	-130.	-118.	-36.	-143.	-19.	-54.	-28.
-103.	-40.	-81.	-11.	-118.	-50.	-20.	-42.	-85.	-83.	-116.	-121.	-129.	-105.	-39.	-30.
-37.	-137.	-50.	-47.	-88.	85.	-5.	-123.	-197.	-177.	-86.	-159.	22.	-139.	-12.	-39.
-56.	-49.	-112.	-180.	-166.	-67.	1.	-89.	-125.	-26.	88.	-94.	-60.	-94.	9.	-123.

X0=3959 Y0=4076 XSTEP= 2 YSTEP= 1

MTF AND PTF 07:52:30 09-SEP-81

SPATIAL FREQUENCY C/MM	MTF	PTF	SPATIAL FREQUENCY C/MM	MTF	PTF	SPATIAL FREQUENCY C/MM	MTF	PTF	SPATIAL FREQUENCY C/MM	MTF	PTF
0.0	1.000	0.0	3.9	1.001	2.6	7.8	0.972	5.0	11.6	0.932	7.6
15.5	0.881	9.9	19.4	0.820	12.3	23.3	0.754	14.7	27.2	0.683	17.2
31.1	0.612	19.6	34.9	0.540	22.0	38.8	0.468	24.3	42.7	0.401	26.6
46.6	0.337	29.0	50.5	0.276	30.9	54.3	0.218	33.1	58.2	0.164	34.9
62.1	0.116	36.4	66.0	0.073	38.5	69.9	0.035	42.1	73.8	0.001	68.9
77.6	0.028	41.0	81.5	0.054	44.9	85.4	0.076	45.9	89.3	0.091	46.6
93.2	0.106	48.0	97.0	0.116	49.2	100.9	0.126	51.1	104.8	0.131	52.3
108.7	0.134	53.9	112.6	0.136	54.8	116.4	0.136	56.2	120.3	0.134	56.9
124.2	0.130	59.0	128.1	0.125	61.2	132.0	0.120	62.0	135.9	0.111	63.9
139.7	0.104	65.8	143.6	0.095	67.7	147.5	0.085	69.6	151.4	0.075	70.8
155.3	0.064	72.5	159.1	0.055	73.8	163.0	0.044	74.0	166.9	0.034	72.7
170.8	0.027	71.4	174.7	0.018	67.2	178.6	0.014	62.5	182.4	0.009	41.4

X0=3959 Y0=4076 XSTEP= 2 YSTEP= 1

Figure 3.2.2-3. Measured Point Spread Function and MTF of a Magnetic Focus Image Tube Having a 6 Micrometer, Intagliated, Fiber Optic Screen (600 nm). The 5 Micrometer Optical Input was Centered on the Interface Web Between Two Fibers.

Sheet 2 of 2

Section 4

A FILM DENSITOMETRY METHOD FOR COMBINED TUBE AND FILM SPATIAL FREQUENCY RESPONSE MEASUREMENT

This section describes the means used to measure the spatial frequency response of an image tube and film combination. As in the electronic method, this method uses the Fourier Transform relationship between the line spread function and the MTF.

Figure 4-1 illustrates the test setup used for the film exposures. It is basically the same setup used for the previous film tests. The notable differences for the present tests are the use of a 600 nm center wavelength filter versus the previous 500 nm filter and a 5x NA 0.1 lens versus the previous 10x NA 0.25 lens for the test image input.

The image of the narrow slit of light was projected onto the photocathode. Film was held in pressure contact with the image tube fiber optic window. Recorded in the film were multiple images of the output slit in an exposure series. A second piece of film from the same roll recorded a contact copy of a calibrated gray scale step wedge. Both films, the gray scale and the slit image films, were developed in the same baths at the same time. Other details about the film and experimental technique are in the earlier report.

A microdensitometer was used to extract the slit image profile from the film. Tests of the microdensitometer resolution using different sampling apertures, 2 x 2 micrometers square and 100 x 1 micrometers rectangular, showed its spatial frequency response to be in excess of 100 c/mm at 50 percent modulation.

Before the slit image profile can be used as input data to the Fourier Transform process, the data must be converted to intensity values. This is the role of the step wedge photograph. The measured density versus intensity data are curve fit to an analytical function. Figure 4-2 is an example of the characteristic curve for the film used for the tests. The film has a great deal of contrast; the gamma for the mid-section of the curve is 2.7.

In the following sections, the image profiles are density space data and are so labeled. The linespread functions are intensity space data and are derived from the density data using each film sample's characteristic curve. It is the intensity space data that is ultimately used in the MTF computation.

The image tube used for the following film tests was the same tube used for the electronic MTF tests.

4.1 RESULTS OF THE DENSITOMETRY TESTS OF THE 10 MICROMETER INTAGLIATED FIBER OPTIC PLATE AND FILM COMBINATION

Figure 4.1-1 is a series of photomicrographs of one of the

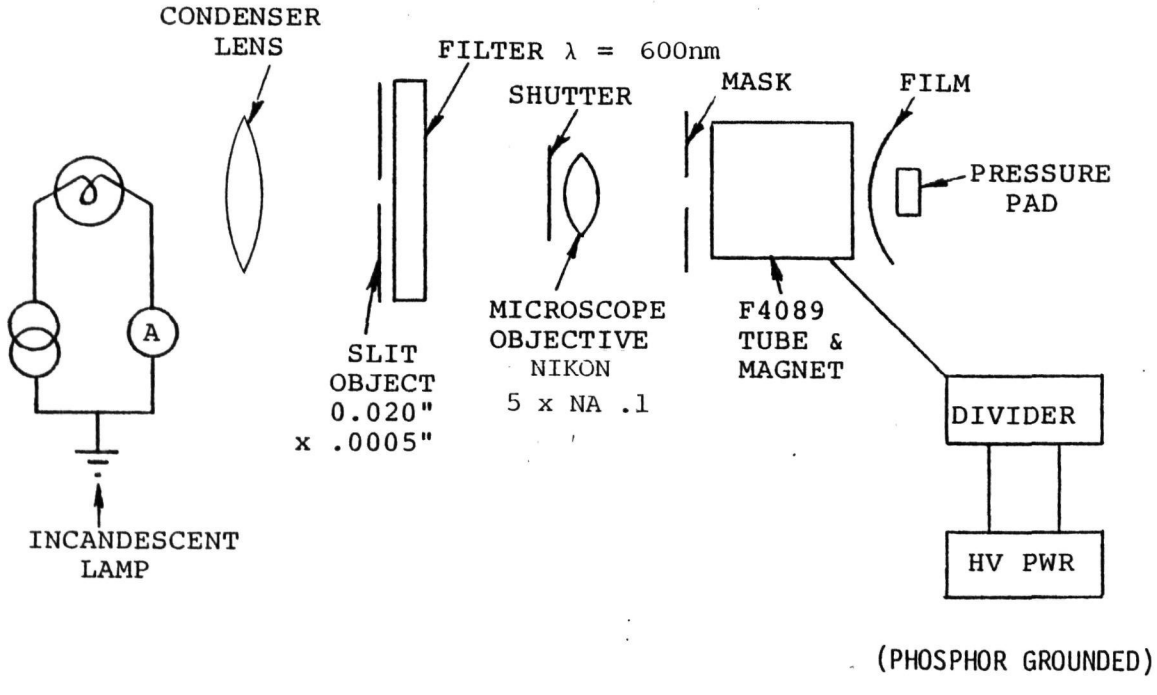

Figure 4-1. Setup for the I^2 - Film Combination Resolution Tests

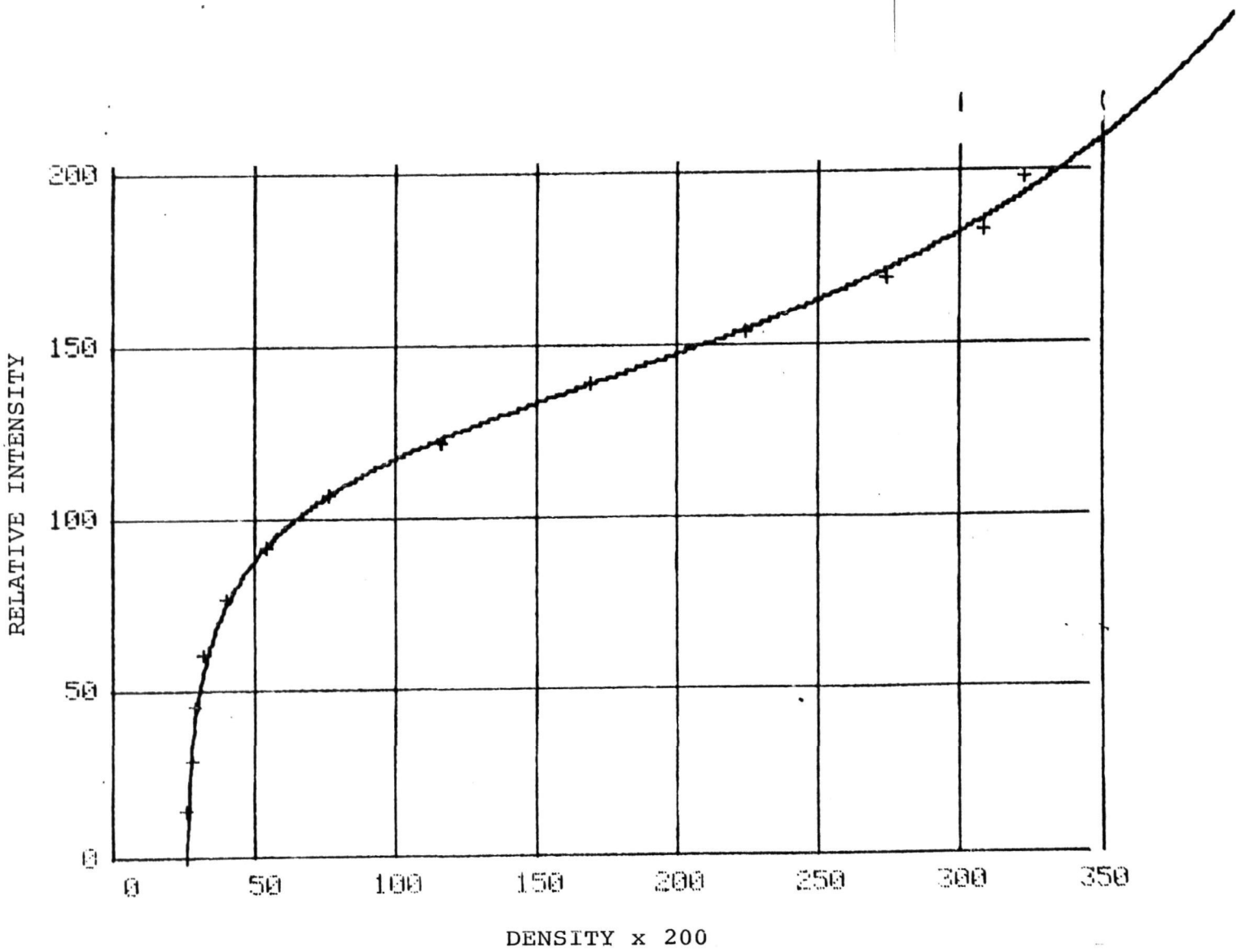

Figure 4-2. Sample of the Density to Intensity Space Conversion Curve Used. The "+" are the Measured Points. The Smooth Curve is the Best Fit of an Analytical Function to the Data.

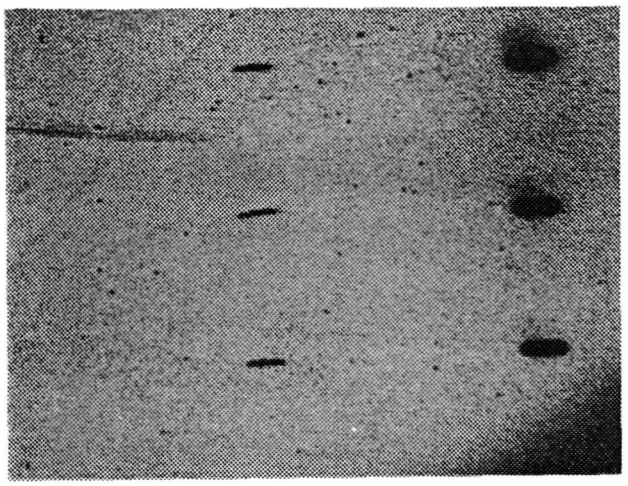

A

RELATIVE MAGNIFICATION
1X

RELATIVE MAGNIFICATION
4X

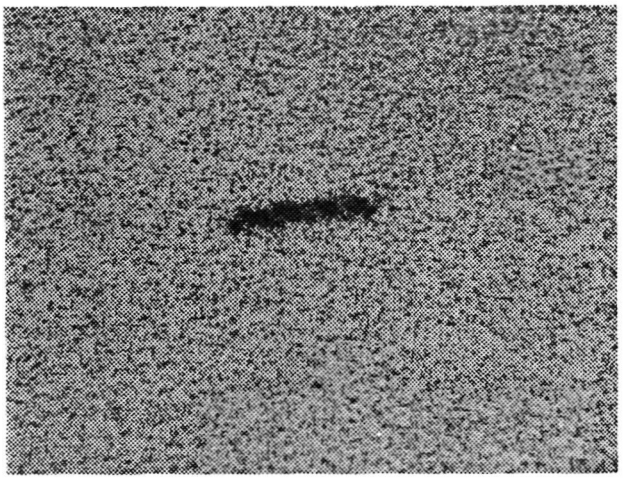

B

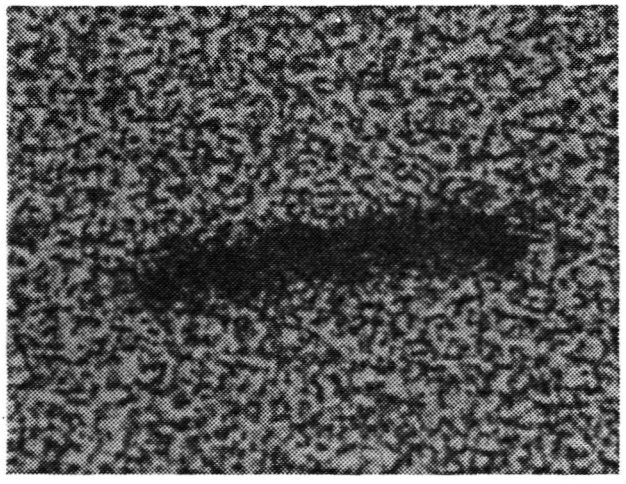

C

RELATIVE MAGNIFICATION
10X

Figure 4.1-1. Photomicrographs of the Slit Image Recorded in the Film for the 10 Micrometer, Intagliated, Fiber Optic Window. (X322-88A-F)

samples exposed using the 10 micrometer intagliated fiber optic plate portion of the image tube. The top photo shows a portion of the exposure series recorded in the film. At higher magnification, the result of the individual exposure of each of the 10 micrometer fibers in the image can be seen. The mathematical dimensions of the recorded features in the film are 100 micrometers x 2.5 micrometers, based upon the calibrated magnifications. The recorded dimensions are about 100 micrometers in the long direction x 15 to 20 micrometers in the shorter direction. The width is approximately two fibers in size. It is interesting to compare the image in Figure 4.1-1B with that of Figure 3.1.1-2. They are both 10 micrometer plate images; both are from approximately the same region of the plate. It could be said that there is sharper definition of the fibers in the electronic case.

Figure 4.1-2 shows the densitometry results of the entire exposure series, part of which is depicted in Figure 4.1-1. The leftmost plot of the groups of three is the density data (log intensity). The middle plot is the intensity plot or line spread function. The rightmost plot is the calculated MTF curve. Each of the groups of three is a different exposure progressing from the minimum exposure to just below saturation. The image in 4.1-1B or C corresponds to 4.1-2B. The densitometer scan was 256 steps of 2 micrometers per step; therefore, the horizontal scale is 512 micrometers long and the spatial frequency scale is zero to 240 c/mm.

4.2 RESULTS OF THE DENSITOMETRY TESTS OF THE 6 MICROMETER INTAGLIATED FIBER OPTIC PLATE AND FILM COMBINATION

Figure 4.2-1 is a series of microphotographs of one of the film samples exposed using the 6 micrometer intagliated fiber optic portion of the image tube. The top photo shows a portion of the exposure series recorded in the film. At higher magnification, the individual fibers do not seem to be resolved. The size of this image recorded in the film is very close to that for the 10 micrometer (Figure 4.1-1) plate.

Figure 4.2-2 shows the densitometry results of the exposure series depicted in Figure 4.2-1. As before, the leftmost plot of the groups of three is that of the line profile (log intensity). The middle plot is the line spread function derived from the profile using the measured film characteristics curve. Each of the groups of three is for different exposure levels, from minimum to just into saturation.

4.3 RESULTS OF THE DENSITOMETRY TESTS OF THE 6 MICROMETER NON-INTAGLIATED FIBER OPTIC PLATE AND FILM COMBINATION

One of the film test samples obtained during the previous study was remeasured during this study. Figure 4.3-1 is a series of microphotographs of this film sample. It was originally exposed using 10x demagnification of the slit onto the photocathode; therefore, the different aspect ratio of the image when compared to the more recent tests. The tube used for the previous tests was a F4089 but had a non-intagliated 6 micrometer fiber optic phosphor screen.

A

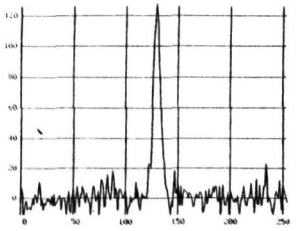

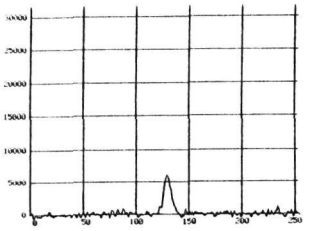

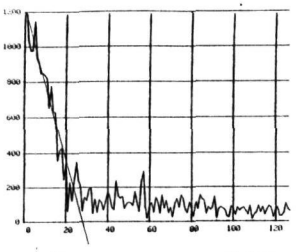

B

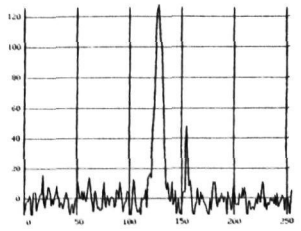

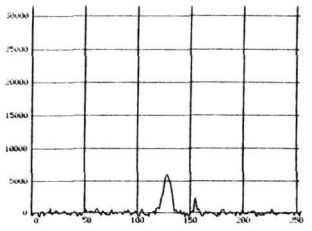

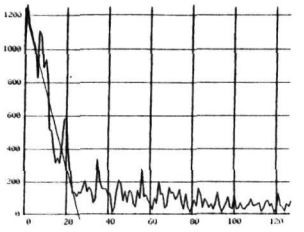

C

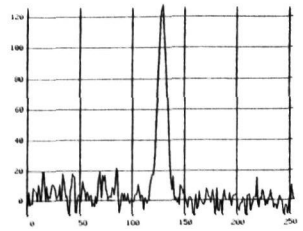

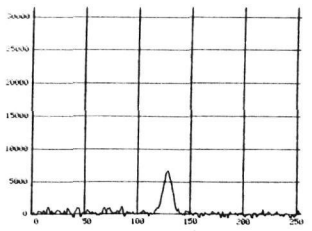

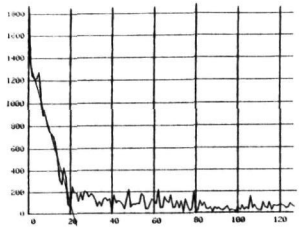

Figure 4.1-2. Densitometry Results and Calculated MTF for 10 Micrometer, Intagliated Phosphor Screen and Film Combination. Plots are Grouped by Increasing Exposure. (X322-88A-F)

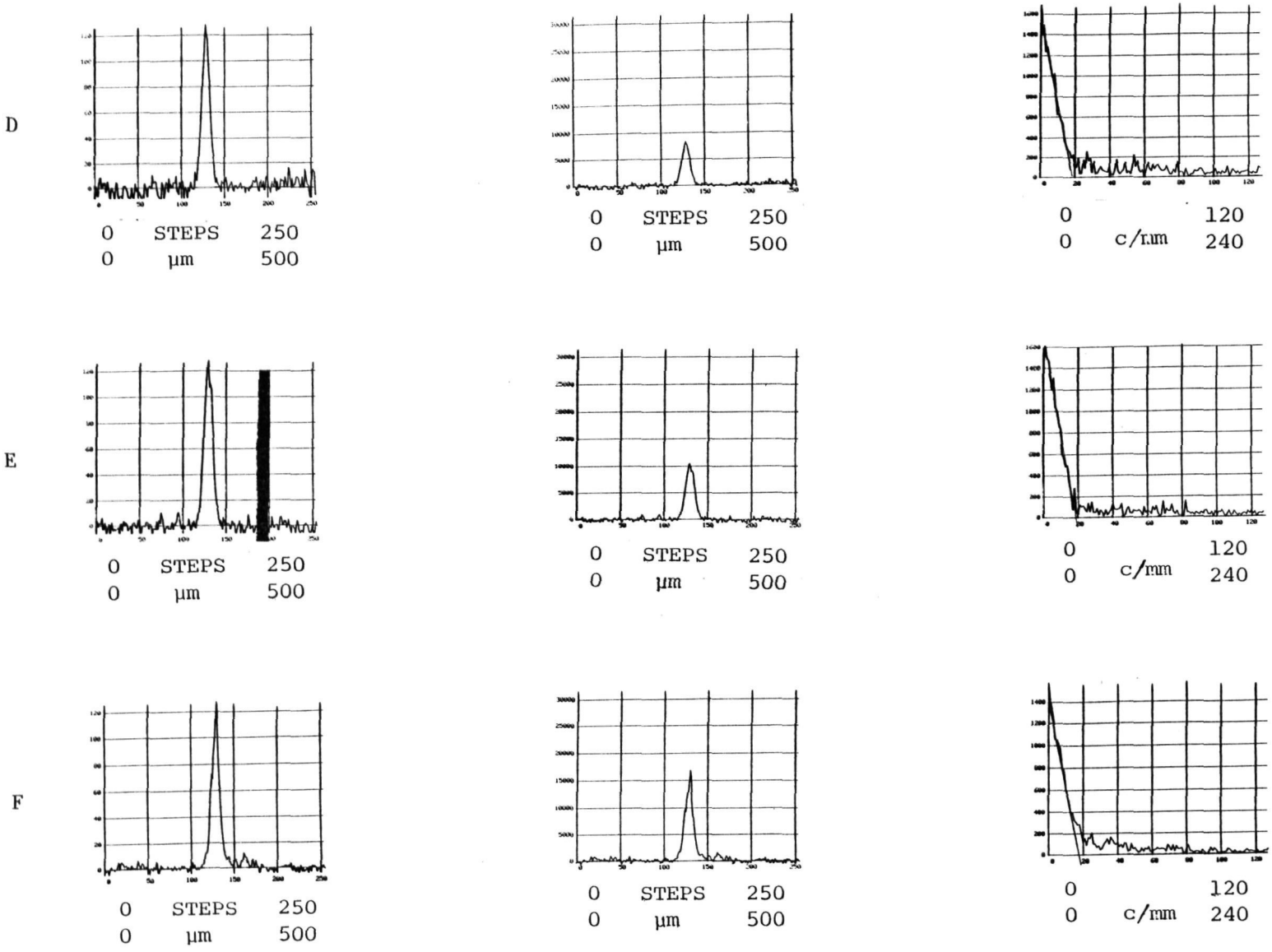

Figure 4.1-2. Densitometry Results and Calculated MTF for 10 Micrometer, Intagliated Phosphor Screen and Film Combination. Plots are Grouped by Increasing Exposure. (X322-88A-F)

Sheet 2 of 2

A

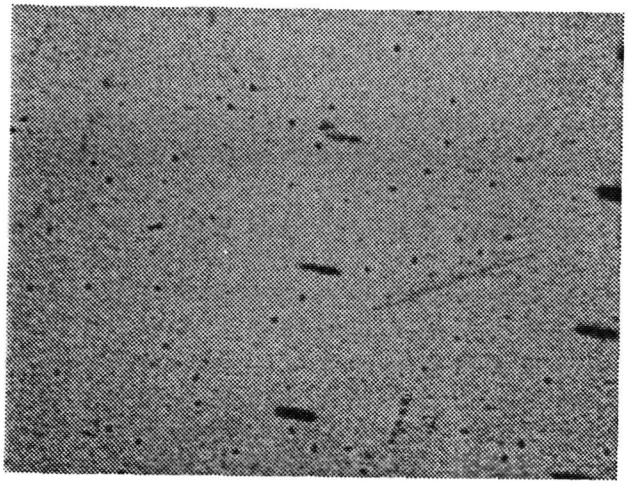

RELATIVE MAGNIFICATION
1X

RELATIVE MAGNIFICATION
4X

B

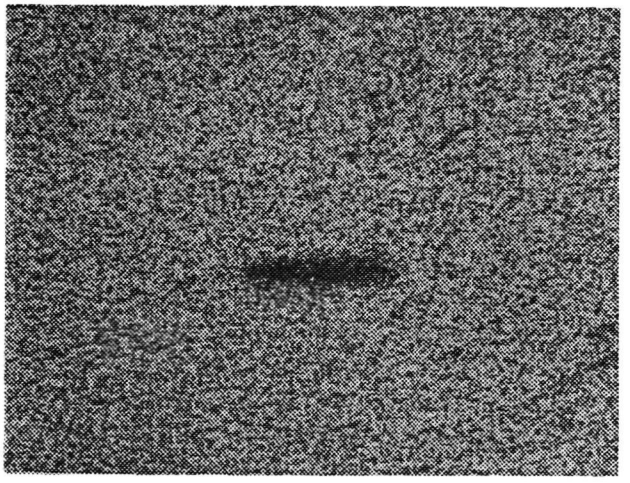

C

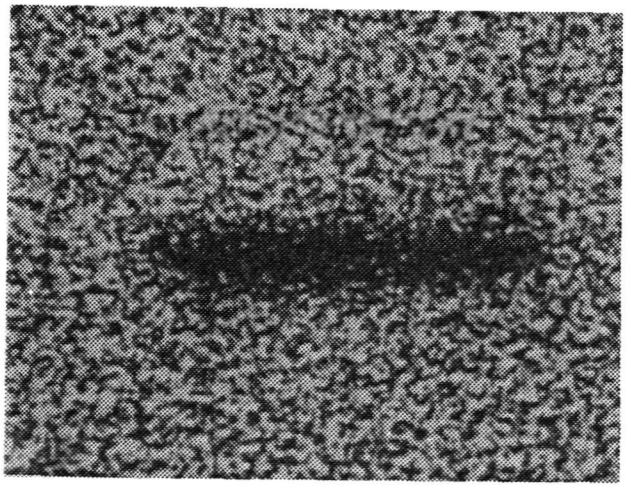

RELATIVE MAGNIFICATION
10X

Figure 4.2-1. Photomicrographs of the Slit Image Recorded in the Film for the 6 Micrometer, Intagliated, Fiber Optic Windows.

A

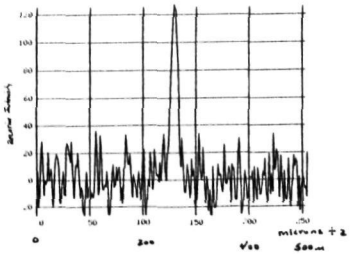

0 STEPS 250
0 µm 500

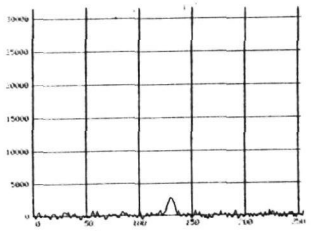

0 STEPS 250
0 µm 500

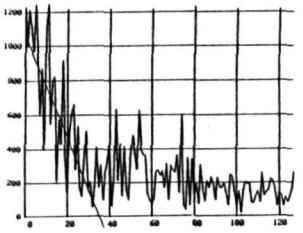

0 120
0 c/mm 240

B

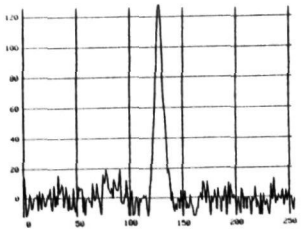

0 STEPS 250
0 µm 500

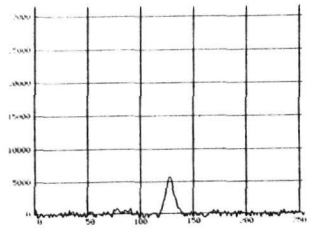

0 STEPS 250
0 µm 500

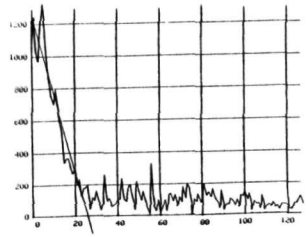

0 120
0 c/mm 240

C

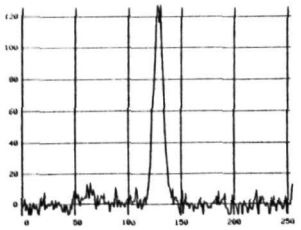

0 STEPS 250
0 µm 500

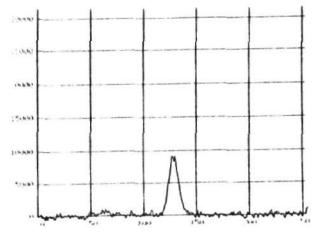

0 STEPS 250
0 µm 500

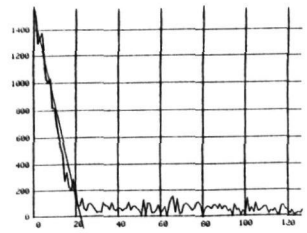

0 120
0 c/mm 240

Figure 4.2-2 Densitometry Results and Calculated MTF for 6 Micrometer, Intagliated Phosphor Screen and Film Combination. Plots are Grouped by Increasing Exposure. (X322-88A-F)

D

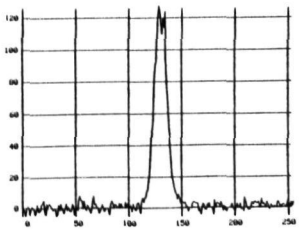

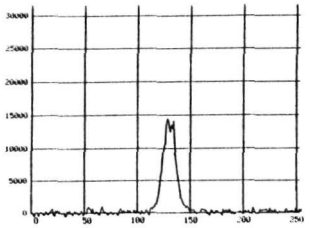

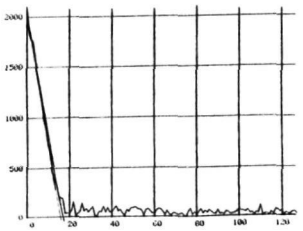

E

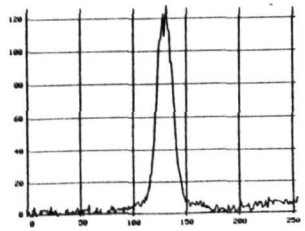

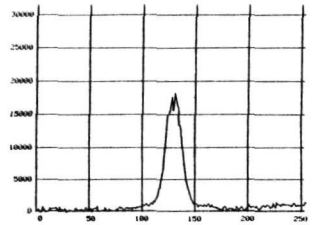

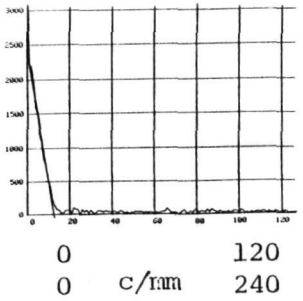

Figure 4.2-2 Densitometry Results and Calculated MTF for 6 Micrometer, Intagliated Phosphor Screen and Film Combination. Plots are Grouped by Increasing Exposure. (X322-88A-F)

Sheet 2 of 2

A

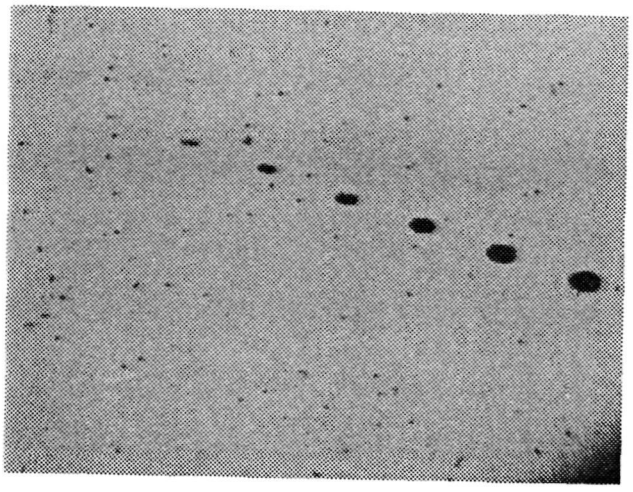

RELATIVE MAGNIFICATION
1X

RELATIVE MAGNIFICATION
4X

B

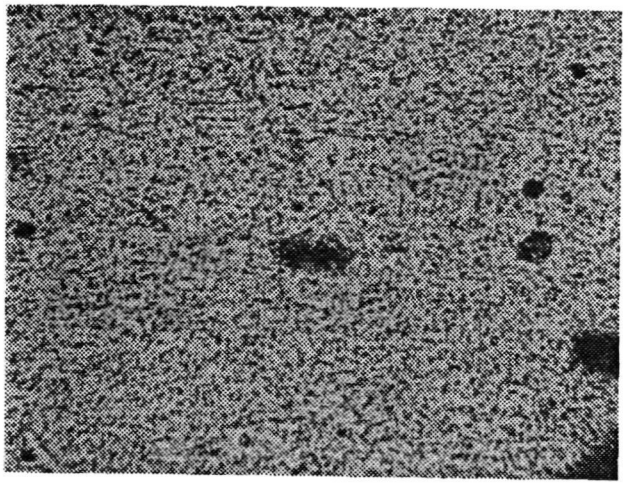

C

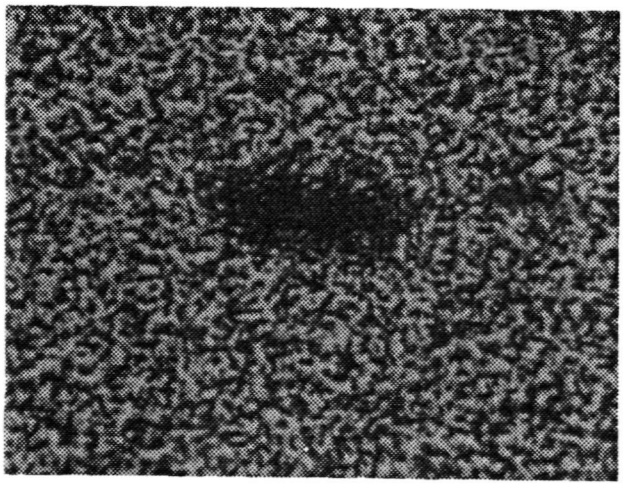

RELATIVE MAGNIFICATION
10X

Figure 4.3-1. Photomicrographs of the Slit Image Recorded in the Film for the 6 Micrometer, Non-Intagliated, Fiber Optic Film Combination. (X322-88A-F). The Projected Slit is One-Half the Size of That Used for Figures 4.1-1 and 4.2-1.

Figure 4.3-2 shows the densitometry results of the exposure series in Figure 4.3-1. Again, the leftmost plot of the group is the line profile (log intensity). The middle plots of the line spread function are missing from this series. The rightmost plot is the MTF. Each of the groups are for different exposure levels, progressing from the minimum exposure to just below saturation.

A

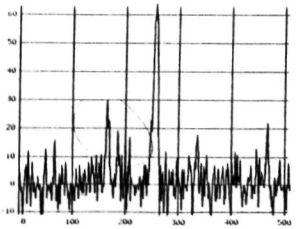

0 STEPS 250
0 µm 500

NO PLOT AVAILABLE

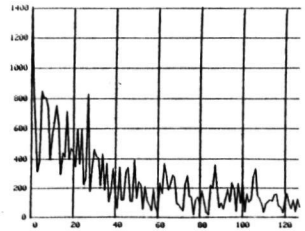

0 120
0 c/mm 240

B

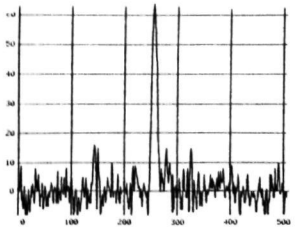

0 STEPS 250
0 µm 500

NO PLOT AVAILABLE

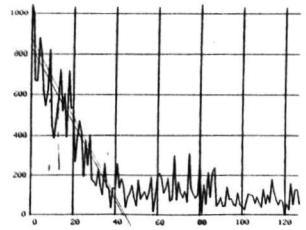

0 120
0 c/mm 240

C

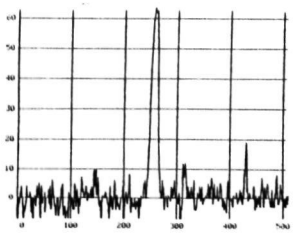

0 STEPS 250
0 µm 500

NO PLOT AVAILABLE

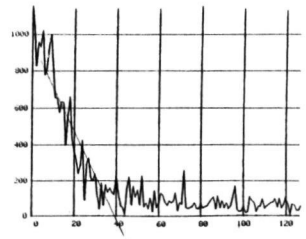

0 120
0 c/mm 240

Figure 4.3-2. Densitometry Results and Calculated MTF for 6 Micrometer, Non-Intagliated, Phosphor Screen and Film Combination. This is Remeasurement of Prior Data. (X322-88A-F)

Section 5

SUMMARY AND CONCLUSIONS

The tube and film combination performance results are summarized in Tables 5-1 and 5-2. Examination of the table entries shows that there is a resolution improvement between the previous 6 micrometer non-intagliated screen tests and the present 6 and 10 micrometer intagliated screen tests. Depending upon the exposure level, the improvement is a few percent to 50 percent increase in the spatial frequency for 50 percent modulation.

The exposure level dependence of the resolution requires some explanation. In the course of this explanation, it is shown that exposure dependence of resolution is a property of film in general and the test film in particular. It is also shown that there remains a significant amount of light that exits the fiber plate at large angles to the plate surface normal and that this light is probably not caused by lateral propagation in the phosphor screen or the fiber plate.

Film response to light is described by a log-exposure versus density curve. There are three important aspects to this curve - the minimum density or fog level, the total exposure scale and its slope, and the maximum density or saturation level. To be detectable, a light exposure must cause a density above the fog level. The total range of recordable light exposures falls between fog and saturation. The film used for these tests had a very steep slope in the linear exposure range, gamma = 2.7. Good line spread functions have a large range of intensity. Consequently, any test exposure is only a small fraction of the entire line profile. The profiles tend to be clipped in width because of the fog level or in amplitude because of an onset of saturation effects. It therefore becomes quite difficult to state a resolution number independent of exposure. The film used for the tests was not the best choice for quantitative line spread analysis. A wide latitude or low gamma film would be better.

The assertion that the stray light affecting film recorded resolution caused by large angle rays can be supported by comparing the electronic and film test results. It must be remembered that the electronic test records rays falling within a 14-degree, half-angle cone of acceptance while film approximates a 90-degree, half-angle cone. Electronically measured line spread functions show relatively steep sides to the 1-3 percent amplitude level; see Figures 3.1.2-2 and 3.2.2-2. At 45 micrometer line widths, the amplitude is 0.5 percent. Film recorded line widths show 10 percent amplitude at 45-60 micrometers. The light rays are, therefore, at large angles.

The source of the large angle rays is still the phosphor screen and the fiber optic plate combination. Intagliation does not eliminate large rays, although it may change their intensity distribution. Intagliation does greatly minimize the propagation of large

Table 5-1. Summary of MTF Results. Table Entries are the Spatial Frequency in c/mm for MTF = 0.50

RELATIVE INTENSITY (PEAK)	FILM RESULTS			ELECTRONIC RESULTS		ZERO THICKNESS PHOSPHOR AND FILM	
	INTAGLIATED 10 MICROMETER	INTAGLIATED 6 MICROMETER	NON-INTAGLIATED 6 MICROMETER	INTAGLIATED 10 MICROMETER	INTAGLIATED 6 MICROMETER	10 MICROMETER	6 MICROMETER
2700		34					
5800		27					
6000	32		20				
6100	27						
6800	22						
8300	18						
9200		21		30	32	60	100
11000	20		No Data				
15000		16					
17000	18						
18000		10					

Table 5-2. Summary of Line Width Results. Table Entries are in Micrometers at 10 Percent/50 Percent of Peak Amplitude

RELATIVE INTENSITY (PEAK)	FILM RESULTS			ELECTRONIC RESULTS	
	INTAGLIATED 10 MICROMETER	INTAGLIATED 6 MICROMETER	NON-INTAGLIATED 6 MICROMETER	INTAGLIATED 10 MICROMETER	INTAGLIATED 6 MICROMETER
2700		25/15			
5800		36/18			
6000	33/16				
6100	37/17				
6800	35/20		No Data		
8300	45/22			22/10	21/9
9200		38/23			
11000	46/24				
15000		51/28			
17000	45/19				
18000		67/35			

angle rays and the resulting adjacent fiber illumination. Intagliation is especially effective when the fiber plate has a numerical aperture greater than or equal to 1 and has good extra-mural absorption properties.

The next improvement in resolution must come from controlling the choice of film to those having very thin emulsions. As noted in Section 2.1.5, scientific films have 10 to 15 micrometer emulsions. High resolution aerial reconnaissance emulsions are 4 to 6 micrometers thick. An interesting variation on the film tests would be the use of an aerial film. Aerial films also have greater latitude. The line spread function using such a film should appear more like electronically measured ones.

In conclusion, the point to remember is that whatever media are used to sense the output image in an intagliated phosphor screen, fiber optically coupled system, the thickness of the detection volume is now important. The image is recorded "in," not "on" the media. The finite thickness is an effective gap between the fiber optic window and an ideal, zero thickness medium.

Intagliated screen image tubes should cascade well, due in part to very thin ($t <$ wavelength) photocathodes. At least one component of the wings on line spread functions is reduced by intagliation. Image tube-charge coupled device combinations should show some degree of resolution loss, depending upon the relative values of the pixel area, the CCD MTF term, and the sensing thickness. Fiber optic vidicons should act like thick film. Their targets are the order of 10 micrometers thick. Particular difficulty might be expected in 1/2 inch or 2/3 inch vidicons because they must have relatively high spatial frequency response to produce a standard TV image on their smaller target areas.

Section 6

CREDITS

The author wishes to express his appreciation to his colleagues at NASA Goddard Space Flight Center, and at ITT-Aerospace/ Optical Division and ITT Electro-Optical Products Division. Without their help and cooperation, very little of the work reported here would have been possible.

The recorded in-film resolution problem was first posed to the author several years ago by Lou Wuellmer of ITT-A/OD. Ted Slecher of NASA-GSFC was the sponsor of this and the previous study.

The intagliated phosphor screens are the work of Dan Duggin of ITT-EOPD at Roanoke, Virginia. The design modifications and special assembly work on the F4089 image tube were done by Al Knight of ITT-EOPD at Fort Wayne, Indiana. Scott Neven of ITT-EOPD handled the logistics of building one tube at two manufacturing facilities several hundreds of miles apart. Scott also arranged the SEM examination of the phosphor screens and provided most of the text for Section 2.3. Ed Eberhardt provided many useful comments and suggestions during the work and preparation of the final report.

Ted Gull of NASA-GSFC expended much time and effort obtaining the densitometry data from the exposed film samples, calibrating and correcting them for the film exposure-density properties, and computing their MTF results.

The services of all are gratefully acknowledged.